

5-2021

A Novel Role for DYRK1A in Kidney Development

Alexandria Blackburn

Follow this and additional works at: https://digitalcommons.library.tmc.edu/utgsbs_dissertations



Part of the [Medicine and Health Sciences Commons](#)

Recommended Citation

Blackburn, Alexandria, "A Novel Role for DYRK1A in Kidney Development" (2021). *The University of Texas MD Anderson Cancer Center UTHealth Graduate School of Biomedical Sciences Dissertations and Theses (Open Access)*. 1068.

https://digitalcommons.library.tmc.edu/utgsbs_dissertations/1068

This Dissertation (PhD) is brought to you for free and open access by the The University of Texas MD Anderson Cancer Center UTHealth Graduate School of Biomedical Sciences at DigitalCommons@TMC. It has been accepted for inclusion in The University of Texas MD Anderson Cancer Center UTHealth Graduate School of Biomedical Sciences Dissertations and Theses (Open Access) by an authorized administrator of DigitalCommons@TMC. For more information, please contact digitalcommons@library.tmc.edu.

A NOVEL ROLE FOR DYRK1A IN KIDNEY DEVELOPMENT

by

Alexandria Blackburn, B.S.

APPROVED:

Rachel K. Miller

Rachel Miller, Ph.D.
Advisory Professor

Pierre D. McCrea

Pierre McCrea, Ph.D.

Rebecca Berdeaux

Rebecca Berdeaux, Ph.D.

Vicki Huff

Vicki Huff, Ph.D.

George T. Eisenhoffer

George Eisenhoffer, Ph.D.

Mir Reza Bekheirnia

Reza Bekheirnia, M.D.

APPROVED:

Dean, The University of Texas

MD Anderson Cancer Center UTHealth Graduate School of Biomedical Sciences

A NOVEL ROLE FOR DYRK1A IN KIDNEY DEVELOPMENT

A

DISSERTATION

Presented to the Faculty of

The University of Texas

MD Anderson Cancer Center UTHealth

Graduate School of Biomedical Sciences

in Partial Fulfillment

of the Requirements

for the Degree of

DOCTOR OF PHILOSOPHY

by

Alexandria Blackburn, A.S., B.S.

Houston, Texas

May, 2021

DEDICATION

I dedicate this dissertation to my children, Emery and Everett. I know that both of you will do great things one day.

ACKNOWLEDGEMENTS

I would like to thank my advisor, Dr. Rachel Miller, for being a great mentor throughout my graduate career. She has been incredibly supportive of me and my future career and has always pushed me to be a better scientist and get out of my comfort zone. She has taught me how to think critically about scientific questions and think about different ways to solve them. Before I came to her lab I had very little scientific writing experience and she was always there to help look over my proposals/papers/CVs and improve my writing. She has always been very supportive of my role as a mother and understanding if I had to leave early or stay home for a sick kid. Rachel, I deeply appreciate the support you have given me over the years both scientific and non. I would like to thank the past and present members of the Miller lab for help with troubleshooting experiments and also to commiserate with when said experiments failed. I want to thank Bridget DeLay for her sound advice whenever I was down because nothing would work. I want to thank Vanja Stankic for her help for all things graduate student-related. She helped me every time I had a milestone to reach and also a shoulder to cry on when I felt overwhelmed. I especially want to thank Mark Corkins who served as my mentor when I rotated and still does to this day. He helped me troubleshoot experiments, listened to me gripe (a lot), helped me learn every new technique I ever needed to learn in lab, and has helped me persevere through all of the failures.

I would like to thank both past and present members of the McCrea lab. They were always around to help if we needed reagents, experimental advice, or an extra set of eyes. I'd like to thank Pierre McCrea for being ever willing to help with all of

my scholarship and fellowship applications, I applied to everything! I would additionally like to thank Malgosia Kloc and past and present members of the Park lab. In addition to the McCrea lab, we all held constructive lab meetings which always led to better presentations and experiments. Furthermore, I would like to thank my wonderful advisory committee members (Pierre McCrea, George Eisenhoffer, Vicki Huff, Rebecca Berdeaux, and more recently, Mir Reza Behkeirnia). Every student I talked to dreaded their committee meetings but I always looked forward to mine. All of my members were incredibly supportive and helpful with new experiments and ideas that have helped pave the way to my success as a student. I always left my committee meetings happy and confident with new experiments/ideas. I especially want to thank Dr. Rebecca Berdeaux and Dr. Vicki Huff for always giving me new things to think about and new experiments to make my research better. I also want to thank Dr. Mir Reza Bekheirnia for giving me clinical insight into my project and, along with Nasim, being great collaborators who have given translational relevance to my project.

I want to thank my program for being such an engaging and social program. It really was like a little family in G&E. All of the faculty were always willing to help with whatever you needed and the students were always there to lend a helping hand, or to empathize with. A huge thank you to G&E program manager Elisabeth Lindheim who is the lifeblood of the G&E community. She is always there for whatever you need, is fantastic to work with, and always has advice for any situation. Elisabeth, you truly are a spectacular human. Thank you to all of the GSBS staff. Lily, Elisabet, Joy, Eric, Bunny and especially Brenda who made GSBS feel like a second home.

Brenda is also an amazing ally who always has something great to say, has given me countless advice, and always makes me feel like 100 bucks. Thank you Dr. Mattox for always helping me with all scholarship and academic related questions. Thank you to the deans for being such a great team throughout my graduate education and for handling the pandemic with your students in mind. Thank you to the Michaels for all IT related issues and especially Michael Orlando for making my best friend so happy through marriage. I am immeasurably grateful to my friends, you made graduate school bearable. You lunched with me, you took coffee breaks and sanity breaks with me. You made the last four years amazing and I will miss the weekly visits and hugs more than anything as we all move on to the next phase of our careers. Mostly, thank you to my other half, my partner in life, my husband, Clint Blackburn, for taking this crazy journey with me. You have supported my dreams and dealt with me being in school for an entire decade! You have helped me through the rough times and have made the good ones. You have made me a mother to two beautiful children and made our house a home. You are the reason I was able to do all of this and love you dearly for it. Lastly, to my family both by blood and by marriage, you have acted as my support system through this process and throughout my life. Especially to my mom, who always told me I could be whatever I wanted to be, and lead me to believe the sky was the limit. I love you so much for that.

A NOVEL ROLE FOR DYRK1A IN KIDNEY DEVELOPMENT

Alexandria Blackburn, B.S.

Advisory Professor: Rachel Miller, Ph.D.

Congenital anomalies of the kidney and urinary tract (CAKUT) are a leading cause of pediatric kidney failure and encompass a wide range of structural malformations resulting from defects in morphogenesis. CAKUT occur in ~1/500 live births and with an average wait time of 3-5 years for a kidney transplant, the need is high for the development of new strategies aimed at reducing the incidence of CAKUT and preserving renal function. Approximately 14% of CAKUT cases have a known genetic component. This low causality suggests that CAKUT is complex and that there are underlying genes and mechanisms which lead to CAKUT that have not been identified. Next-generation sequencing has uncovered a significant number of putative causal genes, including the novel observation that a cohort of patients with DYRK1A haploinsufficiency has a higher prevalence of CAKUT (73% of those assessed), including kidney defects. By using *Xenopus laevis* as a model we determine that DYRK1A is essential for kidney development. Loss of *dyrk1a* in *Xenopus* leads to abnormal kidney formation, which can be rescued. Furthermore, I demonstrate that Dyrk1a perturbations lead to changes in β -catenin during embryogenesis. This dissertation reveals a new gene important for kidney development and disease and also has the potential to impact diagnostic patient treatment strategies for DYRK1A-syndrome patients.

Table of Contents

Signature Page	i
Title Page	ii
Dedication	iii
Acknowledgements	iv
Abstract	vii
Table of Contents	viii
List of Figures	xi
List of Tables	xiii
List of Abbreviations	xiv
Chapter 1: Introduction	1
1.1 Kidney Development	1
1.2 Conservation of the Nephron in <i>Xenopus</i> and Mammals	6
1.3 Wnt Signaling in Kidney Development	10
1.4 Modeling CAKUT in <i>Xenopus</i>	14
1.5 Delineating Molecular Pathways Involved in Kidney Development Using <i>Xenopus</i>	22
1.6 Using <i>Xenopus</i> to Examine Human Genetic Variants	25
1.7 DYRK1A	28
1.8 Approaches to Discover Novel CAKUT Genes	30
1.9 Dissertation Summary	33
Chapter 2: Materials & Methods	34
2.1 Construct Design and <i>in vitro</i> Transcription	34
2.2 Western Blots	36
2.3 Design and Statistical Analyses	37
2.4 Study Participants	38
2.5 Exome Sequencing and Data Analysis	39
2.6 Whole mount <i>in situ</i> Hybridization	40
2.7 <i>Xenopus</i> Embryos and Microinjections	41
2.8 Immunostaining	41

2.9 Imaging	42
2.10 Transgenic <i>Xenopus</i> Lines	42
Chapter 3: Dyrk1a-Related Intellectual Disability Syndrome: A Novel Association With Congenital Anomalies Of The Kidney And Urinary Tract ...	44
3.1 Introduction	44
3.2 Results	46
3.21 CAKUT/Genital Defects Identified in Patients with DYRK1A Variants	46
3.22 A Majority of the Variants Found in DYRK1A are Loss-of-Function and are Found in the Kinase Domain	52
3.23 <i>Xenopus laevis</i> as a Model of Genitourinary Development	53
3.24 <i>dyrk1a</i> is Expressed in the <i>Xenopus</i> Kidney and <i>in vivo</i> Knockdown Demonstrates its Role in Kidney Development	56
3.25 Variants Identified in DYRK1A-related Intellectual Disability Syndrome Fail to Rescue Dyrk1a Loss-of-Function in <i>Xenopus</i>	66
3.26 Other Findings	69
3.3 Discussion	76
Chapter 4: Dyrk1a and Wnt Signaling in Kidney Development.....	79
4.1 Introduction	79
4.2 Results	80
4.21 Dyrk1a Perturbation Alters β -catenin Levels	80
4.3 Discussion	90
Chapter 5: Conclusions, Discussion, and Future Directions.....	93
5.1 Conclusions and Discussion	93
5.11 DYRK1A's Known Interactions with Pathways Involved in Kidney Development	96
5.12 Overall Conclusions.....	100
5.2 Future Directions	100

Chapter 6: Appendix: Loss of P53 Leads to Aberrant Kidney Development in <i>Xenopus</i> and May Lead to Congenital Anomalies of the Kidney and Urinary Tract in Li-Fraumeni Patients.....	105
6.1 Introduction	105
6.2 Results	105
6.21 P53 Knockdown or Knockout Leads to Aberrant Kidney Development in <i>Xenopus</i>	106
6.22 Modeling Dominant Negative mRNA From Li-Fraumeni Patients Leads to Abnormal Kidney Development in <i>Xenopus</i>	112
6.3 Discussion.....	115
Chapter 7: Bibliography	120
Vita	161

List of Figures

Figure 1. Development of the Kidney	3
Figure 2. <i>Xenopus</i> Pronephric and Human Metanephric Nephrons Share Conserved Tubule Segmentation Patterns	5
Figure 3. Expression Patterns are Conserved Between the Human S-Shaped Body and the Early <i>Xenopus</i> Pronephros During Development	9
Figure 4. Wnt Signaling Pathways.....	11
Figure 5. Common Malformations of the Kidney Found in CAKUT	15
Figure 6. Congenital Anomalies of the Kidney and Urinary Tract (CAKUT) Associated with DYRK1A Variants in Patients with DYRK1A-Related Intellectual Disability Syndrome	49
Figure 7. Human and <i>Xenopus laevis</i> Protein Alignment and Short and Long <i>Xenopus</i> Homeolog Alignment for <i>dyrk1a</i> 5'UTR	54
Figure 8. <i>in situ</i> Hybridization of <i>dyrk1a</i> Across Developmental Stages Demonstrates Kidney Expression in <i>X. laevis</i> and <i>X. tropicalis</i>	57
Figure 9. Immunofluorescence of Dyrk1a in <i>Xenopus laevis</i> at Stage 47 Demonstrates it is Expressed in the Kidney	59
Figure 10. The Dyrk1a MO Correctly Targets <i>Xenopus dyrk1a</i> mRNA and Wild- Type, Missense, and Truncated Human DYRK1A Proteins are Expressed in Neurula Stage <i>Xenopus</i> Embryos	60
Figure 11. Dyrk1a Knockdown Disrupts Late Kidney Marker Na ⁺ K ⁺ -Atpase (<i>atp1a1</i>) in <i>Xenopus</i>	62
Figure 12. Loss of Dyrk1a Results in Kidney Anomalies in <i>Xenopus laevis</i> ..	63
Figure 13. Overexpressing <i>DYRK1A</i> ^{R205*} or <i>DYRK1A</i> ^{L245R} Does Not Cause a Gain-of-Function Phenotype	67
Figure 14. Scoring System for <i>Xenopus</i> Embryonic Kidneys	68
Figure 15. Injecting Both Ventral Cells of 4-cell Embryos Does Not Affect Heart Morphology or Cardiac Beating	70
Figure 16. <i>Xenopus dyrk1a</i> Overexpression Leads to Kidney Abnormalities .	72

Figure 17. Nuclei Tracking of Neural Crest Explants Demonstrates That Dyrk1a Loss Leads to Loss of Coordinated Cell Migration	74
Figure 18. Dyrk1a Loss in Neural Crest Cells leads to Craniofacial Anomalies	75
Figure 19. Ventralization Results When Dyrk1a MO is Injected into the Dorsal Cells	82
Figure 20. Knockdown of Dyrk1a Results in Reduced Total β -Catenin Protein	83
Figure 21. Knockdown of Dyrk1a Results in Reduced Active β -Catenin Protein	84
Figure 22. GFP Expression is Increased with <i>dyrk1a</i> Overexpression Upon Lysis of The Nucleus	88
Figure 23. Inhibiting Dyrk1a at a Lower Dose Increases Wnt Signaling	89
Figure 24. How DYRK1A Interacts with the Wnt Pathways	101
Figure 25. p53 Expression Across Developmental Stages	107
Figure 26. The p53 Morpholino Correctly Targets p53 mRNA in <i>Xenopus</i> ...	108
Figure 27. p53 Knockdown Leads to Loss of Kidney Tubules in <i>Xenopus</i> ..	109
Figure 28. p53 Can be Knocked Out with CRISPR/Cas9 Technology in <i>Xenopus</i>	110
Figure 29. p53 Knock Out Leads to Loss of Kidney Tubules in <i>Xenopus</i>	113
Figure 30. Human p53 Wild-type and Mutant Proteins are Expressed in Neurula Stage <i>Xenopus</i> Embryos	116
Figure 31. Mutant Human p53 Disrupts Kidney Development in <i>Xenopus</i> ...	117

List of Tables

Table 1. CAKUT Genes That Have Been Analyzed or Have Kidney Expression in <i>Xenopus</i>	18
Table 2. Demographics, Molecular Data, and Phenotype of 19 Patients With SNVs and Small Indels (<10bp) in <i>DYRK1A</i> Identified by Clinical Exome Sequencing	47
Table 3. Available Information about Genitourinary Phenotype of Patients Reported in This Study	50
Table 4. Figure 12F p-Values for Each Experimental Condition as Determined by Two-Tailed T-Test	65
Table 5. Figure 12G p-Values for Each Experimental Condition as Determined by Two-Tailed T-Test	65
Table 6. <i>Xenopus</i> Embryos Used for Edema Experiment	65

List of Abbreviations

ADPKD: autosomal dominant polycystic kidney disease

ACE: angiotensin converting enzyme

APC: adenomatous polyposis coli

ASD: autism spectrum disorder

BMP: bone morphogenetic protein

CAKUT: congenital anomalies of the kidney and urinary tract

CaN: calcineurin

Cas9: CRISPR associated protein 9

CDC42: Cell division control protein 42

CDK: cyclin-dependent kinase

CKD: chronic kidney disease

CK1 α : casein kinase 1 α

CRISPR: clustered regularly interspaced short palindromic repeats

DAAM1: dishevelled-associated activator of morphogenesis

DAG: Diacylglycerol

DVL: dishevelled

DYRK1A: dual specificity tyrosine phosphorylation regulated kinase 1A

ESRD: end-stage renal disease

GD-CNV: genomic disorder-associated copy number variations

GDNF: glial cell line-derived neurotrophic factor

GSK3: glycogen synthase kinase 3

FGF: fibroblast growth factor

FZD: frizzled

IP3: inositol trisphosphate

JNK: c-Jun N-terminal kinase

LRP5/6: low density lipoprotein receptor related protein 5/6

MAPK: mitogen-activated protein kinases
MCDK: multicystic dysplastic kidney
MM: metanephric mesenchyme
MO: morpholino
NDD: neurodevelopmental disorder
NFAT: nuclear factor of activated T-cells
NLK: nemo like kinase
NLS: nuclear localization sequence
NMD: nonsense-mediated decay
NPHP: nephronophthisis
PCP: planar cell polarity
PKC: Protein kinase C
PLC: Phospholipase C
ROCK: Rho-associated kinase
ROR: retinoid-related orphan receptor
RYK: receptor like tyrosine kinase
RV: renal vesicle
SNV: single-nucleotide variants
TAK1: transforming growth factor beta-activated kinase 1
TCF/LEF: T-cell factor/lymphoid enhancer factor
UB: ureteric bud
WNT: wingless/integrated
WT1: wilms tumor 1

CHAPTER 1: INTRODUCTION

This chapter is modified from Blackburn ATM, Miller RK. Modeling congenital kidney diseases in *Xenopus laevis*. Dis Model Mech. 2019 Apr 9;12(4). pii: dmm038604. doi: 10.1242/dmm.038604. <https://dmm.biologists.org/content/12/4/dmm038604>. Dis Model Mech articles are published under a CC BY license, which establishes that authors retain copyright in their articles.

1.1 Kidney Development

The kidney is an excretory organ that functions by reabsorbing nutrients and excreting waste and excess fluid in the form of urine. Humans have two kidneys that each drain through a separate tube called a ureter into the bladder. The structural and functional unit of the kidney is the nephron. Each kidney contains around 1 million nephrons which are tubules that filter blood. Through this process, the kidneys maintain salt, water, and pH homeostasis, as well as removing metabolic waste byproducts (1). Additional functions of the kidney include regulating blood pressure, converting vitamin D into its active form, stimulating red blood cell production, and maintaining phosphate and calcium levels (2).

Anatomically, the kidney consists of three sections: the renal cortex, the renal medulla and the renal pelvis. The renal cortex is the outermost part of kidney, while the renal medulla is the innermost. All nephrons empty the blood ultrafiltrate through their tubules into the collecting duct system which leads to the renal pelvis and then drains into the ureter and bladder. There are two types of nephrons that exist. A majority of nephrons (~85%) are cortical nephrons which have short loops of Henle

that just dip into the outer medulla (1). The remaining 15% are called juxtamedullary nephrons. They have long loops of Henle that descend deeply into the medulla which allow for the concentration of urine (1).

In humans, nephrogenesis starts at around 5 weeks of gestation and completes between weeks 34-36 (3). Environmental factors such as vitamin A deficiency or exposure to teratogenic substances can affect proper kidney development (4, 5). Retinoic acid signaling is important for embryonic kidney patterning and is derived from vitamin A, therefore deficits of it can lead to anomalies (4). Additionally, taking angiotensin converting enzyme (ACE) inhibitors during pregnancy can lead to congenital anomalies of the kidney and urinary tract (CAKUT), as the kidney is essential in maintaining blood pressure through the renin-angiotensin-aldosterone system (5).

The kidney is a unique organ in that it develops from successive forms that replace the previous structure (Figure 1A-C) (6). These forms are the pronephros, the mesonephros, and the metanephros. As each sequential form of the kidney is superseded by the next, the organizational complexity increases (6). In mammals, both the pro- and mesonephros are replaced by the metanephros, which persists as the adult kidney (Figure 1) (2). It is important to note that although the pronephros is non-functional in mammals, it is required for the subsequent formation of the mesonephros and metanephros and the urogenital tract.

In mammals, the kidney arises from the intermediate mesoderm, which gives rise to the nephric duct (Wolffian duct) and the metanephric mesenchyme (MM).

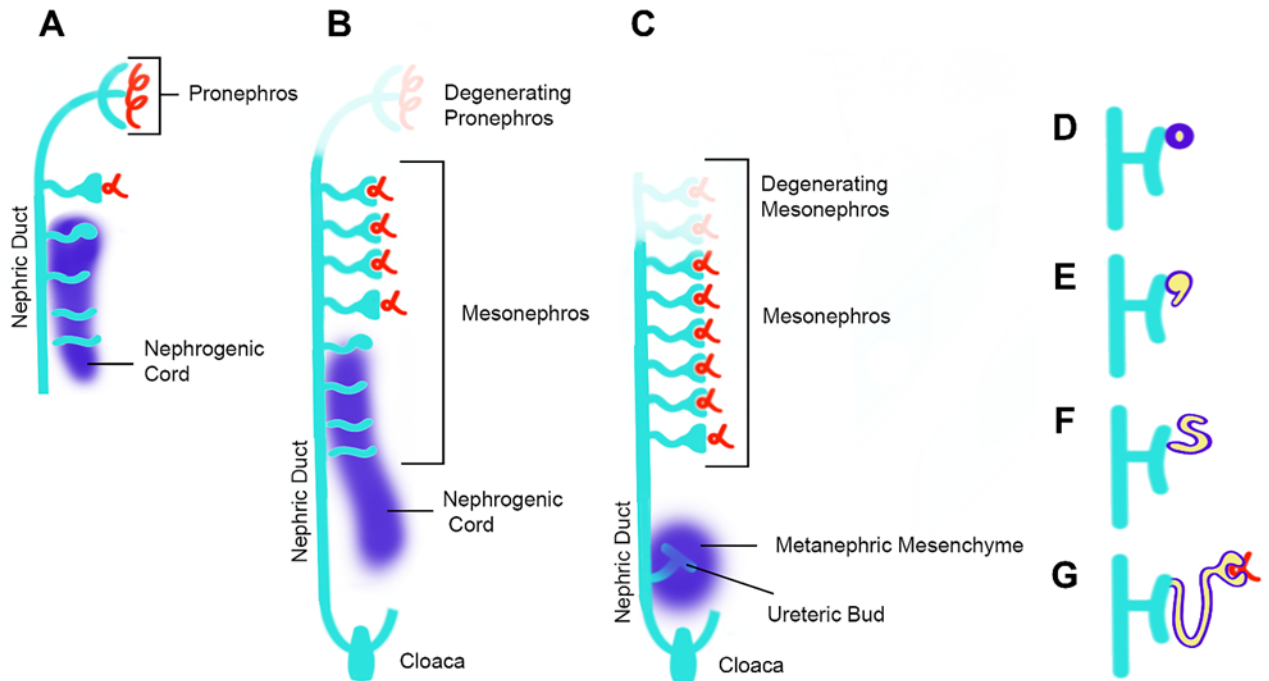


Figure 1. Mammalian Kidney and Nephron Development.

The kidney develops from the intermediate mesoderm (labeled here as the nephrogenic cord) in three successive forms, the pronephros, the mesonephros, and the metanephros, which occurs in a cranial to caudal fashion. (A) In mammals the pronephros arises from the nephrogenic cord and is a transient and non-functional structure which degenerates. (B) Mesonephric nephrons are functional and develop more caudally from the nephrogenic cord along the nephric duct/Wolffian duct but also degenerate. (C) The metanephric nephrons form from the metanephric mesenchyme which condenses around the ureteric bud to form (D) polarized renal vesicles. (E) A cleft in the renal vesicle leads to formation of the comma-shaped body. (F) An additional cleft leads to the formation of the S-shaped body, which (G) elongates and fuses to the ureteric bud to form a mature metanephron that is patterned along the proximal-distal axis where the proximal end becomes the podocytes and the distal end becomes the distal tubule. The ureteric bud will become the complex arborized collecting duct system which is induced from signals from the metanephric mesenchyme. Although the pronephros is non-functional in mammals, it is required for the subsequent formation of the mesonephros, metanephros, and the urogenital tract, which arises from or along the nephric duct. (B-C) The cloaca is a temporary structure during embryogenesis.

The formation of nephrons and collecting ducts occurs through reciprocal interactions between the MM and the ureteric bud (UB) (2, 7). The UB grows from the nephric duct and will branch into a complex arborized network which gives rise to the collecting duct system (7). This growth and branching is directed by signals from the surrounding MM, which can be found around the branches of ureteric tips (2). The MM is likewise induced by the UB to promote nephrogenesis which occurs at the nephrogenic zone near the outer edge of the kidney (8). The cells closest to the UB tips undergo epithelialization and form the renal vesicle (RV) which forms all parts of the nephron (Figure 1D) (2). The RV forms a single cleft which creates the comma-shaped body (Figure 1E), which is followed by another cleft to form the S-shaped body (Figure 1F) (2, 9). The S-shaped body is patterned along the proximal-distal axis where the proximal end becomes the podocytes and the distal end becomes the distal tubule, with the proximal tubules and loop of Henle patterned in between (2, 8).

An adult human kidney contains approximately one million nephrons (10) whereas an adult mouse kidney has over ten thousand (11). Mammalian nephrons develop asynchronously, making them challenging to study (12). In contrast, *Xenopus laevis*, or frog embryos contain only one functional pronephric nephron on either side of their body, which serves as the embryonic kidney (Figure 2). In amphibians, the mesonephros serves as the adult kidney which replaces the pronephros upon metamorphosis. Although the arrangement of kidneys differs, the structural and functional unit of the kidney, the nephron, remains the same. Therefore, the fully functional *Xenopus laevis* pronephric nephron serves as a

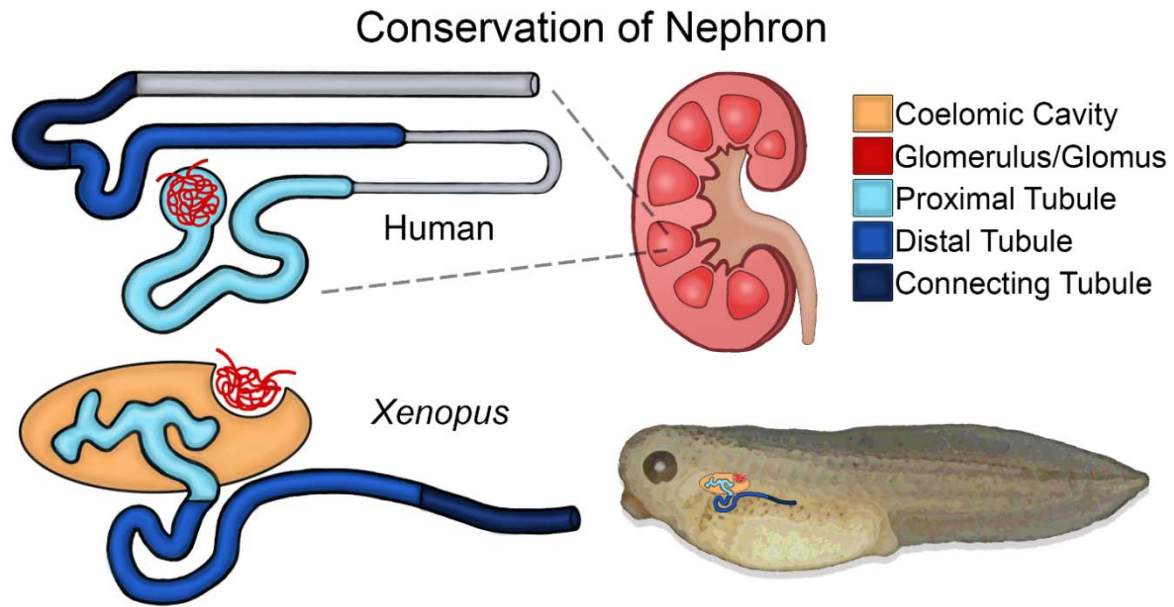


Figure 2. The *Xenopus Laevis* Pronephric and Human Metanephric Nephrons Share Conserved Tubule Segmentation Patterns Based on Gene Expression Data.

The schematic represents nephron segments, designated by different colors, in the mammalian metanephric nephron (top) and the *Xenopus laevis* pronephric nephron (bottom). The glomus/glomerulus filters blood across capillary walls into the proximal tubule, which filters various wastes out of the body through the remaining distal and connecting tubules. There are noted differences between the glomus and glomerulus in that the glomus deposits blood filtrate into the coelomic cavity. Additionally, *Xenopus laevis* does not have a loop of Henle (grayed out in human schematic) or a true collecting duct (grayed out in human schematic), but instead has a region analogous to the connecting tubule closest to the distal tubule of the mammalian metanephric nephron (13).

simplified model for mammalian meso- and metanephric nephron development (Figure 2).

1.2 Conservation of the Nephron in *Xenopus* and Mammals

The pronephros forms from the intermediate mesoderm in both mammals and amphibians. In *Xenopus laevis* embryos (hereafter referred to simply as *Xenopus*) the nephric primordia is induced by signals from the surrounding tissues and forms during neurula stages 12-15 (~16-20 hours post-fertilization), which will later generate the tubules of the pronephros (14). Pronephros specification in *Xenopus* occurs through interactions between the transcription factors *Ors1/2*, *Pax8*, *Lhx1*, and *Hnf1 β* , among others (15–18). Morphogenesis of the pronephros begins at the early tailbud stage 21 (~23 hours post-fertilization) (<http://www.xenbase.org/anatomy/alldev.do>).

In mice, the *Ors1* gene is essential for the formation of renal structures and can be found in the intermediate mesoderm, while *Osr2* is found later on in the mesonephros and is not essential (16). Consistent with *Xenopus* (19, 20), mice that lack *Lhx1* or *Pax2/8* have severe kidney defects, though *Pax2/8* seem to have redundant functions in mice (21, 22). Finally, *Hnf1 β* is expressed in the ureteric bud as well as comma- and S-shaped bodies and mutations in this gene lead to kidney cyst formation in mice (23). In addition, WNT (Wingless/Integrated), FGF (fibroblast growth factor), BMP (bone morphogenetic protein) and GDNF (glial cell line-derived neurotrophic factor) signaling pathways are involved in both *Xenopus* and mammalian kidney development (9, 24).

Analogous to the mammalian nephron, the amphibian pronephros is segmented along its proximal-distal axis (25). Mammals have a glomerulus to filter blood, proximal tubules for reabsorbing water and various nutrients, a loop of Henle to concentrate urine, distal tubules for reabsorbing water and various nutrients, and a collecting duct that reabsorbs water and carries urine from the kidneys to the bladder (2). Similarly, *Xenopus* embryos have a glomus for filtering blood, proximal and distal tubules for reabsorbing water and nutrients and a connecting tubule, which opens out to the cloaca (Figure 2). In mice, the glomerulus forms at the most proximal end of the S-shaped body which makes it linked to the development of the rest of the nephron. *Xenopus* however, can develop a glomus independently from the tubules, which may make understanding how the glomus forms more accessible (26). In addition, at the tips of the proximal tubules, the amphibian also has multi-ciliated cells called nephrostomes, which cause fluid influx from the coelomic cavity into the proximal tubules (27).

Each segment of the nephron has a specific function, which is reflected by distinct cell morphologies (25) and gene expression signatures (13, 28). Strikingly similar to mammals, the proximal tubules in *Xenopus* are responsible for reabsorbing ions, water, glucose, and amino acids (13, 28–31). The most distal part of the *Xenopus* proximal tubule is analogous to the mammalian proximal straight tubule (13). Because *Xenopus* is an aquatic freshwater frog, it is unlikely that the amphibian pronephros requires a true loop of Henle for concentrating urine. Within the literature, the *Xenopus* intermediate tubules have been defined using markers that are co-expressed in the proximal and distal tubules of the mouse kidney (13,

32). Thus, assessment of a marker that is exclusive to this region is necessary to confirm or refute the existence of this structure and will be called early distal in this dissertation. The *Xenopus* distal tubule is analogous to the thick ascending limb of the loop of Henle and the distal convoluted tubule in mammals (13), and it functions to transport ammonium, reabsorb magnesium ions and is important for urine acidification (13, 28, 33, 34). The pronephric connecting tubule of *Xenopus* connects the distal tubules to the cloaca to excrete urine and is only analogous to mammals in the region neighboring the distal tubule (13). The pronephros does not have a collecting duct to further concentrate urine or connect multiple nephrons to a secondary structure, as is necessary for the mammalian metanephros.

Recently, it has been shown that human and mouse nephron protein expression signatures in the renal vesicles and S-shaped bodies are very similar (35). Not surprisingly, *Xenopus* shares similar gene expression signatures during early pronephric development in the kidney (Figure 3). Although this figure only illustrates four gene expression signatures, it is important to note that of the 29 expression signatures identified in the human embryonic kidney (35), 18 can also be found in the *Xenopus* kidney (Xenbase.org). Additionally, a comparison of gross expression signatures in the kidney demonstrated similarities between mouse and *Xenopus* in both overlapping transcription factors such as *Pax8* and additional ones such as *Foxc1* and *Sal1* (36). Furthermore, some of the proteins analyzed in humans have not been studied in *Xenopus*, potentially leading to an underestimate of the similarities. This overall conservation on the molecular, genetic, structural, and functional levels supports the use of the *Xenopus* pronephros as an appropriate

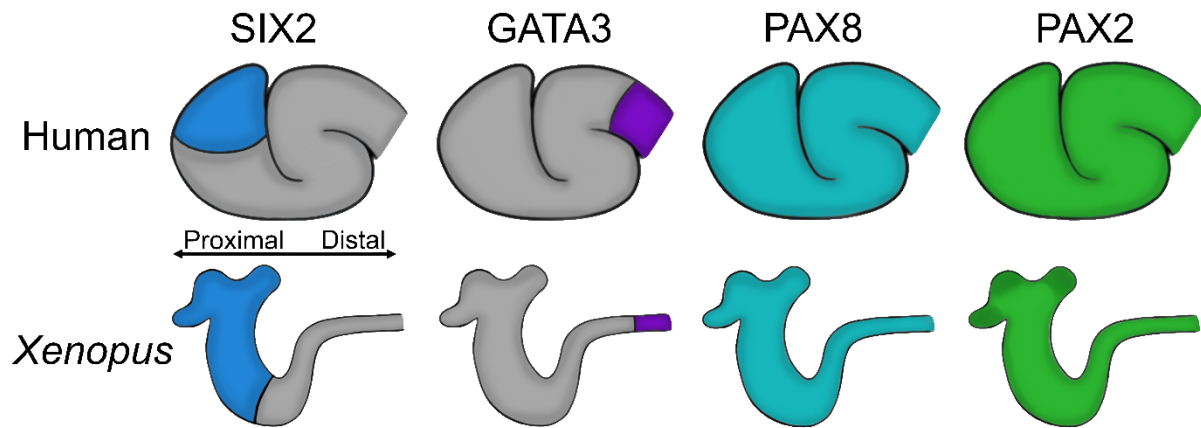


Figure 3. Expression Patterns are Conserved Between the Human S-shaped Body and the Early *Xenopus* Pronephros During Development.

Four different expression patterns (shown in different colors) of fundamental kidney proteins/mRNA were chosen to demonstrate the similarities between the developing human and *Xenopus* nephron. Schematics indicate where immunostaining of S-shaped body nephrons of week 16 to 17 human fetal kidneys is present (top) (35), as well as *in situ* expression patterns of stage 33 *Xenopus* nephrons (bottom) (Xenbase.org). Schematics are positioned so that the proximal and distal regions of the human and *Xenopus* nephron expression patterns can be easily compared. The *Xenopus* kidney stage was chosen to match the approximate developmental time point of human S-shaped body nephrons, as both are representative of recently epithelialized nephrons. Note that *pax2* is slightly more enriched at the nephrostomes in *Xenopus* (dark green).

model for the study of congenital kidney anomalies.

1.3 Wnt Signaling in Kidney Development

The Wnt signal transduction pathway is an evolutionarily conserved pathway where Wnt glycoproteins are secreted to nearby cells. Wnt signaling has been implicated in embryonic organogenesis, fate determination, cell polarity, cell migration, and neural patterning (37). There are three major pathways for Wnt signaling: canonical/ β -catenin, non-canonical planar cell polarity, and the non-canonical calcium pathway (Figure 4). The upstream event of all pathways is the same: Wnt ligands are secreted from one cell and bind the extra-cellular domain of a Frizzled (FZD) receptor of a neighboring cell which is then transduced to the neighboring cell's interior to the phosphoprotein Dishevelled (DVL) (37–39). After that, to activate the planar cell polarity (PCP) pathway, either Dishevelled-associated activator of morphogenesis 1 (DAAM1) or Rac are recruited to modulate actin polymerization to alter the cytoskeleton (Figure 4B) (37). The Wnt/calcium pathway recruits a trimeric G-protein which leads to PLC activation and calcium release (Figure 4C) (37). In canonical Wnt signaling, in the absence of a Wnt ligand, the cytoplasmic protein β -catenin is targeted for degradation by the destruction complex. The destruction complex is composed of Axin, adenomatous polyposis coli (APC), casein kinase 1 α (CK1 α), and glycogen synthase kinase 3 (GSK3) (Figure 4A) (37, 39). While in this complex, CK1 α and GSK3 phosphorylate β -catenin which targets it for ubiquitination and proteasomal degradation. However, in the presence

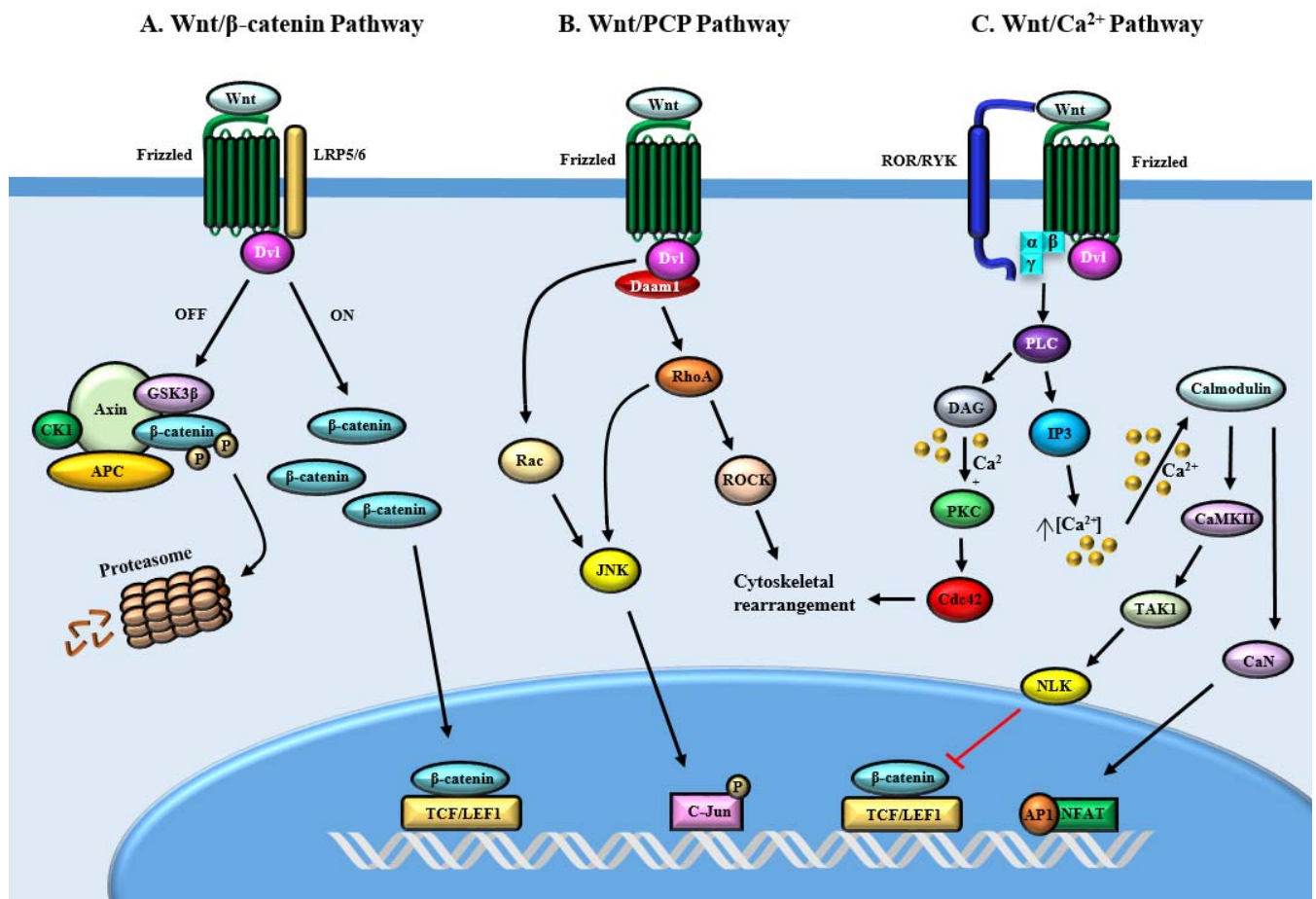


Figure 4. Wnt Signaling Pathways.

There are three major pathways for Wnt signaling: canonical/ β -catenin, non-canonical planar cell polarity, and the non-canonical calcium pathway. The upstream event of all pathways is the same: Wnt ligands are secreted from one cell and bind the extra-cellular domain of a Frizzled (FZD) receptor of a neighboring cell which is then transduced to the neighboring cell's interior to the phosphoprotein Dishevelled (DVL) (37–39). (A) In the absence of a Wnt ligand, the destruction complex (Axin/APC/CK1/GSK3 β) targets β -catenin for proteasomal degradation (OFF). When a Wnt ligand binds, LRP5/6 binds to a FZD receptor which inhibits the destruction complex from phosphorylating β -catenin. β -catenin is then able to translocate to the nucleus and bind TCF/LEF1 which leads to activation of canonical Wnt target genes. (B) To activate the planar cell polarity (PCP) pathway, either DAAM1 or Rac are recruited. DAAM1 activates RhoA which activates Rho-associated kinases (ROCK) and leads to cytoskeletal rearrangements. Alternatively, Rac or RhoA lead to c-Jun n-terminal kinase (JNK) which controls cell polarity and movement (40). (C) The Wnt/calcium pathway requires Wnt ligand to bind leading to FZD receptor interaction co-receptor retinoid-related orphan receptor/ receptor like tyrosine kinase (ROR/RYK) leading to recruitment of a trimeric G-protein. This leads to phospholipase C (PLC) activation which can activate diacylglycerol (DAG) through protein kinase C (PKC) to stimulate cell division control protein 42 (CDC42) mediated cell movements (37). Additionally, PLC activation can lead to inositol trisphosphate (IP3) activation which releases intracellular calcium to activate Calmodulin. Activation of Calmodulin causes transforming growth factor beta-activated kinase 1 (TAK1) to activate nemo like kinase (NLK) which inhibits β -catenin/TEF function. Alternatively, Calmodulin can lead to calcineurin (CaN) and NFAT activation (37).

of a Wnt ligand, the destruction complex is disassembled, leading to β -catenin stabilization. This stabilization allows β -catenin to translocate to the nucleus and bind to transcription factor T-cell factor/lymphoid enhancer factor (TCF/LEF) to activate Wnt target genes (37). This occurs when FZD binds to the low density lipoprotein receptor related protein (LRP5/6), recruiting DVL which leads to phosphorylation of LRP5/6 which in turn recruits Axin and disrupts the destruction complex (39).

The canonical Wnt/ β -catenin pathway has been identified as a key regulator in kidney development in both mammals (41, 42) and *Xenopus* (43, 44). Wnt signaling is necessary for nephron induction in mice (45) and is essential for renal branching morphogenesis (46), as well as maintaining the nephron progenitor pool (47). In humans, loss-of-function mutations in canonical Wnt ligand *WNT4* have been associated with renal hypodysplasia, a condition characterized by dysplastic kidneys with a reduced number of nephrons (48). Studies in *Xenopus* demonstrate that Wnt4 protein controls the medio-lateral patterning of the pronephros (49). Additionally, knockdown of Wnt4 protein in *Xenopus* results in complete loss of kidney tubules (43).

In addition to Wnt ligands, other proteins have been found to regulate Wnt signaling. In humans, *Wilms Tumor 1* (*WT1*) is a known regulator of canonical Wnt signaling. Mutations that affect *WT1* result in nephroblastoma, more commonly known as Wilms tumor (50). Knockdown of Wt1 protein expression was shown to reduce Wnt4 expression in the prospective pronephros of *Xenopus* embryos (51). Both overexpression or loss of canonical Wnt signaling in *Xenopus* leads to loss of

kidney tubules whereas overexpression of β -catenin in the mouse kidney leads to severe polycystic lesions that affect the entire nephron (52). These studies in both *Xenopus* and mouse models demonstrate that too much or too little Wnt signaling results in kidney abnormalities, suggesting that endogenous levels must be tightly maintained to achieve proper nephrogenesis.

1.4 Modeling CAKUT in *Xenopus*

CAKUT are a leading cause of pediatric kidney failure, accounting for 40–50% of pediatric chronic kidney disease (CKD) worldwide (53). CAKUT encompasses a wide range of structural malformations resulting from morphogenetic defects, including Wilms tumor and renal hypodysplasia (Figure 5) (54). With an average five-year wait time for a deceased donor kidney transplant (United Network for the Organ Sharing), the need to find alternative treatments that preserve renal function is essential. Monogenic disease with strong genetic causality only accounts for 14% of CAKUT (55), and polygenic causes are speculated to occur but are largely unknown (56). Next-generation sequencing has helped to uncover novel causative genes of CAKUT, but a high-throughput strategy to test their function in the kidney is needed. To understand how CAKUT arises, it is crucial to understand how the kidneys and urinary tract develop to uncover the genetic mechanisms that coordinate these events. Mice and zebrafish have been the predominant models used in kidney research, while recent advances have made kidney organoids useful for nephrotoxicity screening as well as modeling kidney diseases (57). However,

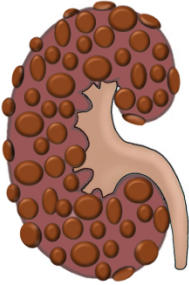
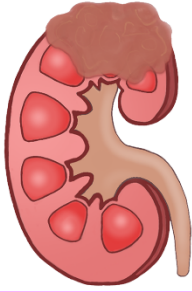
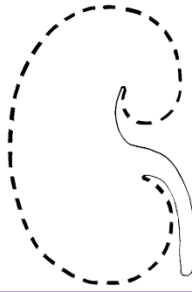

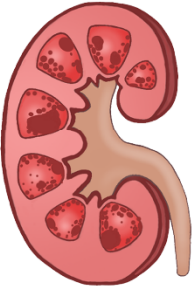
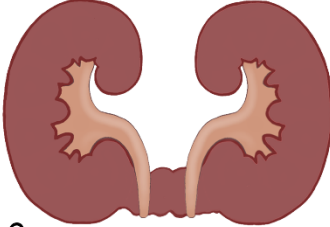
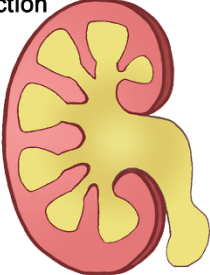
<p>Dysplasia/Polycystic Kidney</p>  <p>1</p>	<p>Tumor</p>  <p>2</p>	<p>Aggenesis</p>  <p>3</p>
<p>Hypoplasia</p>  <p>4</p>	<p>Nephronopthisis</p>  <p>5</p>	<p>● <i>BICC1, FOXC2, GATA3, HNF1B, LHX1, LMX1B, PKD1/2, SALL1</i></p> <p>● <i>TSC1, WT1</i></p> <p>● <i>GDNF, HNF1B, RET,</i></p> <p>● <i>ANKS6, BMP4/7, EYA1, FOXC1, HNF1B, NRIP1, PAX2, SALL1, SIX1/2, WNT4</i></p> <p>● <i>ANKS6, INVS, NEK8, NPHP3</i></p> <p>● <i>FOXC2, HNF1B</i></p> <p>● <i>BMP7, NRIP1, PAX2, SALL1, SOX17</i></p>
<p>Horseshoe Kidney</p>  <p>6</p>	<p>Ureter Malformation/Obstruction</p>  <p>7</p>	

Figure 5. Common Malformations of the Kidney Found in CAKUT.

Renal malformations resulting from inherited kidney diseases are depicted in colored boxes. The colors correspond to the color coding for genes whose loss results in the given phenotype. (1) Green represents renal cysts that are large and cover the majority of the kidney, as seen in renal dysplasia, multicystic dysplastic kidney (MCDK) and autosomal-dominant polycystic kidney disease (ADPKD). (2) Magenta represents a tumor, as seen in tuberous sclerosis and Wilms tumor. (3) Purple represents kidney agenesis. (4) Teal represents renal hypoplasia, which is one of the most common CAKUT phenotypes. (5) Orange represents nephronophthisis, with maroon spots depicting corticomedullary cysts, which are generally small. (6) Blue represents horseshoe kidney, where both kidneys are fused together. (7) Red represents ureter malformations and blockages, which result in urine backflow into the kidney (shown in yellow in the schematic). Genes listed in the key have been studied or are expressed in the *Xenopus* kidney. Colored boxes and numbers that correspond to the aforementioned phenotypes can also be found in Table 1 under 'Renal phenotype'

Xenopus possesses many qualities that make it an effective *in vivo* model to study congenital kidney diseases.

Xenopus share a relatively close evolutionary history with mammals because they are tetrapods. Thus, this model has the advantage of rapid development, like zebrafish, but evolutionarily, it lies closer to mammals. Additionally, *Xenopus* and human genomes have long stretches of gene colinearity and 79% of identified human disease genes have a verified ortholog in *Xenopus* (58). The embryonic kidney of *Xenopus* has many characteristic features of a mature mammalian kidney (Figure 2) (13, 28). Thus, many genes and processes necessary for *Xenopus* kidney development are also important in mammalian kidney development. Furthermore, a number of kidney disease-causing genes have been analyzed in *Xenopus* or are expressed in its embryonic kidney, introducing potential paths for future kidney research (Figure 5 and Table 1). Though relatively few in number, the *Xenopus* genes studied have been shown to function in kidney development as their mammalian orthologs do in mammalian kidneys, and they result in similar nephron phenotypes when their expression is disrupted. Additionally, *Xenopus* possesses unique qualities that other *in vivo* model systems lack.

With a simple hormone injection, *Xenopus* produces large clutch sizes with hundreds of embryos that develop externally. Their kidneys can easily be visualized and imaged through their transparent epidermis, and they develop a fully functional kidney in ~56 hours (15). Additionally, cleavage-stage *Xenopus* embryos have been fate-mapped, which allows for the tracking of specific blastomeres as they develop

Gene Symbol	Renal Phenotype	Human disease	Contribution of <i>Xenopus</i>	Mode of inheritance	References
<i>ACE</i>	renal dysgenesis	Renal tubular dysgenesis	ACE activity detected at high levels in kidney and testes	recessive	(59, 60)
<i>AGT</i>	renal dysgenesis	Renal tubular dysgenesis	Mitochondrial targeting in liver cells	recessive	(60, 61)
<i>ANKS6</i> (NPHP16)	Renal cysts ⁵ , renal hypoplasia ⁴	Nephronophthisis, situs inversus	<u>Role in early tubule morphogenesis</u>	recessive	(62, 63)
<i>BICC1</i>	Renal cysts, renal dysplasia ¹	Renal disease	<u>Regulates renal epithelial cell differentiation, defects in left-right patterning</u>	N/A	(64–67)
<i>BMP4</i>	Renal hypodysplasia ⁴	Microphthalmia, syndromic 6 Orofacial cleft 11	Important for ventral mesoderm formation, BMP signaling mediates pronephric tubule and duct formation	dominant	(68–70)
<i>BMP7</i>	UVJ obstruction ⁷ , hypodysplasia ⁴	CAKUT	Expressed in pronephros	dominant	(71, 72)
<i>CLCNKB</i>	Hypochloremia, proteinuria	Bartter Syndrome type III	<u>Important for chloride conductance</u>	recessive	(33, 73, 74)
<i>EYA1</i>	Renal hypodysplasia ⁴	Branchio-oto-renal syndrome	Important for normal ear development, not analyzed in pronephros	dominant	(75, 76)
<i>FOXC1</i>	Renal hypoplasia ⁴	CAKUT, Axenfield-Rieger Syndrome	Expression in pronephros	dominant	(77, 78)
<i>FOXC2</i>	Hydronephrosis, horseshoe kidney ⁶ , proteinuria, renal cysts ¹	Lymphedema-distichiasis syndrome with kidney disease and diabetes mellitus	Required for podocyte gene expression	dominant	(79, 80)
<i>GATA3</i>	Renal dysplasia ¹	HDR Syndrome	Expressed in pronephric duct.	dominant	(81, 82)
<i>GDNF</i>	Kidney agenesis ³ , renal dysgenesis, nephrotic syndrome	CAKUT, Hirschsprung Disease	Expressed in pronephros	N/A	(83, 84)
<i>HNF1β</i>	Renal hypodysplasia ⁴ , sporadic renal dysplasia, renal cysts ¹ , renal agenesis ³ , horseshoe kidney ⁶	MODY5, Renal cysts and diabetes syndrome	<u>Distinct renal phenotypes based on specific human mutations</u>	dominant	(23, 85–89)
<i>INVS</i> (NPHP2)	Renal cysts ⁵ , tubular lesions	Nephronophthisis, situs inversus	<u>Role in early tubule morphogenesis</u>	het and homo	(62, 90)
<i>LHX1/XLI M1</i>	MCDK ¹	CAKUT	Important for proper renal development	N/A	(20, 87)

<i>LMX1β</i>	Renal cysts ¹ , microscopic haematuria, proteinuria	Nail-patella syndrome, nephrotic syndrome, nail-patella-like renal disease	Critical for glomus development, Found its position in gene regulatory network of podocyte specification	dominant	(80, 91–93)
<i>NEK8 (NPHP9)</i>	Renal cysts ⁵	Nephronophthisis, Meckel–Gruber syndrome	<u>Role in early tubule morphogenesis</u>	recessive	(62, 94)
<i>NPHP3</i>	Renal cysts ⁵ , tubular lesions	Nephronophthisis, <i>situs inversus</i> , Meckel–Gruber syndrome, Renal-Hepatic-Pancreatic Dysplasia	<u>Role in early tubule morphogenesis</u>	het and homo	(62, 95)
<i>NRIP1</i>	Renal hypo/dysplasia ⁴ , VUR ⁷	CAKUT	<u>Important for proper renal development</u>	dominant	(96)
<i>PAX2</i>	Renal hypoplasia ⁴ , VUR ⁷ , Renal-coloboma syndrome	Pallilorenal syndrome	Essential for tubule differentiation	dominant	(19, 97)
<i>PKD1</i>	Renal cysts ¹	ADPKD type 1	<u>Expressed in pronephros</u>	dominant	(67, 98, 99)
<i>PKD2</i>	Renal cysts ¹	ADPKD type 2	<u>Post-transcriptionally positively regulated by BicC via repression of miR-17</u>	dominant	(65, 100, 101)
<i>RET</i>	Renal agenesis ³	CAKUT, Hirschsprung disease	Expressed in pronephric duct	dominant	(102, 103)
<i>SALL1</i>	Renal hypodysplasia ⁴ , MCDK ¹ , PUV, UPJ obstruction, VUR ⁷	CAKUT, Townes-Brocks syndrome	Expressed in pronephros	dominant	(72, 104)
<i>SIX1</i>	Renal hypodysplasia ⁴	Branchio-oto-renal syndrome	<u>Potential <i>six1</i> gene targets expressed in kidney</u>	dominant	(105, 106)
<i>SIX2</i>	Renal hypodysplasia ⁴	CAKUT	Conserved enhancers regulate pronephros specific expression	dominant	(69, 107)
<i>SOX17</i>	VUR, UPJ obstruction ⁷	CAKUT	Important for endoderm formation	dominant	(108, 109)
<i>TSC1</i>	Kidney tumors ²	Tuberous sclerosis	Down regulated by miRNAs to control proximal tubule size	dominant	(110)
<i>WDPCP (FRITZ)</i>	Renal malformation, genital abnormalities	Bardet-Biedel syndrome	<u>Controls septin localization at cilia, linked mutations in human <i>wdpcp</i> to Bardet-Biedl and Meckel-Gruber syndromes</u>	recessive	(111, 112)
<i>WNT4</i>	Renal hypodysplasia ⁴	Mullerian aplasia and hyperabdrigenism, SERKAL syndrome	Patterns the proximal pronephric primordia, Regulated by notch, wt1 and sox11	dominant	(42, 43, 48, 49, 51)

<i>WT1</i>	Kidney tumors ²	Wilms-tumor type 1, Denys-Drash syndrome, Frasier syndrome, Nephrotic syndrome type 4	Key regulator of glomus development, Regulates wnt4 expression in the pronephros	dominant	(50, 51, 80)
------------	----------------------------	--	---	----------	--------------

Table 1. CAKUT Genes That Have Been Analyzed or Have Kidney Expression in *Xenopus*.

Colors and superscripts 1-7 correspond to the numbers found in Figure 5 (1, green; 2, magenta; 3, purple; 4, teal; 5, orange; 6, blue; 7, red). Underlined indicates studies were performed in *Xenopus* to validate that specific mutations cause human kidney phenotypes. CAKUT, congenital anomalies of the kidney and urinary tract; Het, heterozygous; Homo, homozygous; MCDK, multicystic dysplastic kidney; PUV, posterior urethral valves; UPJ, ureteropelvic junction obstruction; UVJ, ureterovesical junction obstruction; VUR, vesicoureteral reflux.

from an early stage embryo into a differentiated body plan (113, 114). This facilitates unilateral tissue-targeted injections that are specific to organs such as the kidney (115) and permits using the uninjected side as an internal control. In addition, researchers have developed assays to study kidney function in *Xenopus*.

Xenopus oocytes and early embryos can easily be injected with DNA, mRNA, protein, and/or morpholinos (MO) to overexpress or knock down proteins. A common assay in *Xenopus* involves disrupting genes/proteins in both kidneys by injecting MOs or CRISPR sgRNAs and Cas9 protein in both ventral cells of four-cell embryos. If the gene/protein is important for kidney formation, its loss will result in edema, characterized by swelling in the chest cavity due to fluid retention. This technique allows for disruption of the kidney while avoiding the heart and liver (xenbase.org), two other common causes of edema, generating tissue-targeted knockdown or knockout embryos. Upon edema formation researchers can then use an excretion assay, allowing visualization of the passage of fluorescent molecules through the kidney and out through the cloaca which can show if the kidneys are still functioning (28). Though not directly comparable to the Cre/loxP systems used in mouse studies, this edema assay, which is unique to *Xenopus*, allows for some evaluation of tissue specificity.

Knockdown of Pkd2, a protein involved in autosomal dominant polycystic kidney disease (ADPKD), in *Xenopus* embryonic kidneys results in edema (65). Similar edema phenotypes occur due to the loss of other proteins implicated in CAKUT such as Pax2 and Pax8 (19). These established techniques demonstrate that *Xenopus* possesses distinctive qualities suitable for disease modeling, and new

technologies continue to improve the experimental opportunities in this model system.

Genetic screens of the allotetraploid *Xenopus* are becoming more feasible with the development of the CRISPR/Cas9 system (116) and the ability to target CRISPR-mediated genetic manipulation to the kidney is unique to *Xenopus* (20). Additionally, inducible systems such as Gal4-UAS (117), Tet-On (118), heat-shock inducible (86, 89), and the Dex-inducible strategy (119) have been successfully used in *Xenopus* embryos, which allows for temporal or spatial control of gene expression. These tools make *Xenopus* a valuable model for studying the kidney, can aid in our understanding of the mechanisms through which the kidney develops, and can help identify new genes important for renal function.

1.5 Delineating Molecular Pathways Involved in Kidney Development Using *Xenopus*

Xenopus has been historically used to elucidate molecular mechanisms and signaling cascades involved in early developmental processes (120). More recently, *Xenopus* has been used to model various human genetic diseases (121). Importantly, *Xenopus* has played a vital role in identifying the function of genes that are involved in CAKUT.

Mutations in the RNA-binding protein BICC1, a negative Wnt regulator, result in a cystic kidney phenotype in mice and renal anomalies in patients (66). Prior studies in *Xenopus* indicate that Bicc1 inhibits the microRNA *miR-17*, preventing *miR-17* from destabilizing the *pkd2* transcript (65). This was demonstrated by

showing a rescue of the kidney phenotype when both *miR-17* and *Bicc1* were knocked down in tadpoles simultaneously (65). Interestingly, loss of the *Pkd1* gene product, polycystin-1, downregulates BICC1 expression in mouse kidneys and mouse cell lines (67). The connection between BICC1 downregulation and polycystin-1 loss in mice and *Bicc1* stabilizing *pkd2* mRNA in *Xenopus* suggests that disruption of *BICC1* may induce cystic phenotypes through polycystin signaling. Similarly, targeted deletion of *Hnf1 β* , a key transcription factor involved in kidney development, decreases *Bicc1* and *Pkd2* mRNA expression in the mouse kidney (88). HNF1 β in the mouse (88, 122) and BICC1 in mice and *Xenopus* (65) regulate the *Pkd2* transcript, and mutations in either gene can lead to kidney cysts in mouse models (23, 65). Thus, it is likely that these genes act through the same or similar pathways. *Xenopus* would be an ideal model for looking at the components of this pathway because molecular strategies to assess these components have already been established (64, 65).

Another common congenital kidney disease whose pathway has been elucidated using *Xenopus* is Nephronophthisis (NPHP). NPHP is a ciliopathy, which results in either abnormal formation or function of cilia. NPHP is a rare birth defect, but it is the most common cause of kidney failure, or end-stage renal disease (ESRD), in the first three decades of life (123). Studies in *Xenopus* linked several genes with NPHP or clarified components of the mechanism that causes the disease. First, targeted kidney knockdown of the Wnt signaling inhibitor *Invs* (Inversin/NPHP2) demonstrated that Inversin is important for morphogenetic cell movements during tubule elongation (124). This knockdown led to impaired ventral

proximal pronephros extension and distal tubule differentiation (124). Later, it was discovered that several genes that cause NPHP form a distinct complex that contributes to kidney development. In *Xenopus*, Anks6 was identified as an NPHP family member which assembles a protein complex of the NPHP-associated proteins Nek8, Inversin, and Nphp3 to regulate kidney development (62). This study showed that Anks6 localizes to the base of the cilium and that knockdown of its protein expression results in kidney anomalies (62). The study also linked *ANKS6* mutations in patients with a nephronophthisis-like clinical syndrome (62). Additionally, knockdown of either Anks6 or Nphp3 protein in *Xenopus* embryos results in edema, which suggests they may be important for kidney function (62). Likewise, edema in *Xenopus* has been shown to occur due to depletion of Invs protein (124).

Although *Xenopus* has helped uncover some of the causative NPHP genes and their role in kidney development and function, only ~40% of patients have a mutation in one of the 20 known NPHP-related genes (125, 126). A recent Genome-Wide Association Study has uncovered epigenetic signatures of chronic kidney disease including *NPHP4* (127). Some NPHP patients may suffer from epigenetic alterations of NPHP genes rather than a mutation in the gene itself. Future research using *Xenopus* may lead to the identification of new NPHP-causing genes and may uncover further epigenetic regulation of known genes as amphibians have been used to study epigenetics.

A notable CAKUT-causing gene encodes the transcription factor *LMX1 β* , where mutations can lead to Nail-patella syndrome, a rare cause of autosomal dominant ESRD (93). Additionally, mutations in *LMX1 β* can result in

glomerulopathies. Mouse studies suggest that *Lmx1 β* is necessary for the maintenance of podocytes, which are highly specialized cells that wrap around capillaries of the glomerulus and restrict the passing of macromolecules into the kidney (91). In *Xenopus*, *lmx1 β* is expressed in the glomus, which is analogous to the mammalian glomerulus, and is also known to have a role in podocyte specification (80, 92). MO knockdown of Lmx1 β protein in *Xenopus* showed that the glomus was reduced in size, and the development of the proximal tubules was reduced (92). Taken together, these studies demonstrate the usefulness of *Xenopus* in uncovering the role of proteins important for kidney development and function. Additionally, they show that *Xenopus* is capable of recapitulating specific kidney disease phenotypes found in humans.

1.6 Using *Xenopus* to Examine Human Genetic Variants

In human studies, missense mutations are often analyzed via software programs such as PredictSNP (128) and Meta-SNP (129). These programs predict the functional relevance of an amino acid change and suggest if they are likely to be pathogenic. One drawback of this method is the surprising data from 1000 Genomes indicating that people with predicted pathogenic variants do not suffer from the expected disease (130). *Xenopus* can be used to verify the pathogenicity and expressivity of potential disease-causing genetic variants *in vivo*.

Work in mouse models found that the ion channel protein CLCNKB is important for concentrating urine (131). In humans, *CLCNKB* mutations cause a salt-losing tubulopathy known as Bartter syndrome type III (73). Because *Xenopus*

oocytes are equipped with all of the necessary machinery for development upon fertilization they have been used broadly to study channel proteins. In fact, the first genotype/phenotype correlation for Bartter syndrome type III was validated by functional analyses of eight missense and two nonsense mutations in *Xenopus*. By performing voltage clamp experiments in *Xenopus* oocytes, it was found that nine of the ten mutations significantly decreased normal conductance (74), indicating altered salt homeostasis. This work verified that the reported human genetic mutations were, in fact, Bartter syndrome type III-causing mutations (74). Given the large number of ion channels present in the kidney, this system can be readily exploited to study patient mutations in various channels and their effects on conductance.

A similar study demonstrated that dysregulation of NRIP1-dependent retinoic acid signaling in both *Xenopus* and mouse disrupted kidney formation (96). In *Xenopus*, knockdown of Nrip1 protein causes kidney anomalies that can be rescued with wild-type human *NRIP1* mRNA but not with the truncated *NRIP1* mRNA identified in patients (96). *Xenopus* can also serve to assess the distinct effects of different mutations in a single gene.

HNF1 β mutations have been shown to manifest as distinct renal diseases in humans (85). An attempt to model these differences in *Xenopus* was successfully executed using different methods in two separate studies. In the first study, *Xenopus* transgenic lines expressing two different human *HNF1 β* mutants using a heat shock-inducible Cre/loxP system were generated. One transgenic line expressed an insertion mutation, while the other line expressed a deletion mutation. The deletion

led to reduced pronephric development, while the insertion enlarged the pronephros, with both phenotypes primarily affecting the proximal tubules (89). The second study compared nine different human *HNF1 β* mutations including indels (insertions/deletions), missense, and nonsense mutations by injecting mutant mRNA. The mutations led to distinct renal disease phenotypes in *Xenopus*, as they do in humans (85). In *Xenopus*, six of the mutants resulted in an enlargement of the pronephric structures, while the other three mutations led to a reduction or loss of the tubules and the anterior part of the duct (85). Additionally, a new transgenic line has the potential to make modeling human variants easier.

The *cdh17:eGFP* frog line has recently been developed in which GFP is expressed in the epithelium of the pronephros and mesonephros (132). This permits live imaging of the developing kidney, which can also be used to assess kidney disruption upon specific gene knock down/out without the need for immunostaining or *in situ* hybridization. This *Xenopus* line has the potential to streamline large-scale screens of kidney disease-causing genes and environmental factors that affect renal development. Also, bypassing the need to process embryos will expedite drug discovery screening in *Xenopus* (133), that may ultimately lead to clinical applications.

The above data demonstrate that the range of kidney phenotypes seen in *Xenopus* recapitulate the kidney phenotypes observed in humans. This potentially allows for a correlation between an observed patient phenotype with a specific mutation in the *HNF1 β* gene. Studies like these are an efficient way to identify pathogenic genetic variants and can represent the variation of expressivity seen in

patients. Additional variants found in the *DYRK1A* human gene have been examined using *Xenopus* and will be further discussed in Chapter 3.

1.7 DYRK1A

The dual-specificity tyrosine phosphorylation-regulated kinase (DYRK) family is composed of DYRK1A, DYRK1B, DYRK2, DYRK3, DYRK4 (134) and they phosphorylate their substrates at serine or threonine residues. DYRKs belong to the CMGC group of kinases, which includes cyclin-dependent kinases (CDKs), mitogen-activated protein kinases (MAPKs), glycogen synthase kinase-3 (GSK3), CDK-like kinases, serine/arginine-rich protein kinases, cdc2-like kinases, and RCK kinases (135). Most protein kinases function as molecular switches that require an upstream kinase to adopt an active conformation. The DYRK family is unique in that they do not require an upstream event, but rather they autophosphorylate on a tyrosine residue in their activation loop (135, 136), which earned them their name “dual-specific”. This autophosphorylation event allows them to maintain an active conformation, which makes DYRK’s extremely dose dependent. Another commonality to the DYRKs is that they contain a DYRK homology (DH) box just N-terminal to the kinase domain (135). Both DYRK1A and DYRK1B contain additional homology by having nuclear localization signals (NLS) and a PEST motif (135). DYRK1A is the only member that contains a histidine repeat motif and a serine/threonine-rich motif (135). Of all the DYRK family members, DYRK1A is the most well-studied (137).

DYRK1A is highly evolutionarily conserved and has been implicated in cell survival, differentiation, and neurogenesis (136, 138). DYRK1A has a different consensus sequence (RPXS/IP) (139) than DYRK2/3 (RXS/IP) (140) which gives them differences in the substrates that they phosphorylate (140). DYRK1A was first described in the literature in 1986, in *Drosophila* as minibrain, where it lead to a smaller brain size in flies (141). The mammalian homolog was not studied until almost a decade later (142) and shortly after that it was found to be a candidate gene for intellectual disability in Down syndrome because of its chromosomal location within the “Down syndrome critical region” (21q22.2) and its neurogenic defects in *Drosophila* (141, 143). Further studies have indicated that DYRK1A overexpression in Down syndrome is causative for intellectual disability (138, 144). Similarly, haploinsufficiency of DYRK1A causes intellectual disability, developmental delay, microcephaly, dysmorphic facial features, and seizures (145). Collectively, *DYRK1A* haploinsufficiency is known as DYRK1A-related intellectual disability syndrome (DYRK1A syndrome). Because DYRK1A is always catalytically active and loss or gain of a *DYRK1A* allele has severe phenotypic consequences, it is believed that DYRK1A may be controlled by subtle changes (146). There are several ways DYRK1A is transcriptionally regulated. It was found that Activator protein 4 is a transcriptional repressor of *DYRK1A* in non-neural cells. Also, the transcription factor E2F1 was shown to positively regulate *DYRK1A* by promoting enhancer activity (146, 147). Additionally, NFATc1 was found to upregulate DYRK1A in bone marrow macrophages which serves as a negative feedback loop given that DYRK1A maintains inactive NFAT (146). Furthermore, DYRK1A’s PEST motif suggests that it

may undergo rapid protein turnover, as PEST motifs are thought to act as a degradation tag for proteasomal destruction. One study demonstrated that in HEK293 cells DYRK1A has a half-life of 14 hours and that a conserved region in its N-terminus, not its PEST domain, was responsible for β TrCP-mediated degradation (147). Given that DYRK1A promotes cell cycle exit and therefore inhibits proliferation, dysregulation of DYRK1A may play a role in different disease states (147).

Because of its neurological implications DYRK1A has been heavily studied in the brain. There, it has been found to play a role in many different signaling pathways including calcium signaling, Sonic Hedgehog signaling, and canonical Wnt signaling (148–150). It also has been found to inhibit N-WASP *in vitro* and in the rat hippocampus which may disrupt cell migration by inhibiting filopodia formation (151). Due to DYRK1A's association with multiple neurological defects, it has only been studied in a handful of other tissues. But phenotypic clues from *DYRK1A* loss have lead us to look into the urogenital system. Whole exome sequencing has identified a cohort of 19 patients with DYRK1A syndrome that have increased prevalence of urogenital abnormalities (~73%) including renal agenesis and hypospadias. This prompted the start of my dissertation research: to understand if DYRK1A was the cause of this increased prevalence of CAKUT.

1.8 Approaches to Discover Novel CAKUT Genes

Monogenic disease only accounts for 14% of CAKUT cases (55). Genetic diagnosis of CAKUT is complicated by having genetic and phenotypic heterogeneity,

variable penetrance, and a high level of sporadic cases (53). A potential reason for the variability seen among patients with mutations in the same gene is dosage. Different mutations, such as those that affect DNA binding, could lead to a difference in protein expression of that gene during kidney development which could ultimately lead to phenotypic variability.

In the age of omics, exome-sequencing has identified many potential genes involved in CAKUT. An additional approach is through genome-wide analysis. In a recent study, genome-wide analysis of almost 3000 CAKUT patients identified 45 different genomic disorder-associated copy number variations (GD-CNV) at 37 loci (152). Interestingly, 6 of the loci were found in 65% of CAKUT patients, which are likely to code for regulators of urogenital development (152). Potentially, even more edifying is that specific urogenital anomalies and kidney malformations were associated with specific types of genomic changes. For instance, patients with vesicoureteral reflex and posterior urethral valves mostly had genomic duplications, whereas obstructive uropathies had mostly deletions, and horseshoe kidney and lower urinary tract malformations such as bladder anomalies were not associated with either (152). This could indicate that efforts in searching for vesicoureteral reflex pathologies should be spent looking for genes that are sensitive to gene dosage, whereas those looking for lower urinary tract malformations should focus on individual genetic mutations. This method can also identify non-coding sequences that may be important regulatory elements involved in kidney development (153). Additionally, this type of analysis may be able to identify specific pathways or genes that are involved with specific renal outcomes. For instance, a specific CNV may

mainly cause obstructive uropathies and a specific receptor or ligand was found within the CNV which could implicate a new pathway in ureter formation.

Because monogenic disease accounts for a fraction of CAKUT cases, epigenetic alterations are likely to play a role. Epigenetic alterations can be tested through assays such as ChIP-sequencing. One study compared samples of nephron tubules in healthy patients to those of patients with chronic kidney disease. They showed methylated regions that were different between the two groups overlapped with enhancer regions and contained binding motifs for transcription factors such as *SIX2*, which is essential for kidney development (154). Epigenetic alterations are reversible, but they are also sensitive to environmental factors.

There are several *in utero* environmental factors that are risk factors for developing CAKUT including maternal diabetes mellitus and maternal overweight/obesity (154). Additional environmental risk factors include fetal exposure to alcohol, tobacco, vitamin A deficiency, and maternal medication exposures such as ACE inhibitors and glucocorticoids (155–157). These environmental risk factors can lead to changes in epigenetic marks that may repress or activate genes during different stages of renal development which can lead to CAKUT.

Given the toolbox we now have to find novel CAKUT genes, more are likely to be implicated in pathogenesis in the future. Epigenetic analysis can elucidate our understanding of how important regulators of kidney genes are controlled during nephrogenesis. This type of dysregulation could ultimately affect the structure of the kidneys, ureter, nephrons or even the total nephron count. It would not be surprising

to find that dysregulation of gene dosage by epigenetic or environmental factors rather than genetic mutations may play a significant role in maintaining proper urogenital development.

1.9 Dissertation Summary

Congenital anomalies of the kidney and urinary tract account for 40–50% of pediatric chronic kidney disease worldwide. Although important advances have been made in basic nephrology research, there are still missing pieces in the molecular basis of kidney organogenesis. Being able to uncover novel genes and pathways involved will give us a better understanding of kidney development as a whole. Next-generation sequencing has uncovered many putative causal genes, including *DYRK1A*. A cohort of patients with *DYRK1A* intellectual disability syndrome which results from haploinsufficiency has a higher prevalence of CAKUT (73% of those assessed), including kidney defects. Using *Xenopus laevis* we found that *DYRK1A* is important for kidney development. Loss of *dyrk1a* in *Xenopus* leads to abnormal kidney formation, which can be rescued by adding wild-type human *DYRK1A* mRNA. Furthermore, we found that altered expression of *Dyrk1a* leads to altered canonical Wnt signaling during *Xenopus* embryogenesis. This may suggest *Dyrk1a* can alter Wnt signaling in other instances such as during nephrogenesis. This dissertation fills a major gap in understanding how CAKUT arises in *DYRK1A* syndrome patients and defines a novel protein involved in nephrogenesis and kidney disease.

CHAPTER 2: MATERIALS AND METHODS

This chapter is modified from Blackburn ATM, Bekheirnia N, Uma V, Corkins ME, Xu Y, Rosenfeld JA, Bainbridge MN, Yang Y, Liu P, Madan-Khetarpal S, Delgado MR, Hudgins L, Krantz I, Rodriguez-Buritica D, Wheeler PG, Al Gazali L, Mohamed Saeed Mohamed Al Shamsi A, Gomez-Ospina N, Chao HT, Mirzaa GM, Scheuerle AE, Kukolich MK, Scaglia F, Eng C, Rankin Willsey H, Braun MC, Lamb DJ, Miller RK, Bekheirnia MR. DYRK1A-related intellectual disability syndrome: a novel association with congenital anomalies of the kidney and urinary tract. *Genetics in Medicine*. 2019 July 2. <https://doi.org/10.1038/s41436-019-0576-0>. *Genetics in Medicine* establishes that authors retain copyright of their articles.

2.1 Constructs, Construct Design, and *In Vitro* Transcription

A pCS2-*Xenopus*-Dyrk1a-HA construct (158) was used in transcribing *Xenopus dyrk1a*. Cloning for adding a GFP tag was executed by generating PCR cDNA from a pCS2-*Xenopus*-Dyrk1a-HA construct (158) using a Bio-Rad C1000 Touch™ Thermal Cycler (Bio-Rad), following Addgene's protocol for PCR cloning. PCR with OneTaq (NEB) was used to amplify wild-type *Xenopus dyrk1a* excluding the nucleotides coding for the stop codon. Forward primer 5'-TTTGGATCCATGCATACAGGAGGAGAGAC-3' was used to create the control *dyrk1a* construct while forward primer 5'-TTTGGATCCATGA-GACTTGAAAGAGGACGATGCATACAGGAGGAGAGAC-3' was used to create the *dyrk1a* + 5' UTR construct, which added part of Dyrk1a's endogenous 5' UTR that is recognized by the Dyrk1a MO. The same reverse primer 5'-

TTTTTCTAGACGAGCTTGCCACAGGACTCTG-3' was used to generate both cDNA fragments. BamHI and XbaI were used to insert cDNA fragments into a pCS2-GFP vector, placing the construct immediately upstream and in-frame with a GFP tag. Cloning for the rescue experiment was executed by traditional cloning methods and PCR cloning. The wild-type human *DYRK1A* cDNA was cut from the pMH-SFB-DYRK1A construct (Addgene) and inserted into a pCS2-HA vector using XhoI and contains a gateway vector site 5' to the cDNA. PCR cloning was used to generate the *DYRK1A*^{R205*} variant. Site-directed mutagenesis was used to generate the *DYRK1A*^{L245R} variant. Forward primer 5'-AATGCGGAATTCAGACAAG-TTTGTACAAAAAGCAGGC-3' and reverse primer 5'-TAGAGGCTCGAGTCACACTTCTATC-TGTGCTTGATTGAG-3' were used to amplify the truncated cDNA plus the gateway vector site 5' to the cDNA from the wild-type human pCS2-HA-DYRK1A vector. Forward primer 5'-CTGTCCTACAACCGCTATGACTTGCTG-3' and reverse primer 5'-CAGCAAGTCATAGCGGTTGTAGGACAG-3' were used for site-directed mutagenesis. The truncated cDNA was then inserted into a pCS2-HA vector using EcoRI and XhoI sites. Prior to *in vitro* transcription, the reading frame of each construct was confirmed by Sanger sequencing (Eurofins). The cDNA templates were linearized for transcription using NotI. Capped mRNAs encoding the constructs were generated using the SP6 mMessage mMachine Kit (Thermo Fisher Scientific). The transcribed mRNA products were evaluated by a 1% agarose gel using RNA gel loading dye and by optical density (OD 280/260) obtained from a NanoDrop® ND-1000 Spectrophotometer (Thermo Fisher Scientific). For the p53 appendix, Mark E.

Corkins generated the two point mutant constructs, C742T, p53^{R248W} and C844T, p53^{R282W}, with site-directed mutagenesis from a wild-type human pCdna3-Flag-p53 vector with the following primers I designed: forward primer 5'-GGCGGCATGAA-CTGGAGGCCCCATCCTCACCATCAT-3' and reverse primer 5'-ATGGGCCTCCAG-TTCATGCCGCCCCATGCAGGAAG-3' were used to create p53^{R248W} while forward primer 5'-CCTGGGAGAGACTGGCGCACAGAGGAAGAGAATCT-3' and reverse primer 5'-TCTGTGCGCCAGTCTCTCCCAGGACAGGCACAAAC-3' were used to create p53^{R282W}.

2.2 Western Blots

Ten-twenty embryos were collected at various stages (159) to make protein lysates as previously described (160). One embryo equivalent of lysate was run in each well of a 7.5% or 10% SDS-PAGE gel. Protein was transferred onto a 0.45 µm PVDF membrane (Thermo Fisher Scientific) and blocked for 1 hour at room temp or overnight in KPL block (SeraCare) at 4°C. Blots were incubated one of the antibodies listed: rabbit anti-green fluorescent protein (anti-GFP) (1:500, iclLab), rabbit anti-β-catenin (1:1000, McCrea lab), mouse anti-HA (1:1000, Sigma 12CA5), anti-active β-catenin (1:1000, Cell Signaling 8814), mouse anti-p53 (1:1000, Abcam ab16465), mouse anti-Flag (1:1000, Sigma M2), or rabbit anti-glyceraldehyde 3-phosphate dehydrogenase (anti-GAPDH) (1:1000, Santa Cruz) for 3 hours at room temperature or for 24 hours at 4°C. Blots were washed with TBS-T, incubated in goat anti-rabbit or goat anti-mouse IgG horseradish peroxidase secondary antibody (1:3000; Bio-Rad) for 1 hour at room temperature, and washed again with TBS-T

prior to imaging with Bio-Rad ChemiDoc XRS+ (Bio-Rad) using SuperSignal West Pico PLUS Chemiluminescent Substrate (Thermo Fisher Scientific). To validate knockdown of protein expression by Dyrk1a MO or p53 MO, Western blot analysis was carried out on lysates derived from embryos injected at the single cell stage. Forty ng of either Dyrk1a morpholino 5'- TGCATCGTCCTCTTTCAAGTCTCAT-3' (Gene Tools LLC) (158), or standard morpholino 5'-CCTCTTACCTCAGTTACAA-TTTATA-3' (Gene Tools LLC) was co-injected with 1 ng mRNA (either *Xenopus dyrk1a* control, or *Xenopus dyrk1a* + 5' UTR) along with 1 ng membrane-RFP RNA (161). For p53 knock down, the same dose of 40 ng for either p53 MO 5'-GCCGGTCTCAGAGGAAGGTTCCATT-3' (Gene Tools LLC) or standard MO was injected into embryos and analyzed by Western blot. For p53 knockout, 500 ng of either sgRNA p53.1 5'- CTAGCTAATACGACTCACTATAgGTAACAGCTCCTG-TATGGGAgTTTTAGAGCTAGAAATAGCAAG-3' sgRNA p53.2 5'- CTAGCTAATACGACTCACTATAgCGCGGCTCCATTCTCCGGGCTAgTTTTAGAGCTAGAAATAGCAAG-3' or slc45a2 control 5'-CTAGCTAATACGACTCACTATAgTTACATAGG-CTGCCTCCAgTTTTAGAGCTAGAAATAGCAAG-3' plus 1 ug of Cas9 protein and a lineage tracer were injected into single cell embryos. Lysates were made from 10 embryos at stage 10-11. Underlined sequence is the guide sequence designed from CHOPCHOP.cbu.uib.no.

2.3 Design and Statistical Analyses

Error bars represent standard error of experiments that were repeated four to eight times. The total number of *Xenopus* embryos and significance are as follows:

(Figure 12F) Control: 166, Dyrk1a MO + β -gal: 125, Dyrk1a MO + *DYRK1A*: 140, Dyrk1a MO + *DYRK1A*^{R205*}: 94. * (asterisk) = p<0.001 comparing individual experimental groups to Standard MO + β -gal. # (pound sign) = p<0.006 comparing Dyrk1a MO + *DYRK1A* to Dyrk1a MO + *DYRK1A*^{R205*}. (Figure 12G) Control: 75, Dyrk1a MO + β -gal: 80, Dyrk1a MO + *DYRK1A*: 57, Dyrk1a MO + *DYRK1A*^{L245R}: 74. * (asterisk) = p<0.001 comparing Standard MO + β -gal to Dyrk1a MO + β -gal or Dyrk1a MO + *DYRK1A*^{L245R}. # (pound sign) = p<0.05 comparing Dyrk1a MO + *DYRK1A* to Dyrk1a MO + *DYRK1A*^{L245R}. As expected, no statistical difference was seen between Dyrk1a MO + β -gal and Dyrk1a MO + *DYRK1A*^{R205*} or Dyrk1a MO + *DYRK1A*^{L245R}. Statistical significance was established using a two-tailed T-test.

(Figure 12J) The graph demonstrates a significant difference in edema and kidney abnormalities in embryos injected with either Standard MO or Dyrk1a MO. Error bars represent standard error of experiments that were repeated three times. The total number of *Xenopus* embryos and significance are as follows: Dyrk1a MO: 114 total, 45 of which had edema, Standard MO: 97 total, 2 of which had edema. * (asterisk) = p<0.008 comparing Standard MO to Dyrk1a MO embryos with edema, defects in one, and defects in both kidneys. Statistical significance was established using a two-tailed T-test.

2.4 Study Participants

The index patient was seen in the Renal Genetics Clinic (RGC) at Texas Children's Hospital. Subsequently, patients who had exome sequencing in a clinical diagnostic laboratory (Baylor Genetics) were queried for *de novo* (except P1, P12,

and P15) pathogenic (except P10 [likely pathogenic], and P5, P7, and P17, called as variants of uncertain significance in the initial report) variants in *DYRK1A*. Inclusion criteria also included (1) variant confirmation using Sanger sequencing, and (2) lack of other variants that could explain the phenotype observed. Exclusion criteria included multiple additional candidate genes that may be related to the phenotype. The final size of our cohort after applying those filters was 19 patients. Clinical phenotype information was collected from initial exome sequencing requisition form or contacting referring physicians. The Institutional Review Board at Baylor College of Medicine approved the study protocol for the Protection of Human Subjects. Consent was obtained for clinical genetic testing/exome sequencing from each family participating in this study.

2.5 Exome Sequencing and Data Analysis

Exome sequencing was performed by previously published methods at Baylor Genetics (162–164). In brief, an Illumina paired-end precapture library was constructed with 1 ug of DNA, according to the manufacturer's protocol (Illumina Multiplexing_SamplePrep_Guide _- 1005361_D), with modifications as described in the BCM- HGSC Illumina Barcoded Paired-End Capture Library Preparation protocol (162). Four precaptured libraries were pooled and then hybridized in solution to the HGSC CORE design (52 Mb, NimbleGen) according to the manufacturer's protocol (NimbleGen SeqCap EZ Exome Library SR User's Guide Version 2.2), with minor revisions. Sequencing was performed in paired-end mode with the Illumina HiSeq 2000 platform, with sequencing-by-synthesis reactions extended for 101 cycles from

each end with an additional cycle for the index read. With a sequencing yield of 12 Gb, 92% of the targeted exome bases were covered to a depth of 20x or greater. Illumina sequence analysis was performed with the HGSC Mercury analysis pipeline (<https://www.hgsc.bcm.edu/-/software/mercury>), which moves data through various analysis tools from the initial sequence generation on the instrument to annotated variant calls (SNVs and intraread indels). Variant interpretation was performed according to the most recent guidelines published by the American College of Medical Genetics and Genomics (ACMG) (165). Accordingly, only variants that met strict criteria were called pathogenic. Sanger sequencing confirmed all variants reported in this dissertation.

2.6 Whole Mount *In Situ* Hybridization

A Digoxigenin-11-UTP RNA labeling kit was used to generate digoxigenin-labeled RNA probes for *in situ* hybridization. Digoxigenin-11-UTP labeled antisense RNA probe for *dyrk1a* was synthesized from *Xenopus* Genome Collection IMAGE clone 7687837 (166) using Sall restriction enzyme and T7 polymerase. This clone carries the *Xenopus tropicalis* coding sequence for *dyrk1a*, therefore both *X. tropicalis* and *X. laevis* embryos were stained to ensure proper detection of the target. RNA probe *atp1a1* was synthesized using SmaI restriction enzyme and T7 polymerase (167). Embryos were staged, fixed, and stained according to standard procedures (168, 169) using an anti-digoxigenin antibody (1:3000, Sigma 11093274910) and BM Purple (Sigma 11442074001).

2.7 *Xenopus laevis* Embryos and Microinjections

Xenopus eggs were obtained by standard means, placed in 0.3x MMR and fertilized *in vitro* (169). Blastula cleavage stages and dorsal versus ventral polarity were determined by established methods (168). Microinjections were targeted to the V2 blastomere at the eight-cell stage, which provides major contributions to the development of the pronephros (115, 168, 170). Ten nL of injection mix (described below) was injected into embryos. Ten ng of Dyrk1a morpholino 5'-TGCATCGT CCTCTTTCAAGTCTCAT-3' (171) or Standard morpholino 5'-CCTCTTACCTCAGTTACAATTATA-3' was co-injected with 50 pg mRNA (either control β -galactosidase, wild-type human *DYRK1A*, *DYRK1A*^{R205*}, or *DYRK1A*^{L245R}) along with 1 ng membrane-RFP mRNA (161) as a lineage tracer to verify that the correct blastomere was injected.

2.8 Immunostaining

Embryos were staged (168), fixed, and immunostained (172) using established protocols. Proximal tubule lumens were labeled with the antibody 3G8 (1:30, European *Xenopus* Resource Centre, Portsmouth, UK), while the cell membranes of distal and connecting tubules were labeled with antibody the 4A6 (1:5, European *Xenopus* Resource Centre) (173). Rabbit anti-red fluorescent protein (anti-RFP) (1:250, MBL International) antibody was used to detect the RFP tracer. Goat anti-mouse or anti-rabbit conjugated to Alexa Fluor 488 or Alexa Fluor 555 (1:500, Invitrogen) secondary antibodies were used to visualize antibody staining.

2.9 Imaging

Embryos used for *in situ* hybridization were imaged on a Zeiss AxioZoom V16 with a 1x objective, Zeiss 512 color camera (Zeiss), and extended depth of focus processing. Embryos used for immunostaining were scored and photographed using an Olympus SZX16 fluorescent stereomicroscope and Olympus DP71 camera (Olympus); 3G8/4A6 immunostained kidney images were taken using a Zeiss LSM800 confocal microscope (Zeiss). Fixed embryos were cleared with BABB/Murray's clearing solution for confocal imaging (1:2 volume of benzyl alcohol to benzyl benzoate). Images were processed with Adobe Photoshop.

2.10 Transgenic *Xenopus* Lines

Xla.Tg(actc1:GFP)^{Mohun} (NXR_0007) is a cardiac actin:GFP transgenic line where 580bp of *Xenopus laevis actc1b* gene drives GFP expression. GFP is found in the embryonic striated muscle. Expression can be seen in the somites, craniofacial structures, and the heart.

Xla.Tg(WntREs:dEGFP)^{Vlemx} (NXR_0064) also known as pbin7LEF-GFP/Wnt Reporter. The construct contains a minimal TATA box, a synthetic Wnt-responsive promoter which consists of 7 copies of a TCF/LEF1 binding DNA element, and a reporter gene which encodes destabilized EGFP and a polyA sequence. GFP expression consists of dynamic patterns of Wnt/ β -catenin signaling activity.

Xla.Tg(CMV:hist2h2be-RFP)^{Ueno} (NXR_0073). The construct contains a CMV promoter, *Xenopus laevis* Histone 2B, and RFP in a pCS2p+ plasmid. Histone 2B

drives the RFP expression, which is found only in the nucleus. RFP is found in all nuclei, but distinct RFP expression outlines the somites.

CHAPTER 3: DYRK1A-RELATED INTELLECTUAL DISABILITY SYNDROME: A NOVEL ASSOCIATION WITH CONGENITAL ANOMALIES OF THE KIDNEY AND URINARY TRACT

This chapter is modified from Blackburn ATM, Bekheirnia N, Uma V, Corkins ME, Xu Y, Rosenfeld JA, Bainbridge MN, Yang Y, Liu P, Madan-Khetarpal S, Delgado MR, Hudgins L, Krantz I, Rodriguez-Buritica D, Wheeler PG, Al Gazali L, Mohamed Saeed Mohamed Al Shamsi A, Gomez-Ospina N, Chao HT, Mirzaa GM, Scheuerle AE, Kukolich MK, Scaglia F, Eng C, Rankin Willsey H, Braun MC, Lamb DJ, Miller RK, Bekheirnia MR. DYRK1A-related intellectual disability syndrome: a novel association with congenital anomalies of the kidney and urinary tract. *Genetics in Medicine*. 2019 July 2. <https://doi.org/10.1038/s41436-019-0576-0>. *Genetics in Medicine* establishes that authors retain copyright of their articles.

3.1 Introduction

Intellectual disability and autism spectrum disorder (ASD) are heterogeneous neurodevelopmental disorders (NDDs) both clinically and genetically (174). Understanding NDDs is important, as they affect more than 3% of children worldwide (175). There over 1000 loci that attribute to NDDs and because of this genetic heterogeneity there are a limited number of recurrent mutations (175). Though a number of genes have been found to reoccur in NDDs, in 50% of cases the cause remains elusive (175). The advent of whole genome and whole exome studies have led to a significant number of *de novo* mutations in novel candidate genes (176). Between three studies with 8,400 individuals, mutations in *DYRK1A* accounted for 0.1%-0.5% of individuals with NDDs (145, 177–179).

The DYRK family of protein kinases are conserved across species from lower eukaryotes to mammals (135). DYRK family members are activated by autophosphorylating a tyrosine residue in their activation loop (136). DYRK1A is the most extensively characterized member of the DYRK family, which in humans, is encoded by the *DYRK1A* gene located in the Down syndrome critical region of chromosome 21 (137).

A growing body of literature implicates a strong causal relationship between *DYRK1A* haploinsufficiency and a recognizable syndrome known as DYRK1A-related intellectual disability syndrome (137, 145, 179). This syndrome is rare and was first described in medical literature in 2008 (rarechromo.org). In addition to ASD and intellectual disability, other frequently occurring features include intrauterine growth restriction, difficulty feeding with failure to thrive, microcephaly, seizures, dysmorphic facial features, and developmental delays (145), while additional phenotypic features are observed less commonly such as cardiac anomalies (145, 180). Though previous literature has reported incidental genitourinary findings including micropenis, hydronephrosis, pelvic kidney, renal cysts, and unilateral renal agenesis (180), no studies have explored if these anomalies are a direct result of *DYRK1A* loss.

This dissertation presents a cohort of individuals with *de novo* (when both parental samples available) *DYRK1A* single-nucleotide variants (SNVs) or small deletions ≤ 10 base pairs and defines CAKUT and genital defects in DYRK1A syndrome patients. I also provide supporting evidence using *Xenopus* embryos as a model that DYRK1A, which is expressed in embryonic nephrons, is required for

genitourinary development and that two pathogenic variants of human *DYRK1A* are likely responsible for the CAKUT/genital defects phenotype. Together, these findings support the investigation of potential CAKUT/genital defects in the clinical workup of patients with *DYRK1A*-related intellectual disability syndrome.

3.2 RESULTS

3.21 CAKUT/Genital Defects Identified in Patients with *DYRK1A* Variants

The index patient which prompted our research was seen in the Renal Genetics Clinic for the evaluation of intellectual disability, global developmental delay, hypospadias, and congenital chordee. Trio exome sequencing revealed a novel *de novo* pathogenic p.G168fs single base pair deletion in *DYRK1A*. A subsequent query of the exome sequencing database at Baylor Genetics revealed a total of 18 additional individuals with SNVs or deletions ≤ 10 base pairs (as defined in “Materials and Methods”) in *DYRK1A* among approximately 8000 probands. Phenotype and molecular information of these patients are summarized in Table 2 and Figure 6. Probands were mostly children ranging from 2 to 27 years of age. All 19 of these individuals had neurodevelopmental phenotypes consistent with loss-of-function of *DYRK1A* (MIM 614104). All referring physicians were subsequently contacted to obtain further details regarding the CAKUT/genital defect phenotypes. However, CAKUT/genital defect status of four patients remain unknown. Eleven of fifteen (73%) individuals with available information presented with CAKUT, including unilateral renal agenesis and/or genital defects including undescended testis and hypospadias (Table 3). One patient (P6) with unilateral renal agenesis was identified

Case #	Age	M/F	Ethnicity	Nucleotide change	AA change	Novel Variant	DF / FT T	F D	Microcephaly	Seizures	I D	D D	Renal/GU	ASD
P1*	2.3	F	Caucasian	c.452dup T	p.N151fs	-	+	+	+	-	ukn	M,S	+	ukn
P2*	3.3	M	Caucasian	c.461delA	p.K154fs	-	+	+	+	+	+	M,S	+	+
P3	9.5	F	Caucasian	c.489_495del	p.L164fs	+	+	+	+	+	+	M,S	+	+
P4	11	M	Hispanic	c.501delA	p.G168fs	+	-	+	+	+	+	G	+	ukn
P5	2	M	Caucasian	c.517G>T	p.V173F	+	+	+	+	+	ukn	S	nRUS	ukn
P6*	5.1	M	Not specified	c.613C>T	p.R205X	-	-	+	+	-	ukn	U	+	+
P7*	7	F	Vietnamese	c.734T>G	p.L245R	-	-	+	+	-	+	M,S	+	ukn
P8	20.5	M	Caucasian	c.787C>T	p.R263X	-	+	+	+	+	+	M,S	+	+
P9	5.7	M	Caucasian	c.986_995del	p.S329fs	+	+	+	+	+	+	G	+	+
P10	9.8	M	Middle Eastern	c.1042G>A	p.G348R	+	-	+	ukn	+	+	G	nRUS	ukn
P11	13.5	M	Not specified	c.1098+1G>A	N/A	-	-	+	+	+	ukn	G	ukn	+
P12	27.1	M	Not specified	c.1162dupG	p.A388fs	-	+	ukn	+	+	+	G	+	ukn
P13	14.8	F	Not specified	c.1217_1220del	p.K406fs	+	+	ukn	ukn	+	ukn	M	ukn	+
P14	13.8	F	Not specified	c.1309C>T	p.R437X	-	-	ukn	+	-	+	M,S	ukn	Ukn
P15	10.1	F	Hispanic	c.1309C>T	p.R437X	-	-	+	+	+	ukn	S	nRUS	ukn
P16	5.7	F	Filipino	c.1309C>T	p.R437X	-	-	+	+	+	+	G	nRUS	ukn
P17	19.6	F	Caucasian	c.1400G>A	p.R467Q	-	+	+	+	-	+	G	ukn	ukn

P18*	18.5	M	Caucasian	c.1399C> T	p.R467X	-	-	+	+	+	+	M ,S	+	+
P19	9.4	M	Hispanic	c.1478du pT	p.S494fs	+	uk n	+	+	+	+	M ,S	+	+

Table 2. Demographics, Molecular Data, and Phenotype of 19 Patients with SNVs and Small Indels (<10bp) in *DYRK1A* Identified by Clinical Exome Sequencing.

ASD: Autism spectrum disorder (HP:0000717), DD: Developmental delays; Global (G; HP:0001263), Motor (M; HP:0001270), Speech (S; HP:0000750), Unspecified (U), DF/FTT: Difficulty feeding (HP:0011968)/ failure to thrive (HP:0001508), FD: Facial dysmorphism (HP:0001999), GU: Genitourinary; Normal renal ultrasound: nRUS, Unknown: ukn, + denotes phenotype observed (see Table 3 for more details), ID: Intellectual disability (HP:0001249). M/F: male/female. Note that the age is in years. * Denotes published patients. Used with permission from Reza and Nasim Bekheirnia, who made the table. Rachel Miller and I edited the table.

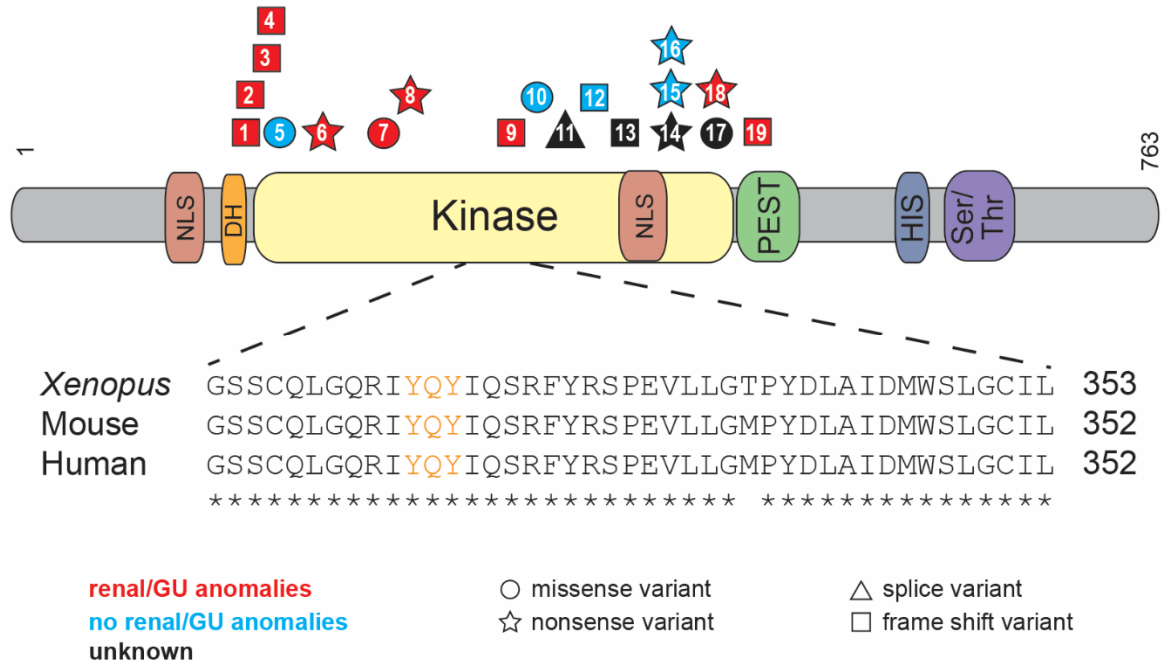


Figure 6. Congenital Anomalies of the Kidney and Urinary Tract (CAKUT) Associated with *DYRK1A* Variants in Patients with *DYRK1A*-Related Intellectual Disability Syndrome.

Schematic shows the *DYRK1A* protein domains. Shapes, which identify the type of variant (squares = frame shift variants, circles = missense variants, stars = nonsense variants, triangles = splice variants), are positioned where *DYRK1A* patient variants impact the amino acid sequence. Patient variants are labeled by patient number as listed in Tables 2 and 3. Variants that result in CAKUT are red, those that do not result in CAKUT are blue, and those in which the effects on CAKUT status are unknown are black. Protein domains are abbreviated as follows: DH; DYRK homology box; HIS histidine; NLS nuclear localization signal; PEST proline (P), glutamic acid (E), serine (S), and threonine (T); Ser/Thr serine/threonine. Inset shows highly conserved sequence surrounding the activation loop (labeled in orange) of the kinase domain. GU; genitourinary. Used with permission from Rachel Miller who made the figure.

Case #	SNV	Segregation	Renal or GU Phenotype
P1	p.N151fs	Mother negative, father's sample unavailable	Mild unilateral pelviectasis (HP:0010946) and frequent UTIs (HP:0000010)
P2	p.K154fs	<i>De Novo</i>	Genital anomalies (HP:0000078)
P3	p.L164fs	<i>De Novo</i>	Kidney abnormalities (not specified; HP:0000077)
P4	p.G168fs	<i>De Novo</i>	Hypospadias (HP:0000047), micropenis (HP:0000054), and congenital chordee (HP:0000041)
P5	p.V173F	<i>De Novo</i>	Renal ultrasound is normal with normal genitalia on exam
P6	p.R205X	<i>De Novo</i>	Left renal agenesis (HP:0000122)
P7	p.L245R	<i>De Novo</i>	Left renal agenesis (HP:0000122)
P8	p.R263X	<i>De Novo</i>	Shawl scrotum (HP:0000049) and history bilateral orchiopexy (HP:0000028)
P9	p.S329fs	<i>De Novo</i>	Hypospadias (HP:0000047) and kidney abnormalities (tiny echogenic foci)
P10	p.G348R	<i>De Novo</i>	Normal renal ultrasound
P11	c.1098+1G>A	<i>De Novo</i>	Unknown
P12	p.A388fs	Mother negative, Father is mosaic	Frequent UTI (HP:0000010)
P13	p.K406fs	<i>De Novo</i>	Unknown
P14	p.R437X	<i>De Novo</i>	Unknown
P15	p.R437X	Mother negative, father's sample unavailable	Normal renal ultrasound
P16	p.R437X	<i>De Novo</i>	Normal renal ultrasound
P17	p.R467Q	<i>De Novo</i>	Unknown
P18	p.R467X	<i>De Novo</i>	Orchiopexy (HP:0000028) and inguinal hernia (HP:0000023)

P19	p.S494fs	<i>De Novo</i>	Bilateral inguinal hernias (HP:0000023) but no renal ultrasound
-----	----------	----------------	---

Table 3. Available information About Genitourinary Phenotype of Patients Reported in This Study.

Eleven patients have genitourinary phenotype. This strongly suggests an important role for DYRK1A in genitourinary tract development. Used with permission from Reza and Nasim Bekheirnia, who made the table. Rachel Miller and I edited the table.

after this newly acquired association of DYRK1A with CAKUT was discussed with the referring physician (181). The probability of loss-of-function intolerance (pLI) score of *DYRK1A* is 1, indicating that this gene is intolerant to loss-of-function variants (182).

3.22 A Majority of the Variants Found in *DYRK1A* Are Loss-of-Function and are Found in the Kinase Domain

Many of the variants found in this cohort are found in the kinase domain (14/17 [82%]), which spans from residues 159 to 479, and 11/17 (65%) are thought to undergo nonsense-mediated decay (NMD), as they result in premature stop codons (<https://nmdpredictions.shinyapps.io/shiny/>) (Figure 6). Of the remaining six variants, one affects splicing, one escapes NMD (p.S494fs), and four are missense variants. The four missense variants are all found in the kinase domain in four individuals. Of these four individuals with missense variants, P7 was diagnosed with unilateral renal agenesis (p.L245R), P5 and P10 had normal renal ultrasounds (p.V173F and p.G348R), and P17 has an unknown CAKUT status (R467Q). Because these variants still lead to other DYRK1A syndrome features such as intellectual disability, they may be important for the catalytic activity or conformational stability of DYRK1A. In fact, in a separate DYRK1A structural study the R467Q variant was found to be a part of a network of electrostatic interactions thought to play a role in the stability of the DYRK1A protein (183). Additionally, the L245R variant was found to prevent autophosphorylation of DYRK1A's activation loop in HEK293 cells (184) and was shown to be catalytically inactive via an *in vitro*

kinase assay (185). Of the three variants not found in the kinase domain, two are just N-terminal (N151fs, K154fs) and the last is found just C-terminal (to kinase domain) in the PEST domain (S494fs). Although theoretically all variants that are more N-terminal should result in NMD, a majority of the variants reside in the kinase domain for unknown reasons that should be studied further.

3.23 *Xenopus laevis* as a Model of Genitourinary Development

DYRK1A's amino acid sequence is highly conserved among amniotes (<https://www.ncbi.nlm.nih.gov/homologene>). Even though the N- and C-terminal regions diverge in invertebrates, the amino acid sequence of the kinase domains are similar indicating the importance of this protein throughout evolution. To model CAKUT associated with human *DYRK1A* loss-of-function variants using *Xenopus* embryos, I first analyzed the conservation of the whole DYRK1A protein sequence, focusing on the kinase domain. Human and *Xenopus* DYRK1A proteins are 91.3% identical over the entire amino acid sequence (Figure 7A). Additionally, the kinase domain, which is where a majority of the variants that cause CAKUT in this study are found, is 97.5% identical to the human protein (Figure 7A). Importantly, the human and *Xenopus* kinase activation loop sequence, which are essential for the kinase activity of DYRK1A, are identical.

Xenopus is a great model for many reasons. Their embryonic kidney, the pronephros, can easily be visualized and imaged through a transparent epidermis, and they develop a fully functional kidney in ~56 hours (15). *Xenopus* was chosen

Figure 7. Human and *Xenopus laevis* Protein Alignment and Short and Long *Xenopus* Homeolog Alignment for *dyrk1a* 5'UTR.

(A) Human *DYRK1A* mRNA transcript variant 1 (NM_001396.4) and *Xenopus laevis* *dyrk1a* short homeolog mRNA (NM_001163197.1) were translated and aligned using Clustal Omega. The overall identity between the protein sequences is 91.3% while the kinase domain has 97.5% identity demonstrating that *DYRK1A* is highly conserved. Grey shading represents the kinase domain of *DYRK1A*. Symbols reflect Clustal Omega's analysis of the residues and examples of specific residue groups that reflect each symbol can be found at their website <https://www.ebi.ac.uk/Tools/msa/clustalo/>. An * (asterisk) indicates positions with a fully conserved residue. A : (colon) indicates conservation between groups of strongly similar properties. A . (period) indicates conservation between groups of weakly similar properties. *DYRK1A* encodes a protein of 763 or 754 amino acid residues which results from alternative splicing with the longer isoform representing the canonical sequence shown above. *Xenopus* is missing residues 70-78 which are the same residues the short isoform of human *DYRK1A* (754 amino acids) is missing. This suggests that *Xenopus* most likely expresses an isoform of *DYRK1A* that is orthologous to the short isoform (NM_001347721.2) in humans. (B) Alignment of *dyrk1a*'s 5'UTR demonstrate in grey shading where the morpholino targets and that it hits both long and short homeologs in *Xenopus*. Underlined text represents the coding sequence of *dyrk1a*. The *Dyrk1a* MO was designed against the short homeolog of *dyrk1a* (top sequence), however, here it is shown it targets both the short and long (bottom sequence) (identified via a BLAT search of Crick <http://genomes.crick.ac.uk/>). The MO does not target *dyrk1a.2* which appears to be a duplication of *dyrk1a* with amino acid conservation only maintained in the kinase domain.

because it is an established model of nephron development, and gene expression studies demonstrate that the developing *Xenopus* nephron is anatomically and functionally similar to the mammalian nephron (13, 28, 186). The embryonic pronephros is the precursor to the mesonephric and metanephric kidney in mammals, and subsequent genitourinary development is dependent upon this structure (Figure 1). Specifically, as the pronephros extends toward the cloaca, the mesonephric nephrons form adjacent to the elongating nephric duct, also known as the Wolffian duct (Figure 1) (187). The ureteric bud, which is required for the development of the collecting duct system in mammals, then branches from this duct. Because the Wolffian duct is required for genitourinary development in males and Müllerian duct elongation, which is necessary for normal female anatomy, depends upon the development of the Wolffian duct (188, 189), the development of the pronephros is critical to both renal and genital development in mammals. Thus, although it is not a well-established model for studying genital formation, the *Xenopus* pronephros is essential for development of the mesonephric/Wolffian duct and subsequently the Müllerian duct, which are required for genitourinary development (190, 191).

3.24 *dyrk1a* is Expressed in the *Xenopus* Kidney and *in Vivo* Knockdown Demonstrates its Role in Kidney Development.

To assess whether *dyrk1a* is expressed in the *Xenopus* kidney, *in situ* hybridization was performed across developmental stages in both *X. laevis* and *X. tropicalis* (Figure 8). *dyrk1a* expression is seen in the pronephros in several stages

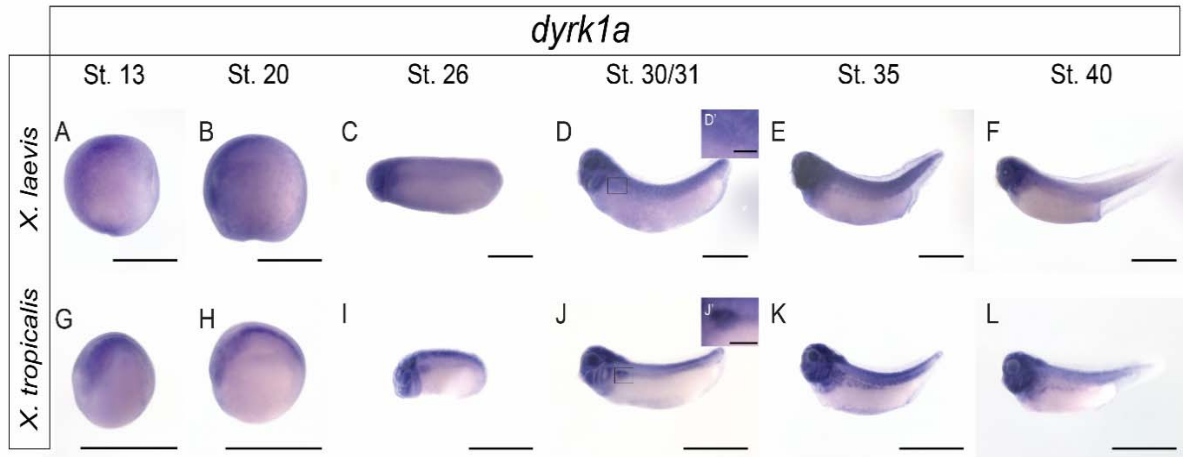


Figure 8. *In situ* Hybridization of *Dyrk1a* Across Developmental Stages Demonstrates Kidney Expression in *X. laevis* and *X. tropicalis*.

To demonstrate spatial-temporal expression of *dyrk1a* in the kidney, *in situ* hybridization was performed. Given that the RNA probe was designed against the *X. tropicalis* sequence, both species were analyzed. Pronephric kidney development occurs between stages 12.5 and 40, which is demonstrated in A-F for *Xenopus laevis* and G-I for *Xenopus tropicalis*. Expression of *dyrk1a* can be visualized in stage 26-40 embryos suggesting Dyrk1a may be important for kidney development. For clarity, insets (D' and J') for stage 30/31 tadpole kidneys with 200 μm scale bars have been added. All other scale bars represent 1000 μm . Used with permission from Helen Wilsey and Yuxiao Xu, who made the figure. I made editions to the figure, as well.

of both *X. laevis* and *X. tropicalis*, a closely related species to *X. laevis*, during kidney development, suggesting that it may be important for nephrogenesis. Furthermore, Dyrk1a protein expression can be seen in the kidney in later stage *Xenopus* tadpoles (Figure 9) which may suggest it is important for kidney maintenance.

To examine *dyrk1a*'s role in renal development in *Xenopus laevis*, an antisense MO that blocks translation was used to knock down endogenous Dyrk1a protein expression. *Xenopus laevis* has two copies of the *dyrk1a* gene because of its allotetraploid genome. Both *dyrk1a* transcripts are targeted by the Dyrk1a MO used in this study (Figure 7B). Two constructs, a control and the experimental construct, were generated with a GFP tag to demonstrate that the MO targets the endogenous 5' untranslated region of *dyrk1a*'s transcript (Figure 10A). Western blot analysis was then used to confirm that the MO correctly targets *Xenopus dyrk1a* mRNA (Figure 10B). Furthermore, knockdown experiments were used to determine whether loss of Dyrk1a function in *Xenopus* results in disruption of kidney development. Embryos were injected in a single V2 blastomere to target a single kidney, leaving the other as an internal control. First, Knockdown with the Dyrk1a MO resulted in loss of proximal tubule convolution by *in situ* hybridization with late kidney marker NA+K+-ATPase (Figure 11B). In addition, Dyrk1a knockdown resulted in abnormal pronephroi when immunostained with antibodies 3G8 and 4A6, which label the proximal tubules and the distal and connecting tubules (nephric duct), respectively (Figure 12B). Loss of Dyrk1a primarily lead to loss of the proximal and distal tubules, with defects in the connecting tubules (nephric duct) occurring only in

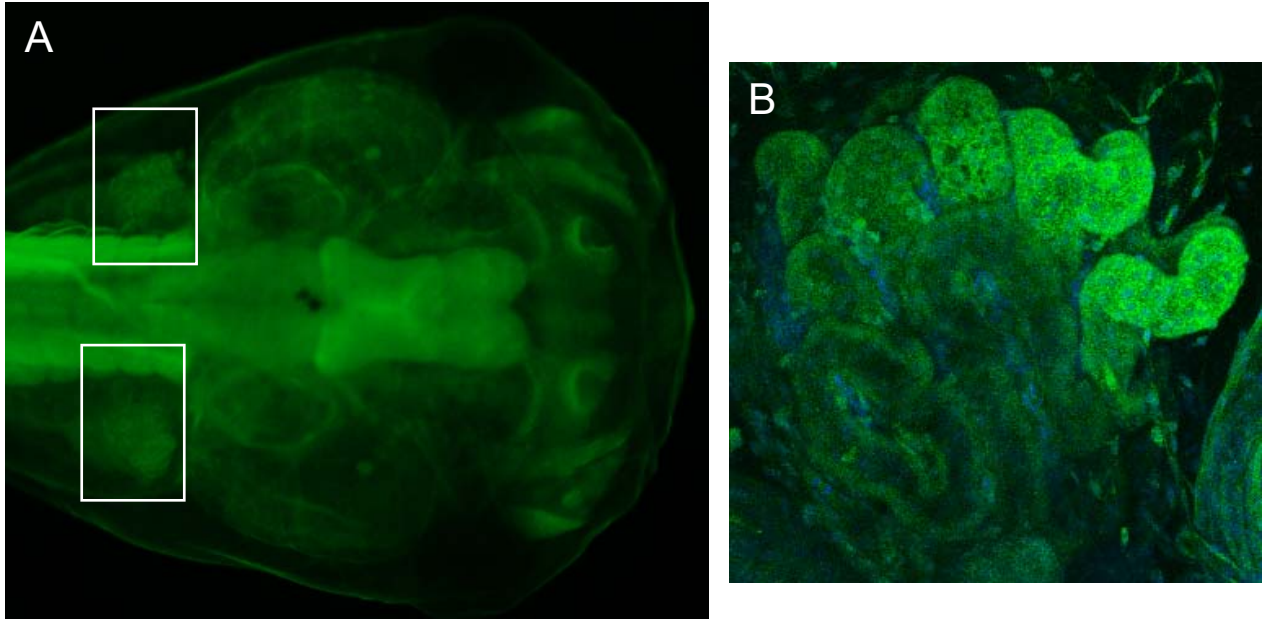


Figure 9. Immunofluorescence of Dyrk1a in *Xenopus laevis* at Stage 47 Demonstrates it is Expressed in the Kidney.

(A) Immunofluorescence shows that the Dyrk1a protein is expressed in later stages of tadpoles in the brain, craniofacial structures, and the kidney (outlined by white rectangles) by dissection scope. (B) Confocal microscopy further demonstrates that Dyrk1a is localized to the cytoplasm at this stage and does not co-localize with DAPI which stains the nucleus.

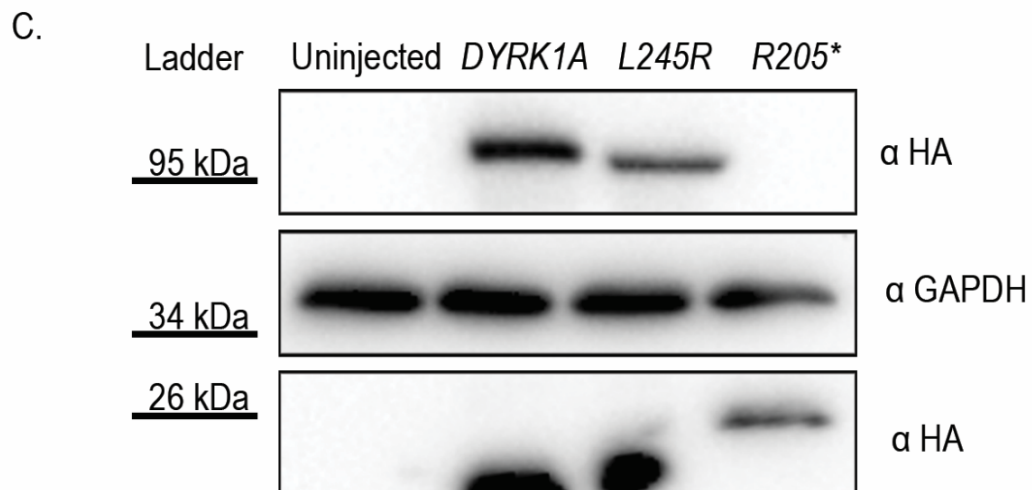
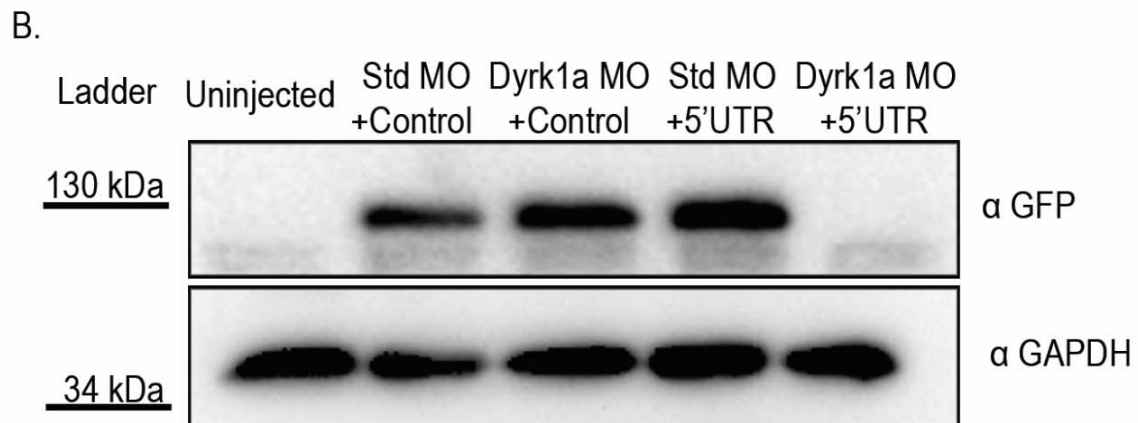
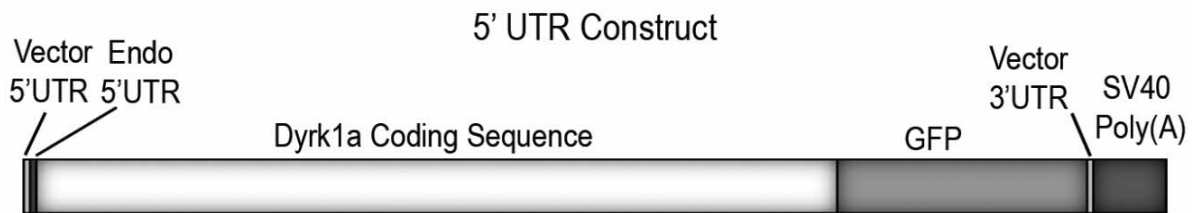
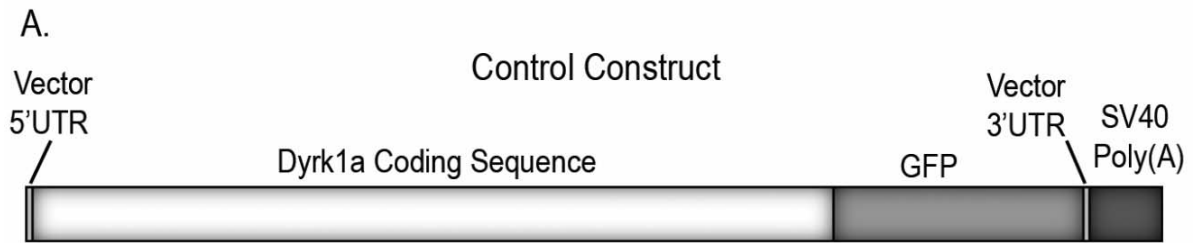


Figure 10. The Dyrk1a MO Correctly Targets *Xenopus dyrk1a* mRNA and Wild-Type, Missense, and Truncated Human DYRK1A Proteins are Expressed in Neurula Stage *Xenopus* Embryos.

Two constructs were generated with a GFP tag to demonstrate that the MO targets the endogenous 5' untranslated region (UTR) of *dyrk1a*'s transcript. (A, bottom) Schematic demonstrates that the 5' UTR construct contains part of *dyrk1a*'s endogenous (endo) 5' UTR that is recognized by the Dyrk1a MO (A, top) while the control construct does not. (B) Single-cell embryos were injected with 10 ng of either Dyrk1a MO or Standard MO (Std MO) and co-injected with 1 ng mRNA (either *Xenopus dyrk1a* control, or *Xenopus dyrk1a* + 5' UTR). Western blot analysis demonstrates complete reduction of GFP protein levels, indicative of loss of exogenous Dyrk1a in neurula stage embryos injected with Dyrk1a MO and *dyrk1a* + 5' UTR mRNA (lane 5) compared to the Standard MO and *dyrk1a* + 5' UTR (lane 4) and Standard MO or Dyrk1a MO and *dyrk1a* control mRNA (lane 2, lane 3). GAPDH was used as a loading control. (C) Wild-type human *DYRK1A* cDNA was inserted into a pCS2-HA vector. *DYRK1A*^{R205*} and *DYRK1A*^{L245R} variants were generated from the wild-type human pCS2-HA-DYRK1A vector. Western blot demonstrates HA protein is present in wild-type, missense (lanes 2 and 3 ~95 kDa), and truncated *DYRK1A*^{R205*} (lane 4 ~25 kDa) lanes, demonstrating *Xenopus* neurula stage embryos can successfully translate human *DYRK1A* mRNA. GAPDH was used as a loading control. Bar under the molecular weight indicates its position on the blot.

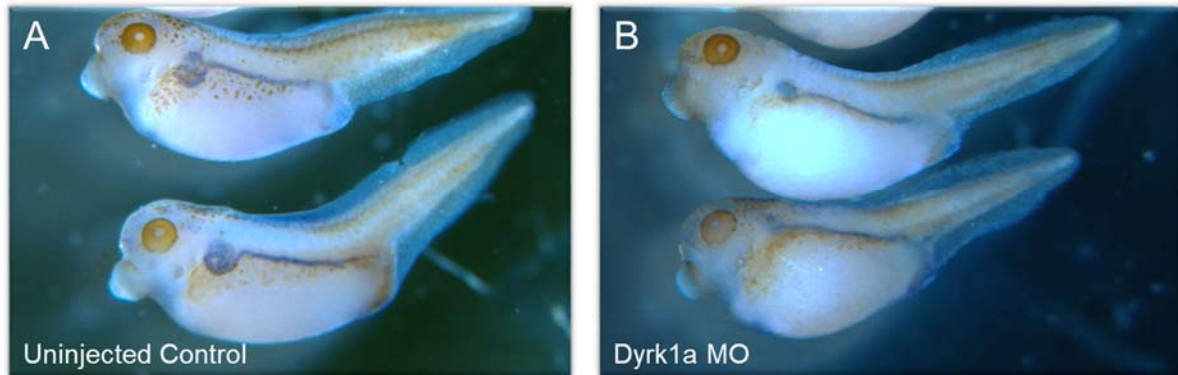


Figure 11. Dyrk1a Knockdown Disrupts Late Kidney Marker Na⁺K⁺-Atpase (*atp1a1*) in *Xenopus*.

Embryos were unilaterally injected at the 8-cell stage with 10 ng of Dyrk1a MO and compared to uninjected embryos. *In situ* hybridization was performed on stage 40 tadpoles which were probed with the late kidney marker Na⁺K⁺-Atpase (*atp1a1*) which binds to the entire kidney. (A) Uninjected kidneys appear normal whereas (B) distinct proximal tubule loss can be seen in embryos injected with the Dyrk1a MO.

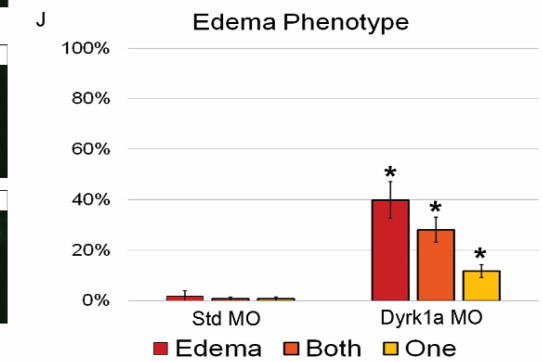
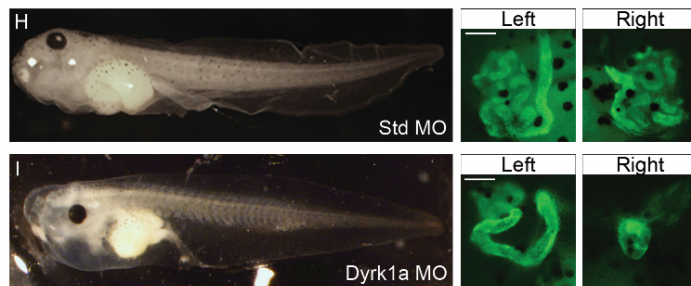
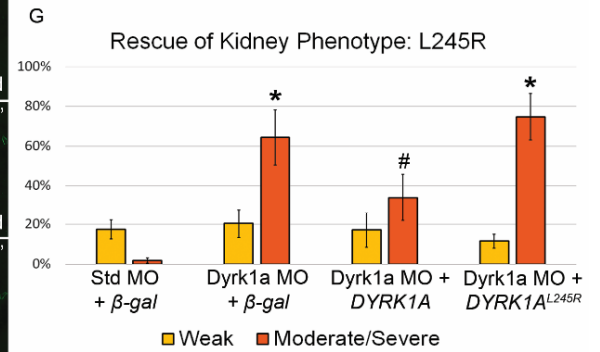
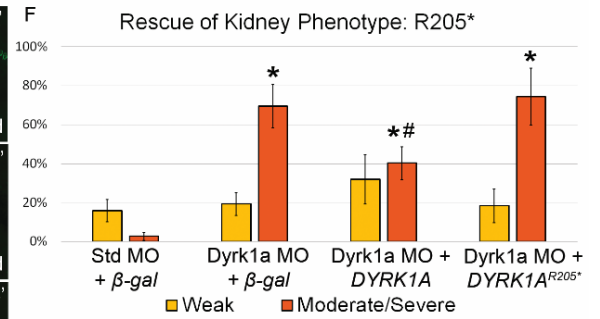
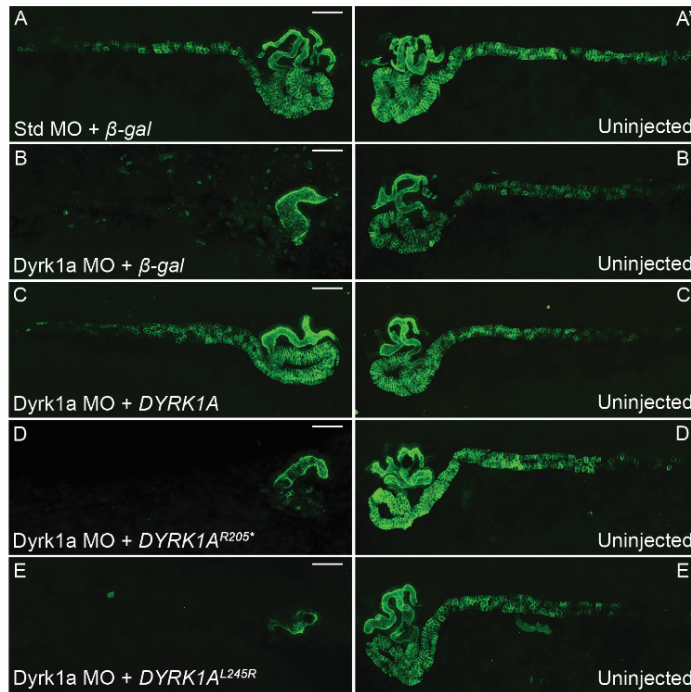


Figure 12. Loss of Dyrk1a results in Kidney Anomalies in *Xenopus laevis*.

(A'–E') Embryos were unilaterally injected at the 8-cell stage with 10 ng of Dyrk1a MO or standard MO (Std MO) along with 50 pg β -galactosidase (β -gal), wild-type, *DYRK1A*^{R205*}, or *DYRK1A*^{L245R} mRNA. Stage 40 tadpoles were stained with kidney antibodies 3G8, which labels the proximal tubules, and 4A6, which labels the distal and connecting tubules. Letters without apostrophes (A–E) represent the injected side, whereas letters with apostrophes (A'–E') represent the uninjected side. (B) Knockdown with a translation-blocking Dyrk1a MO disrupts kidney development, which can be partially rescued (C) by co-injecting with wild-type human *DYRK1A* mRNA but not (D–E) *DYRK1A*^{R205*} or *DYRK1A*^{L245R} mRNA. (A) Co-injection of a standard MO and β -gal serves as a negative control. Scale bars represent 100 μ m. (F) The graph demonstrates a significant difference between embryos injected with either Dyrk1a MO+ β -gal or Dyrk1a MO+*DYRK1A*^{R205*} versus with Dyrk1a MO+*DYRK1A* suggesting successful rescue with human *DYRK1A* but not with the nonsense mRNA. (G) The second graph demonstrates a significant difference between embryos injected with Dyrk1a MO+*DYRK1A*^{L245R} versus with Dyrk1a MO+*DYRK1A*, which suggests that the missense mRNA also fails to rescue the kidney phenotype. Significance was established against embryos that had a moderate or severe kidney phenotype (orange bar) and excluded embryos that had a weak phenotype (yellow bar). (F) Asterisk (*) indicates $p < 0.001$ comparing individual experimental groups with standard MO+ β -gal. Pound sign (#) indicates $p < 0.006$ comparing Dyrk1a MO+*DYRK1A* with Dyrk1a MO+*DYRK1A*^{R205*}. (G) Asterisk (*) indicates $p < 0.001$ comparing standard MO+ β -gal with Dyrk1a MO+ β -gal or Dyrk1a MO+*DYRK1A*^{L245R}. Pound sign (#) indicates $p < 0.05$ comparing Dyrk1a MO+*DYRK1A* with Dyrk1a MO+*DYRK1A*^{L245R}. For edema assays, embryos were injected at the 4-cell stage in both ventral cells to target both kidneys while avoiding the dorsal cells fated to become the heart and liver, which can also lead to edema. (H) Embryos injected with the standard MO did not develop edema while embryos injected (I) with the Dyrk1a MO did develop edema and also suffered from abnormal kidney formation. (J) The graph demonstrates a significant difference in edema and kidney abnormalities in embryos injected with either standard MO or Dyrk1a MO. Asterisk (*) indicates $p < 0.008$ comparing standard MO with Dyrk1a MO embryos with edema, defects in one, and defects in both kidneys. Error bars represent standard error. For ease of comparison of (n) and p-values across conditions, please refer to Tables 4–6.

Figure 12F	Standard MO + β -gal	Dyrk1a MO + β -gal	Dyrk1a MO + WT DYRK1A	Dyrk1a MO + DYRK1A R205*
<i>Xenopus</i> embryo	166	125	140	94
Standard MO	1	3.42E-08	0.0008	5.98E-07
Dyrk1a MO		1	0.0051	0.5867
Dyrk1a MO			1	0.0055
Dyrk1a MO				1

Table 4. Figure 12F p-values for each experimental condition as determined by two-tailed T-test.

Figure 12G	Standard MO + β -gal	Dyrk1a MO + β -gal	Dyrk1a MO + WT DYRK1A	Dyrk1a MO + DYRK1A L245R
<i>Xenopus</i> embryo	75	80	57	74
Standard MO	1	0.0006	0.1449	0.0003
Dyrk1a MO		1	0.0649	0.7735
Dyrk1a MO			1	0.0457
Dyrk1a MO				1

Table 5. Figure 12G p-values for each experimental condition as determined by two-tailed T-test.

	Standard MO	Dyrk1a MO
<i>Xenopus</i> embryo (n)	97	114
Edema (n)	2	45
2 abnormal kidneys	0	31
1 abnormal kidney (n)	1	14

Table 6. *Xenopus* embryos used for edema experiment.

embryos with a more severe phenotype.

3.25 Variants Identified in DYRK1A-Related Intellectual Disability Syndrome

Fail to Rescue Dyrk1a Loss-of-Function in *Xenopus*

To assess if patient DYRK1A variants lead to pronephric anomalies as they do in *Xenopus*, rescue experiments were carried out upon MO-mediated Dyrk1a knockdown in *Xenopus*. To express human DYRK1A in *Xenopus*, three constructs with HA tags were generated: wild-type human *DYRK1A*, a truncating patient variant *DYRK1A*^{R205*}, and a missense patient variant *DYRK1A*^{L245R}. Western blot analysis was used to confirm that the wild-type human *DYRK1A* and *DYRK1A*^{L245R}, ~95 kDa, and the truncated human *DYRK1A*^{R205*} mRNA constructs, ~25 kDa, could be successfully expressed in *Xenopus* (Figure 10C). Overexpression of the rescue dose (50 pg) of either *β-galactosidase* (*β-gal*), wild-type *DYRK1A*, *DYRK1A*^{R205*}, or *DYRK1A*^{L245R} mRNA demonstrated no gain-of-function phenotype of either DYRK1A variant (Figure 13). The kidney anomalies caused by Dyrk1a knockdown were partially rescued by co-injecting wild-type human *DYRK1A* mRNA (Figure 12C). However, neither *DYRK1A*^{R205*} or *DYRK1A*^{L245R} mRNA rescued these anomalies (Figure 12D, E). Due to many factors, rescue experiments rarely give a full rescue. Therefore, significance for Figure 12 was established against embryos that had a moderate or severe kidney phenotype (orange bar) and excluded embryos that had a weak phenotype (yellow bar). Detailed descriptions of how embryos kidney severities are scored can be found in Figure 14.

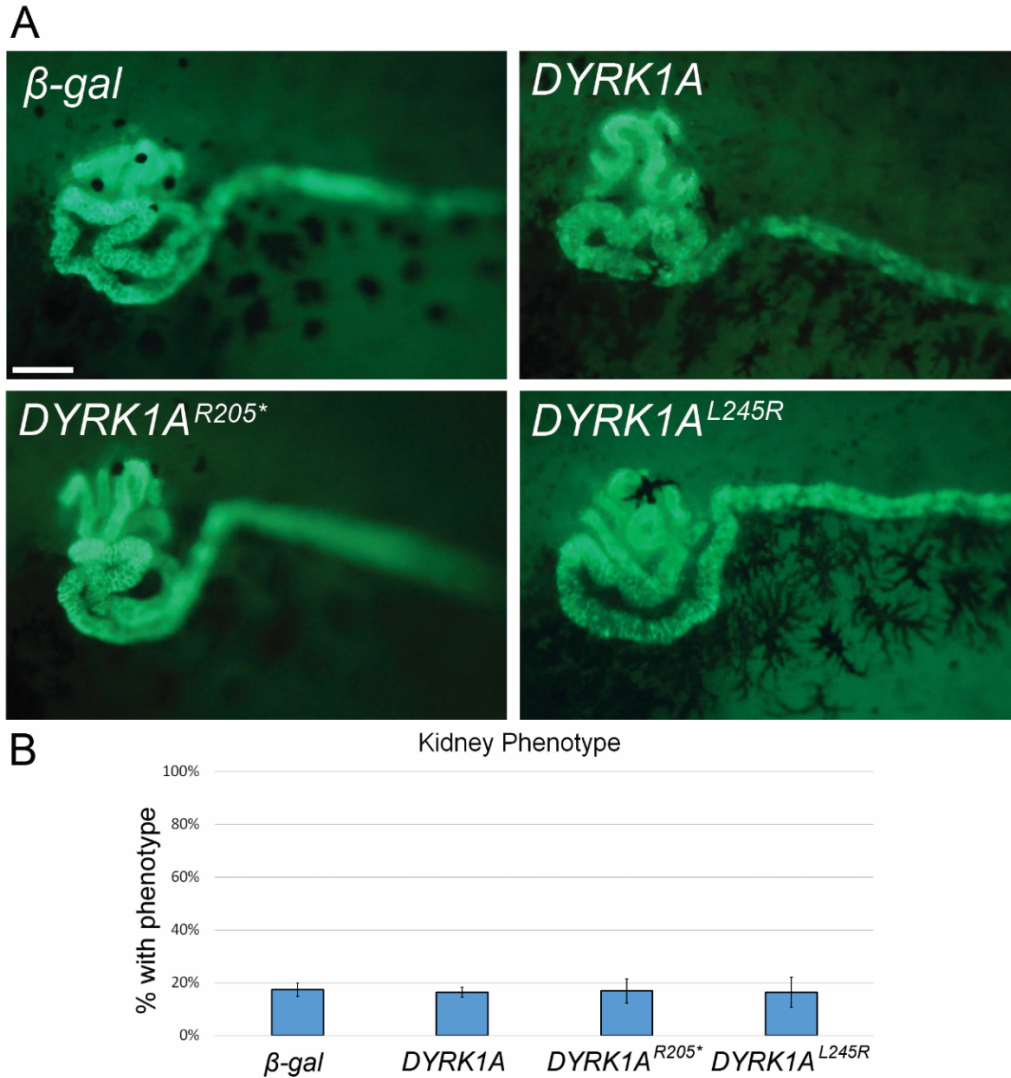


Figure 13. Overexpressing Wild-type *DYRK1A*, *DYRK1A*^{R205*} or *DYRK1A*^{L245R} Does Not Cause a Gain-of-Function Phenotype.

(A) *Xenopus* embryos were injected at the 8-cell stage with the rescue dose (50 pg) of either β -gal, wild-type *DYRK1A*, *DYRK1A*^{R205*}, or *DYRK1A*^{L245R} mRNA. (B) No significant difference ($p > 0.7$) was found between either β -gal and wild-type *DYRK1A*, *DYRK1A*^{R205*}, or *DYRK1A*^{L245R} suggesting neither variant elicits a gain-of-function phenotype. It should be noted that some embryos injected with wild-type human *DYRK1A* mRNA had slightly underdeveloped kidneys suggesting *DYRK1A* overexpression may also affect kidney development. Experiments were repeated three times with error bars representing standard error. The total number of *Xenopus* embryos are as follows: β -gal: 67, *DYRK1A*: 76, *DYRK1A*^{R205*}: 88, *DYRK1A*^{L245R}: 65. Scale bar represents 100 μ m.

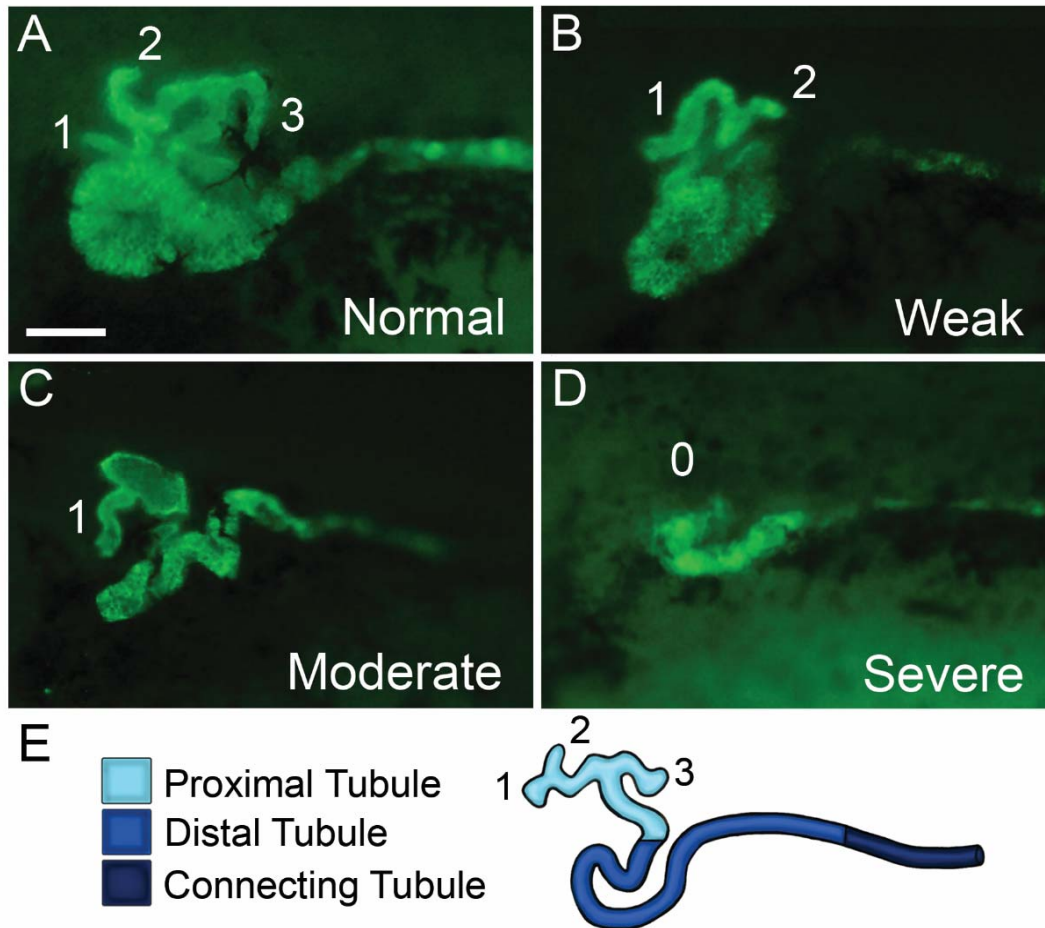


Figure 14. Scoring System for *Xenopus* Embryonic Kidneys.

Kidneys were scored at Nieuwkoop and Faber stage 40 (168). (A) A normal kidney consists of three branches in the proximal region with a “trunk” connecting to the convoluted looping of the early distal region, and strong immunostaining of the late distal region. (B) A weak phenotype consists of loss of one of the branches in the proximal region and possibly less early distal looping and/or partial loss of late distal immunostaining. (C) A moderate phenotype consists of loss of two of the branches in the proximal region with moderate loss of early distal looping and possible loss of late distal immunostaining. (D) A severe phenotype consists of complete loss of proximal tubules with severe or complete loss of early distal looping and the late distal region. (E) The schematic represents a stereotypical *Xenopus* embryonic kidney with proximal tubules in light blue, distal tubules in blue, and connecting tubules in dark blue. Scale bar represents 100 μm .

To assess whether Dyrk1a depletion affects kidney function, an assay was performed evaluating edema formation (172). Edema can be caused by a disruption in the kidneys' ability to excrete excess fluid, but it can also be caused by heart or liver failure. Both the heart and liver arise from dorsal cells in *Xenopus* (Xenbase.org). To prevent knockdown in these tissues, embryos were injected with Dyrk1a MO or standard MO in both ventral cells at the four-cell stage to affect both kidneys. Embryos injected with the Dyrk1a MO suffered from edema and abnormal kidneys, characterized by swelling in the chest cavity due to fluid retention (Figure 12I) while embryos injected with the standard MO did not (Figure 12H). Though the ventral cells do not give rise to the heart or liver, which also can lead to edema if perturbed, I still assessed the heart of *Xenopus* embryos, as DYRK1A syndrome patients also have heart anomalies (145, 180). Embryos injected with Dyrk1a MO have normal heart morphology and similar cardiac beating as the standard MO control embryos (Figure 15). These techniques suggest that the edema is due to loss of kidney function in *Xenopus*. Taken together, these data support a role for DYRK1A in pronephric development and strongly suggest that the *DYRK1A*^{R205*} and *DYRK1A*^{L245R} variants are responsible for the kidney anomalies observed in these patients.

3.26 Other Findings

In addition to understanding how Dyrk1a loss alters the kidney, I have preliminary data suggesting that overexpression also leads to kidney abnormalities. First, I found that overexpressing 50 pg of *Xenopus dyrk1a* mRNA lead to dilated

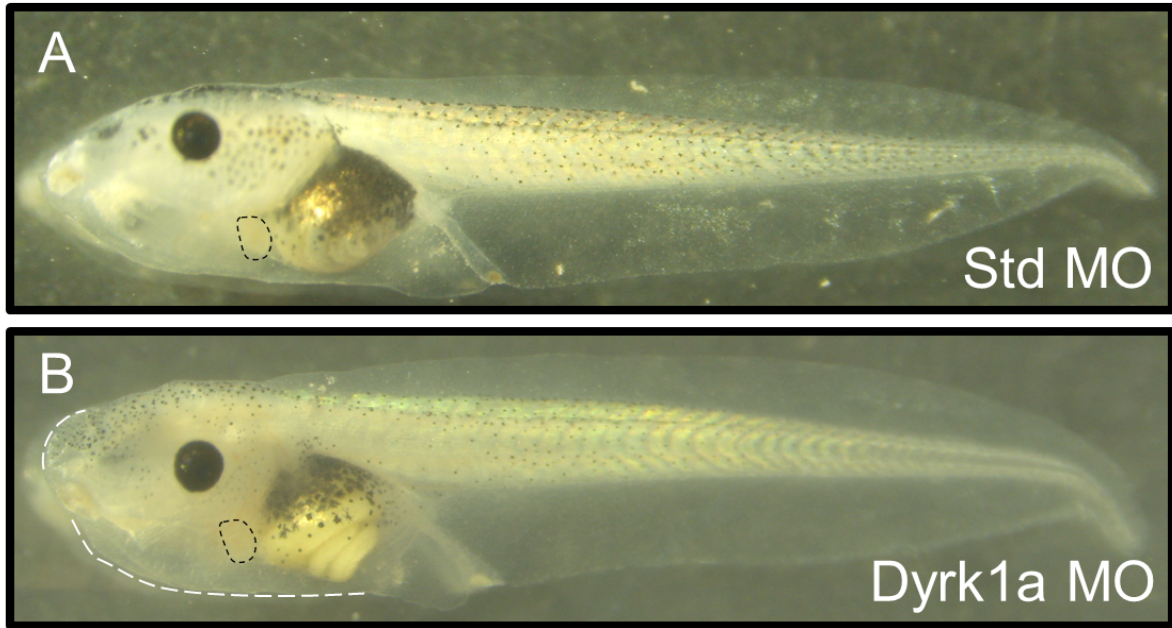


Figure 15. Injecting Both Ventral Cells of 4-Cell Embryos Does Not Affect Heart Morphology or Cardiac Beating.

(B) Embryos injected with 10 ng of Dyrk1a MO in both ventral cells at the 4-cell stage do not affect heart morphology compared to the (A) standard MO control, as seen by the black dashed lines. White dashed line indicates edema formation in the Dyrk1a MO tadpole.

Additionally, Dyrk1a MO injected embryos show cardiac beating

(<https://www.youtube.com/watch?v=EwE2uVfql7I>) similar to the standard MO control

embryos (<https://www.youtube.com/watch?v=vbU5hhVbkhw>).

and/or cyst-like formation in the kidney in several embryos (Figure 16). Cyst formation, dilated tubules, and ectopic tubule formation can also be seen with Dyrk1a MO knockdown in the kidneys. Though this experiment needs to be repeated, I have overexpressed 50 pg of human *DYRK1A* mRNA and found that the *Xenopus* kidney looks slightly different compared to age-matched controls (Figure 13). Though there is no significant difference for overall kidney morphology, there is loss of convolution in the distal tubules and shorter proximal tubules which is indicative of underdevelopment. Though not seen often, I also noted several embryos had tubule dilation as seen with overexpressing *Xenopus dyrk1a* mRNA. In Down syndrome patients who have an extra copy of *DYRK1A*, renal cysts and tubule dilation have been recorded (192, 193). Given that these specific kidney phenotypes occur with both Dyrk1a loss and overexpression this suggests dysregulation of Dyrk1a needs to be tightly regulated. I also have looked at other tissues outside of the kidney that were interesting to me where *dyrk1a* was expressed.

Through discussions with peers who have worked with *DYRK1A* I chose to see if Dyrk1a loss would alter craniofacial structures or neural crest cell migration in *Xenopus*. I have noticed that loss of Dyrk1a alters melanocytes, which are neural crest cell-derived pigment cells. Craniofacial structures likewise arise from the neural crest cells. I utilized a transgenic line where a CMV promoter drives RFP expression in the nucleus called Xla.Tg(CMV:hist2h2be-RFP)^{Ueno}. First, I injected single cell *Xenopus* embryos with 10 ng of Dyrk1a MO and performed neural crest explants on stage 17 embryos and put explants on a glass slip in fibronectin. I then did live

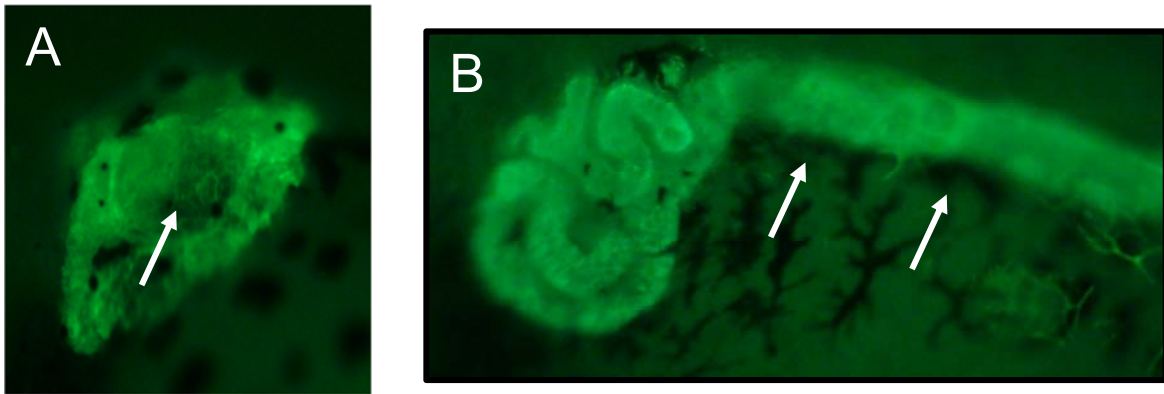


Figure 16. *Xenopus dyrk1a* Overexpression Leads to Kidney Abnormalities.

(A) *dyrk1a* overexpression in the kidney can lead to cyst-like formation or (B) dilated tubules. Both phenotypes are depicted by white arrows. Dilated tubules are also seen with human *DYRK1A* mRNA overexpression.

imaging to track cell migration of the neural crest explants. I used Imaris software to track nuclei from these live imaging videos in order to assess cell migration (Figure 17). The nuclei tracking demonstrates that the wild-type explant cells appear to work together to migrate a certain direction whereas the Dyrk1a MO injected explant fails to move cohesively in a specific direction. Instead, the cells seem to go in circles, seemingly lost as to which direction they should migrate. This suggests that Dyrk1a may be important for proper cell migration in neural crest cells. To further understand if Dyrk1a may be affecting neural crest cells, I next looked at craniofacial structures.

I injected 10 ng of Dyrk1a or standard MO into both dorsal cells of four cell embryos which target the neural crest. I found the embryos injected with the standard MO appeared normal, but embryos injected with the Dyrk1a MO had a range of facial anomalies including coloboma (hole in the iris), narrow head, and loss of eyes (Figure 18). It is also apparent in the Dyrk1a MO injected embryos that the melanocytes are lost or have defects with migration given their haphazard localization compared to control embryos (Figure 18).

Though most of these experiments are outside of the scope of this dissertation, they demonstrate the *Xenopus* serves as a promising model not only of the kidney, but also as a model for other tissues that Dyrk1a may affect. I have shown preliminary data that Dyrk1a loss disrupts neural crest cells through disrupting migration, as well as resulting in abnormalities in melanocytes and craniofacial structures. This opens up a potential new project for the lab to pursue.

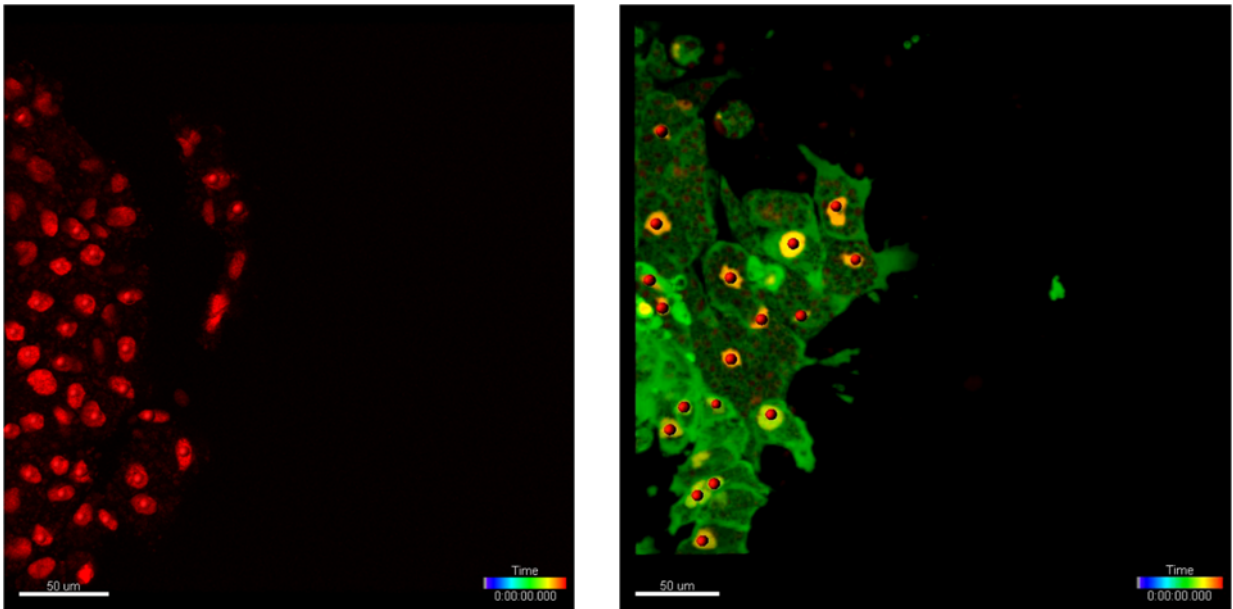


Figure 17. Nuclei Tracking of Neural Crest Explants Demonstrates That Dyrk1a Loss Leads to Loss of Coordinated Cell Migration.

I injected single cell *Xenopus* embryos with 10 ng of Dyrk1a MO along with a GFP cytosolic lineage tracer and performed neural crest explants on stage 17 embryos. Explants were done in the transgenic line $Xla.Tg(CMV:hist2h2be-RFP)^{Ueno}$ where RFP is a reporter for Histone 2B expression in the nucleus. Uninjected $Xla.Tg(CMV:hist2h2be-RFP)^{Ueno}$ embryos served as a control. I utilized live imaging to track cell migration of the neural crest explants. In order to assess cell migration I used Imaris software to track nuclei from the videos made from live imaging. Time is tracked by color where the blue coloring of the lines indicates where the cells first started and the green to red coloring demonstrates where they end. Nuclei tracking demonstrates that the wild type explant cells appear to work together to migrate a certain direction <https://youtu.be/vYa-ellvo1A>, whereas the Dyrk1a MO injected explant fails to move cohesively in a specific direction https://youtu.be/z_vWq5jOQo0. Explants were placed on fibronectin during live imaging.

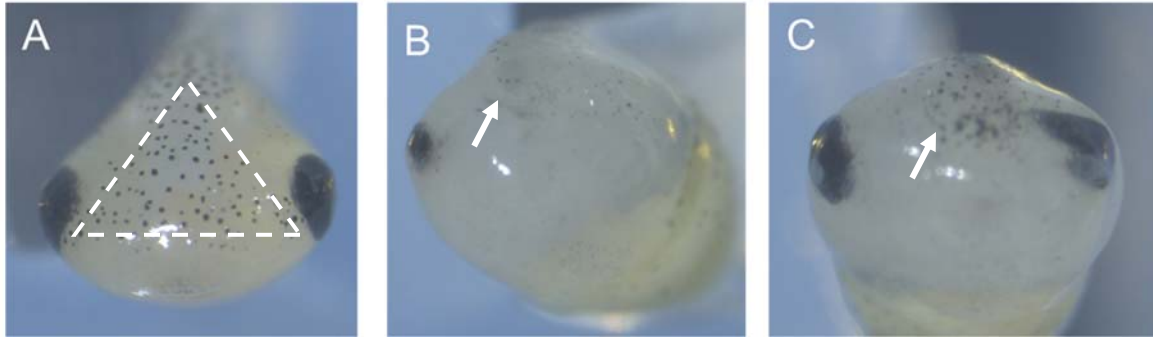


Figure 18. Dyrk1a Loss in Neural Crest Cells Leads to Craniofacial Anomalies.

I injected 4 cell *Xenopus* embryos with 10 ng of standard or Dyrk1a MO in both dorsal cells which target the neural crest cells. (A) Stage 45 Embryos injected with the Standard MO appeared phenotypically normal whereas stage 47 embryos injected with the Dyrk1a MO suffered from (B) dysmorphic facial features, loss of eye structures, and (C) coloboma (smearing-like appearance of the eye). (A) Dashed line demonstrates the normal pattern distribution of melanocytes on the head whereas (B-C) arrows point to abnormal melanocytes, which are also neural crest cell-derived. Staging was assessed by spiraling of the gastrointestinal tract.

3.3. Discussion

Recent discoveries demonstrate that *de novo* pathogenic variants in *DYRK1A* cause a syndromic form of intellectual disability (OMIM 614104). The findings in the current study indicate that CAKUT/genital defects should be included as features associated with this syndrome. CAKUT consist of a heterogeneous clinical spectrum, and how CAKUT arise is largely unknown. Thus, it is important to identify all genes and causal variants involved (194). Strong genetic causality of monogenic disease only accounts for 14% of CAKUT cases (55), and polygenic causes are speculated to occur but are largely unknown (195). Next-generation sequencing, specifically exome sequencing, has improved the discovery of novel causative genes that are important in genitourinary development (196–198). Here, we report on a novel genetic contribution of *DYRK1A* to CAKUT/genital defects. We identified 17 unique variants in *DYRK1A* from clinical exome sequencing in 19 unrelated individuals. As summarized in Table 2, microcephaly, intellectual disability, developmental delay, and seizures are some of the more common features of this syndrome.

Eleven of fifteen (73% of those with available data) individuals in this study (Table 3) have CAKUT/genital defects, with 36% having renal anomalies, in addition to other organ involvement. While renal anomalies have been reported previously (181), broadly based phenotyping for CAKUT was not performed in previous studies. Seven of the *DYRK1A* variants identified in our study were novel as they were absent in ClinVar as well as the gnomAD and ExAC databases. Per inclusion criteria, most of *DYRK1A* variants were *de novo* and included truncating variants.

This suggests a loss-of-function mechanism for variants causing this syndrome, which further supports the findings of another group who proposed reduced kinase function as the cause (183).

In addition, we determined that *dyrk1a* is expressed in the developing *Xenopus* kidney and found that Dyrk1a knockdown results in abnormal tubules or complete loss of the kidney. This phenotype could be partially rescued by human *DYRK1A* mRNA. However, a nonsense (*R205**) and a missense (*L245R*) variants failed to rescue the phenotype, indicating that loss-of-function variants in this gene are likely causative for the observed phenotype in some patients. This also suggests that *DYRK1A*'s kinase domain may be important for kidney development. Furthermore, Dyrk1a MO was injected into both ventral cells at the four-cell stage to affect both kidneys, which resulted in edema suggesting that Dyrk1a is important for both kidney development and function. Although *Xenopus* is an established model of nephron development, it has not been commonly used to study genital defects. However, our findings related to pronephric development are likely relevant to the mammalian urogenital tract, given the dependence of the formation of the male and female urogenital tract upon the nephric duct and the pronephros.

Though it was not explored in this study, *DYRK1A* overexpression in some *Xenopus* embryos led to underdeveloped kidneys. This suggests *DYRK1A* overexpression may also affect kidney development. Interestingly, several studies estimate that the incidence of renal and urogenital anomalies in Down syndrome patients ranges from 3.5–21.4% (192, 193) and my preliminary data shows that both of these occur with overexpression of *Xenopus dyrk1a*. Given that Down syndrome

has a triplication of *DYRK1A*, this gene may affect urogenital and kidney development when its normal dosage is altered. However, I also see both phenotypes, as well as ectopic tubule formation when Dyrk1a is lost, suggesting that it must be tightly regulated to achieve proper nephrogenesis. Furthermore, I demonstrate preliminary data that Dyrk1a loss results in abnormal neural crest cell migration, craniofacial anomalies, and altered melanocyte localization. This suggests that Dyrk1a also may be important for proper neural crest cell migration given that it results in multiple abnormal cell/tissue types that all arise from neural crest cells.

One limitation of this study is that we were not able to obtain genitourinary information from all patients. Future plans for research include identification and studying the phenotype and underlying variants in a larger number of affected families. Furthermore, signaling pathways involved in *DYRK1A*-related CAKUT/genital defects should be investigated. *DYRK1A* has been shown to affect Notch signaling and calcium signaling (150) which are both important for kidney development (199, 200). Additionally, several papers have implicated *DYRK1A* in canonical Wnt signaling (148, 201).

In summary, based on the data we present in this study, the phenotype of *DYRK1A*-related intellectual disability syndrome is now expanded to include CAKUT/genital defects. Our data suggests that *DYRK1A* may affect kidney development through its catalytic activity, though this should be examined further. We empirically recommend that individuals with *DYRK1A* syndrome undergo a renal ultrasound and a thorough genital physical exam, which can improve patient quality of life.

CHAPTER 4: DYRK1A AND WNT SIGNALING IN KIDNEY DEVELOPMENT

4.1 Introduction

It is well-established that canonical Wnt signaling is an important player in kidney organogenesis (41–47). It is necessary for nephron induction in mice (45), and is essential for renal branching morphogenesis, (46) as well as maintaining the nephron progenitor pool (47). Canonical Wnt signaling is also involved in the development of the *Xenopus* pronephros (43, 44). Overexpression or loss of canonical Wnt signaling in *Xenopus* leads to loss of kidney tubules (44) whereas overexpression of β -catenin in the mouse kidney leads to severe polycystic lesions that affect the entire nephron (52). These studies suggest that endogenous levels must be tightly maintained to achieve proper nephrogenesis, though its regulation during nephrogenesis is not completely understood. It could be that DYRK1A acts as a regulator for Wnt signaling during nephrogenesis.

Though canonical Wnt signaling is heavily studied, the precise cause of GSK3 β inhibition to stabilize β -catenin is still unknown and speculated by several different models (202). DYRK1A has been found to phosphorylate GSK3 β at residue T356, which inhibits its activity and leading to increased β -catenin levels *in vitro* and in white adipose tissue in mice (201). Although *Xenopus* does not share the conserved T356 residue, it has at least two possible DYRK1A consensus sequences that could be phosphorylated to inhibit GSK3 β , including T309. Additionally, DYRK1A could modify the Wnt pathway through other Wnt components. It has been found that DYRK1A interacts with both Dickkopf-related protein 3 (DKK3) and DVL1

endogenously by co-immunoprecipitation in HEK293 cells (148). Furthermore, when both DYRK1A and DVL1 are co-transfected in SH-SY5Y neuronal cells transfected with TOPflash Wnt reporter it increases Wnt activity as seen by an increase in luciferase (148). In addition, DKK3 has been found to be decreased in Down syndrome patient samples while it is increased in the Down syndrome Tc1 mouse model (148). Given that the previous studies focused on understanding DYRK1A's effect in cell culture and down-syndrome mouse models, we sought to better understand how DYRK1A modified the Wnt pathway during normal embryogenesis, specifically nephrogenesis. Because Wnt signaling plays a vital role in normal kidney development, it is conceivable that DYRK1A alters β -catenin levels to fine tune Wnt activity during nephrogenesis.

4.2 RESULTS

4.21 Dyrk1a Perturbation Alters β -Catenin Levels

The canonical Wnt pathway is important for many developmental processes, including dorsoventral axis specification with the highest levels of canonical Wnt signaling leading to head formation (203) and lowest levels leading to body trunk formation. Though I did not see abnormalities when overexpressing *dyrk1a* in the dorsoventral axis (data not shown), it was previously shown that co-expressing *dyrk1a* with a subphenotypic dose of *β -catenin* mRNA in *Xenopus* embryos enhanced duplicate axis formation, while kinase dead *dyrk1a* had no such effect (171). Similarly, reduced β -catenin results in ventralization in *Xenopus* embryos (203), and I demonstrate that the same phenotype occurs when Dyrk1a MO is

injected into dorsal cells which give rise to the head (Figure 19). These data suggest that Dyrk1a is altering the canonical Wnt pathway, potentially through β -catenin levels. To test this, I injected single cell embryos with either 40 ng of Dyrk1a MO, 1 ng *dyrk1a*, or 1 ng *β -gal* mRNA. I found that loss of Dyrk1a leads to lowered total β -catenin protein levels (Figure 20, lane 5). This result was somewhat unexpected, as levels of free β -catenin are generally low. It could be that Dyrk1a is somehow affecting the β -catenin pools that are bound to adherens junctions, though my dorsoventral data suggests it is affecting the signaling pool of β -catenin. In order to test this, I utilized an active β -catenin antibody to examine if the signaling pool of β -catenin is being altered.

The active β -catenin antibody, which will only recognize the stable form of β -catenin that is not phosphorylated on residues Ser33/37/Thr41, recognizes what is also known as the transcriptional pool of β -catenin. In addition, to increase specificity, I used our transgenic *Xenopus* line, Tg(pbin7LEF-GFP) canonical Wnt reporter frogs (204). This line contains a construct consisting of a synthetic promoter, seven copies of an optimal binding sequence for LEF/TCF factors, and a minimal TATA box in front of a GFP reporter gene (<https://www.mbl.edu/xenopus>). I injected single cell embryos with either 20 or 40 ng of standard MO as a negative control or 20 or 40 ng Dyrk1a MO then examined active β -catenin and GFP expression by Western blot (Figure 21). The results demonstrated that Dyrk1a loss also reduces the signaling pool of β -catenin. Additionally, even though the active β -catenin antibody shows loss of expression only when 40 ng of the Dyrk1a MO is injected, the GFP antibody demonstrates that GFP expression is also lost with only

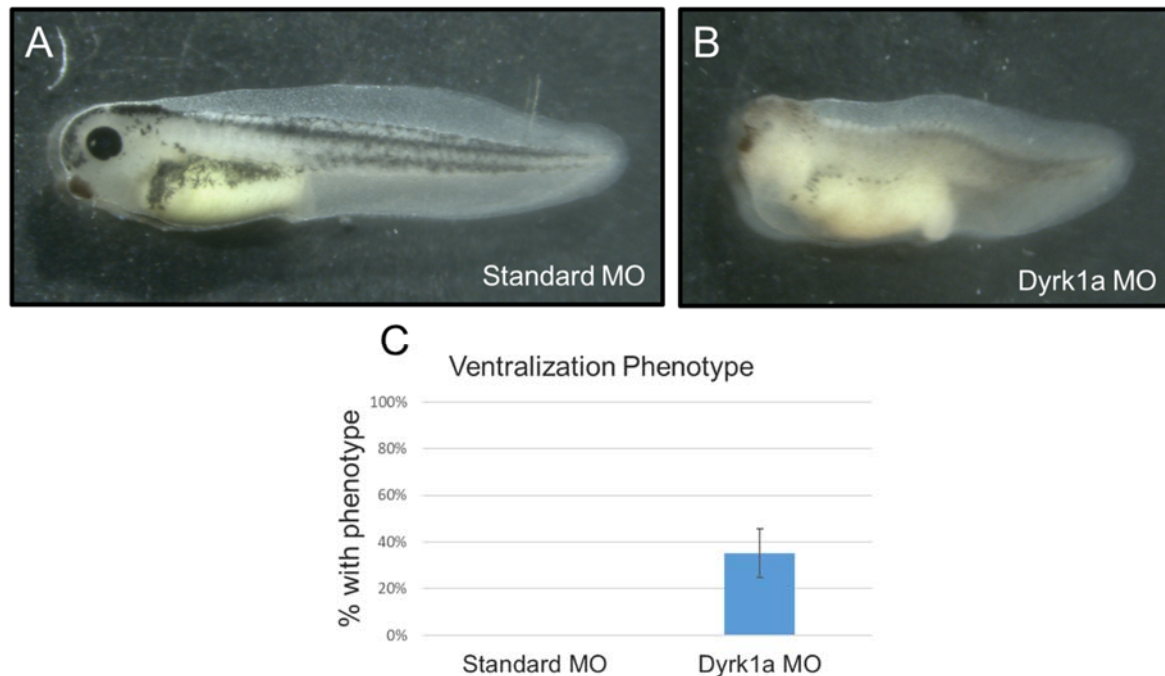


Figure 19. Ventralization Results When Dyrk1a MO is Injected into the Dorsal Cells.

I injected 10 ng of either Dyrk1a or standard MO into both dorsal cells of four-cell embryos. (A) Standard MO injection does not result in ventralization, but (B) Dyrk1a MO injection does. (C) The graph demonstrates almost 40% of Dyrk1a MO injected embryos have a ventralization phenotype whereas no embryos in the control group do. Experiments were repeated three times with error bars representing standard error. The total number of *Xenopus* embryos are as follows: Standard MO: 78, Dyrk1a MO: 43.

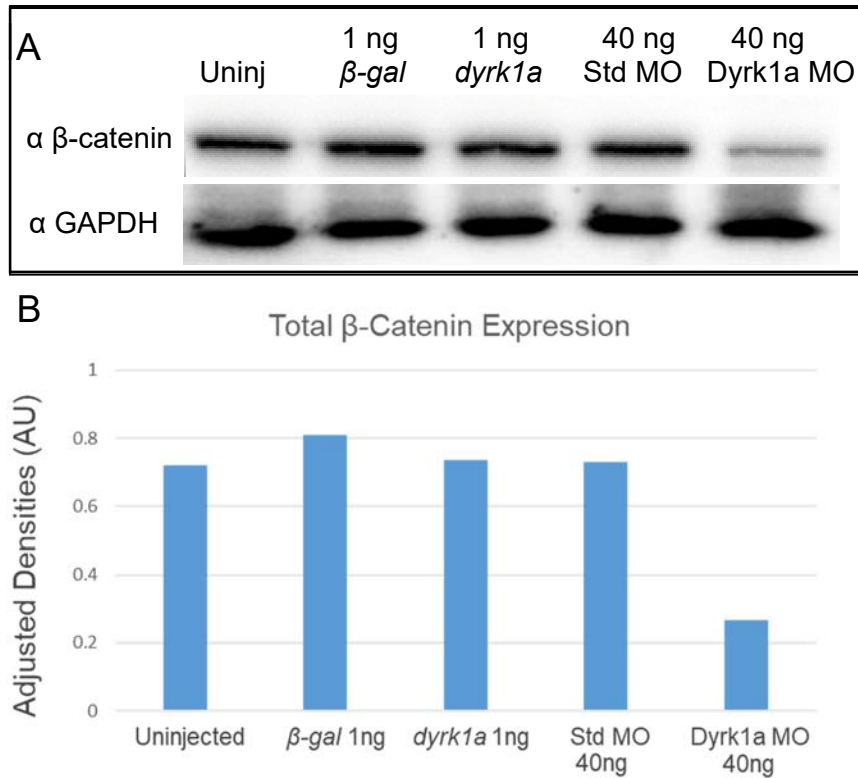


Figure 20. Knockdown of Dyrk1a Results in Reduced Total β-Catenin Protein.

(A) Compared to the uninjected (lane 1) and Standard MO (lane 4) controls, total β-catenin protein is reduced (lane 5) upon Dyrk1a MO knockdown in neurula stage 16-17 embryos.

(B) Adjusted densities were done for (B) total β-catenin expression where expression was normalized against GAPDH which served as a loading control. Overexpressing *dyrk1a* (lane 3) does not increase β-catenin compared to control (lane 2). β-catenin runs at 95 kDa, while GAPDH runs at 37 kDa. Lysates were lysed open with TX Lysis buffer.

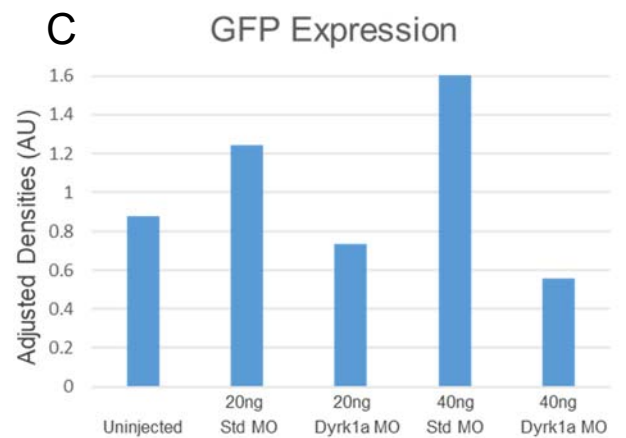
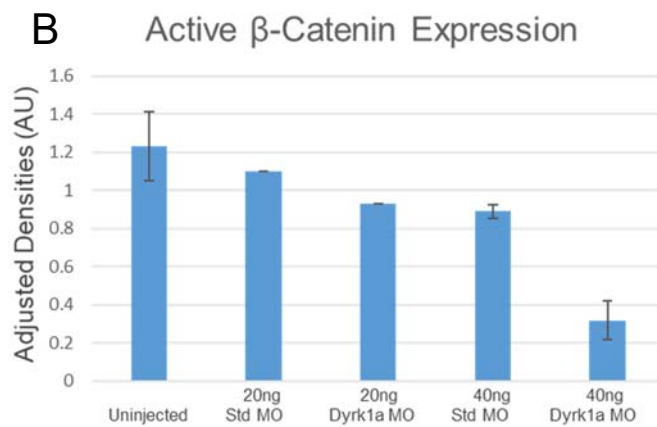
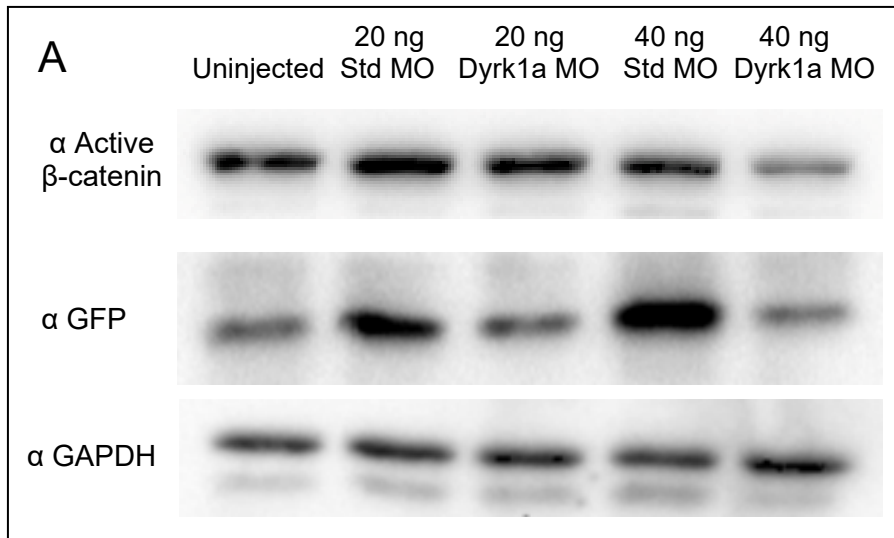


Figure 21. Knockdown of Dyrk1a Results in Reduced Active β -Catenin Protein.

I injected the Tg(pbin7LEF-GFP) canonical Wnt reporter single cell embryos with either 20 ng or 40 ng of Dyrk1a MO or Standard MO as a negative control. (A) Compared to the β -gal (lane 1) and Standard MO (lane 2 and 4) controls, active β -catenin protein is reduced (lane 5) upon Dyrk1a MO knockdown in early tadpole stage 32 embryos. Although not seen with active β -catenin (top row), using 20 ng of Dyrk1a MO reduces GFP protein expression. Adjusted Densities were done for (B) active β -catenin expression and (C) GFP expression where expression was normalized against GAPDH which served as a loading control. Active β -catenin runs at 95 kDa, while GFP runs at 40 kDa, and GAPDH runs at 37 kDa. GAPDH was reblotted after GFP. All injected embryos were selected based on RFP lineage tracer expression. Uninjected embryos were selected based on GFP expression. A potential bias in selecting GFP embryos that were not too dim nor too bright may account for lower GFP expression in uninjected controls. (B) Standard error is shown for uninjected and 40 ng of either Standard or Dyrk1a MO, as I had 2 replicates for them. I only had 1 replicate for 20 ng lysates and therefore they do not have standard error included.

20 ng of Dyrk1a MO. This suggests that the quantification using the GFP antibody is more sensitive to alterations made to the transcriptional pool β -catenin. This is somewhat expected given that it detects only the β -catenin that has bound to TCF/LEF binding sites on the transgenic reporter sequence.

Next, I sought to understand if overexpression of *dyrk1a* would lead to alterations in active β -catenin. I injected the Tg(pbin7LEF-GFP) canonical Wnt reporter single cell embryos with either 250 pg or 500 pg of *dyrk1a* or *β -gal* mRNA as a negative control. My initial studies used TX lysis buffer to dissociate the embryos for lysate use, but upon seeing no change in active β -catenin or GFP expression (data not shown) I changed to a buffer with SDS. This harsh detergent followed by sonication allows for the lysis of the nucleus, where most of the active β -catenin would likely be found. With this detergent I did see a change in GFP, but not active β -catenin expression by Western blot (Figure 22). Given that my previous results demonstrate the quantification of bound β -catenin using the GFP antibody is more sensitive, it is likely because discreet changes in the signaling pool of β -catenin cannot be detected by a typical active β -catenin antibody.

Because minute levels of β -catenin can reach the nucleus and activate Wnt target genes, in some cases differing methods should be utilized even if changes are not seen with a commercial active β -catenin antibody. Dyrk1a may make discreet changes to the Wnt pathway which can still have an effect downstream but may be difficult to detect. I ran into this problem when trying to see if overexpression of *dyrk1a* would lead to increased GFP expression in the kidney of Wnt reporter frogs. Targeted kidney injections with *dyrk1a* overexpression did not show a reliable

amount of increased GFP expression compared to negative controls. I also tried to stimulate canonical Wnt signaling in *dyrk1a* injected embryos by placing the embryos in GSK inhibitor Lithium Chloride (LiCl). First I placed uninjected Wnt reporter embryos at either stage 18 or stage 25 in 25, 35, 45, 55, or 65 mM of LiCl and left them in the molecule overnight. For past lab members 25 mM of LiCl worked to stimulate GFP expression in the kidney whereas 100 mM killed all embryos and lower doses showed no expression. However, I could not find a dose where embryos were healthy enough to grow up to the stage I needed (stage 35). I used the lowest dose of 25mM, to stimulate Wnt signaling in embryos that had been injected with *dyrk1a* or *β -gal* mRNA. Unfortunately, it did not elicit a reliable GFP expression in the kidney, even when immunostained with GFP. The embryos were also extremely sick from being submitted to both LiCl and microinjections. However, I did find an unexpected result when injecting Wnt reporter frogs with the Dyrk1a MO.

I injected a single V2 blastomere in 8-cell embryos with either standard or Dyrk1a MO. Instead of seeing a reduction in expression, as expected, I saw multiple embryos with increased GFP expression (Figure 23B and D) at stages 35 and 40. I also have preliminary data demonstrating that injecting single cell embryos with a lower dose of Dyrk1a MO seems to increase total and active β -catenin expression by Western blot instead of reducing it (Figure 23E-H). This may suggest that DYRK1A alters canonical Wnt signaling differentially in specific circumstances.

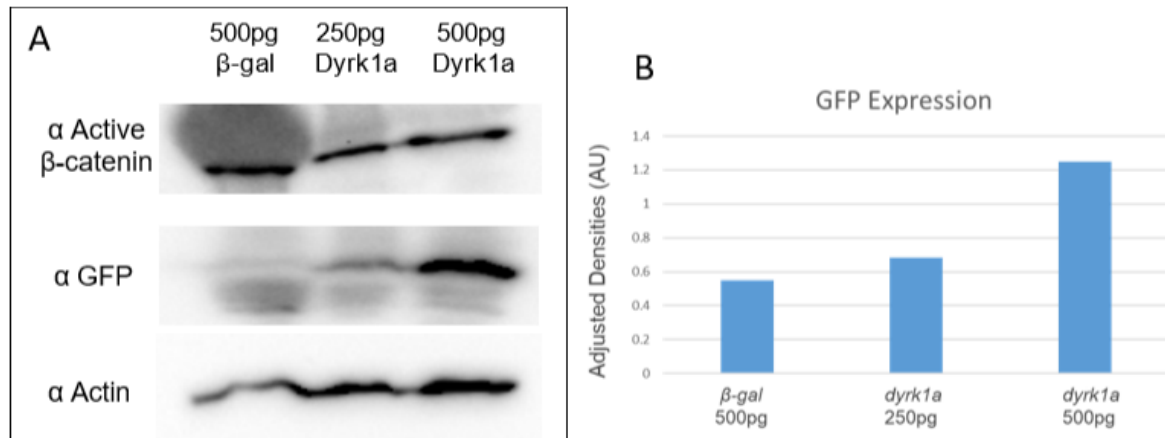


Figure 22. GFP Expression is Increased with *dyrk1a* Overexpression Upon Lysis of the Nucleus.

I injected the Tg(pbin7LEF-GFP) canonical Wnt reporter single cell embryos with either 250 pg of 500 pg of *dyrk1a* or β -gal mRNA as a negative control. I used a buffer with SDS which lyses the nucleus open, where most of the active β -catenin would likely be found. (A)

Adjusted densities were done for (B) GFP expression where expression was normalized against Actin which served as the loading control. GFP expression increases, but active β -catenin expression remained unaltered. This demonstrates that *dyrk1a* overexpression increases the transcriptional pool of β -catenin as seen through GFP.

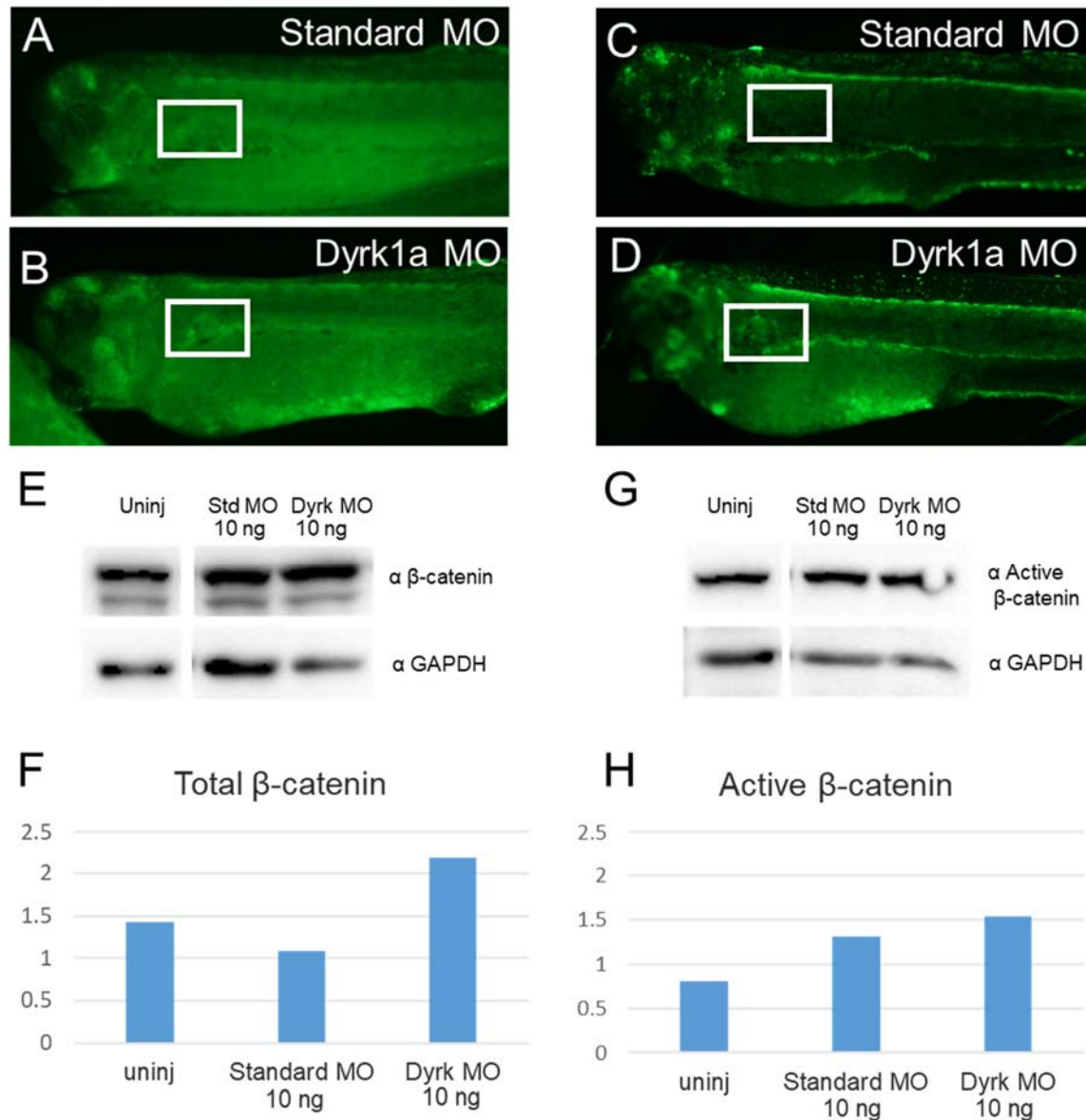


Figure 23. Inhibiting Dyrk1a at a Lower Dose Increases Wnt Signaling.

Dyrk1a knocked down in Wnt reporter line. (A-B) When Dyrk1a is knocked down in targeted kidney injections, a dose of 10 ng leads to (B) increased Wnt expression at stage 35 and (D) stage 40 embryos as seen by GFP immunostaining. White box is over the proximal and early distal kidney tubules. (E-F) Dyrk1a loss leads to increase in total β -catenin compared to loss of β -catenin expression seen with 40 ng of Dyrk1a MO. (G-H) Similar results are seen with active β -catenin expression. Note in (G-H) active β -catenin expression would be similar to (F) if the bubble was not present in the blot. GAPDH was used as a loading control.

4.3 Discussion

Though there are multiple pathways that DYRK1A may be acting through to influence kidney development, my data suggests that it may be acting through the canonical Wnt pathway. This does not exclude the possibility that it also affects other pathways during nephrogenesis, which will need to be illuminated through additional studies. In mice, DYRK1A was shown to phosphorylate and inhibit GSK3 β on the residue T356. Although *Xenopus* does not share the conserved T356 residue, it has at least two possible DYRK1A consensus sequences that could be phosphorylated to inhibit GSK3 β . My data does not directly implicate that Dyrk1a acts through the canonical Wnt pathway by inhibiting GSK3 β , but it clearly demonstrates β -catenin is being altered in whole embryos. My data shows that loss of Dyrk1a leads to reduced β -catenin expression by Western blot and leads to ventralization of embryos when Dyrk1a is specifically reduced in the dorsal cells. I also demonstrate that active β -catenin and GFP expression indicative of Wnt signaling are reduced upon Dyrk1a loss and that GFP expression is increased upon *dyrk1a* overexpression by Western blot. In addition, I also show with preliminary data that a lower dose of 10 ng of Dyrk1a seemed to increase both active and total β -catenin by Western blot (Figure 23E-H) as well as increased GFP expression for targeted kidney microinjections (Figure 23A-D). This suggests that Dyrk1a's interaction with the canonical Wnt pathway may be complex and that in different circumstances or in different doses, it may elicit an alternate outcome of Wnt signaling. Though this is outside of the scope of this dissertation, it is likely that DYRK1A is affecting more than just the canonical Wnt pathway.

Because DYRK1A also alters the cytoskeleton and the calcium pathway it may be that it influences the three main Wnt pathways in kidney development, though most likely not at the same time, if at all: the canonical and non-canonical PCP pathways appear to antagonize each other which prevents both from being active in the same cell at the same time (205). DYRK1A may also affect multiple Wnt pathways in a linear fashion, as it has been found that the calcium/NFAT pathway acts downstream of canonical Wnt ligand Wnt4 (206). It is tempting to speculate that DYRK1A could affect the various Wnt pathways during kidney development or embryogenesis, and even act as a switch between them, though there is no data to support this. DYRK1A has also been shown to regulate another catenin, p120 (158).

Dyrk1a has been found to directly regulate p120 (158), which is another catenin that both transcriptionally regulates Wnt genes and associates with E-cadherin to form adherens junctions. In addition, p120 also regulates small GTPases RhoA and Rac1 (158). Though the study showed that it directly increased the signaling pool of p120 and suggested it may not affect p120 in junctions, no experiments were shown to dispute this. It has been found that siRNA knockdown of p120 in SW48 cells resulted in dose-dependent loss of E-cadherin and complete loss of cell-cell adhesion (207). Thus, it is possible that loss of p120 could lead to loss of a junction, including loss of β -catenin. Given that Dyrk1a loss altered both active and total β -catenin levels, it may be affecting both the transcriptional and non-transcriptional pools of β -catenin.

Although most of my data suggests that Dyrk1a positively regulates the canonical Wnt pathway, I have some experiments that suggest otherwise. I have

preliminary data both by Western blot and by immunofluorescence that suggests loss of lower levels of Dyrk1a lead to increased β -catenin expression (Figure 23). Previous literature demonstrates that increased DYRK1A expression in the Tc1 mouse leads to increased DKK3 expression (148). It may be that loss of DYRK1A could lead to lower levels of Wnt antagonist DKK3, which may lead to increased canonical Wnt signaling in specific circumstances. Given that others and I have seen both inhibitory and activating DYRK1A activity on the canonical Wnt pathway (148), it is likely that these interactions are tissue-dependent, and on other factors including age of the organism, where interactions during development may be vastly different than those that occur in specific disease state, as well as if changes made to DYRK1A are large or discreet.

Although canonical Wnt signaling is essential for kidney development (39–45) its regulation during this time is not completely understood. My data suggests that Dyrk1a alters β -catenin and acts through the canonical Wnt pathway. I have shown that this occurs *in vivo* in whole *Xenopus* embryos in stages when nephrogenesis is occurring. And though most of my experiments only implicated Dyrk1a in acting through the canonical Wnt pathway during embryogenesis, I do have preliminary data suggesting it is also changing Wnt signaling during kidney development (Figure 23). It is possible that this interaction also occurs in mammals, as Wnt signaling is also essential for embryogenesis and kidney development, but further studies will have to decipher this. Though I was not able to ascertain if Dyrk1a is altering β -catenin through GSK3 β inhibition, changes to β -catenin may explain the observed Dyrk1a embryo and kidney phenotypes.

CHAPTER 5: CONCLUSIONS, DISCUSSION, AND FUTURE DIRECTIONS

5.1 Conclusions and Discussion

The kidney is an important excretory organ that eliminates nitrogenous waste, balances the electrolyte levels in the body, controls blood pressure, stimulates red blood cell production, and maintains the density of our bones (2). The structural and functional unit of the kidney, the nephron, filters the blood to regulate water and various soluble substances and reabsorbs what is needed and removes the rest as urine (1). The nephron's function is vital for homeostasis of both blood pressure and volume, acid-base balance, and plasma osmolarity (1). Given the important and vast functions of the kidneys in the human body, it is vital to understand how anomalies arise during development. *Xenopus laevis* contain one functional pronephric nephron on either side of their body, which serves as a simplified model for mammalian meso- and metanephric nephron development (Figure 2). This simplified model can help us understand how CAKUT may arise.

Congenital anomalies of the kidney and urinary tract (CAKUT) are a leading cause of chronic kidney disease in children (53). CAKUT can appear as an isolated feature or be multi-syndromic with extra-renal clinical manifestations (53). Though kidney organogenesis is well-studied, gaps in understanding still remain. This failure to fully grasp how the kidney develops translates into low cure rates for many of the genetic disorders that cause kidney disease. Only 14% of known CAKUT cases have strong genetic causality for monogenic disease (55). Polygenic disease is likely to occur but it is largely unknown how frequently (195). Uncovering more causative

genes will aid in our understanding of how the kidney develops and what processes lead to abnormal development. This dissertation reveals a new gene important for nephrogenesis called *DYRK1A*.

Unpublished clinical findings suggested that patients who suffer from *DYRK1A* haploinsufficiency, known as *DYRK1A* intellectual disability syndrome, had a higher prevalence of CAKUT, but it was not understood why. This dissertation demonstrates that *DYRK1A* mutations are likely causative in CAKUT cases seen in *DYRK1A*-syndrome patients through several key experiments. I use *Xenopus* as a model to show that *dyrk1a* is expressed in the pronephric kidney and *dyrk1a* loss leads to abnormal kidney formation. Additionally, I demonstrate that knockdown of *Dyrk1a* in both kidneys leads to edema formation, likely because kidney function has been lost. Furthermore, I show this kidney phenotype can be rescued by co-injecting human wild-type *DYRK1A* mRNA. However, nonsense (*R205**) and missense (*L245R*) patient mutant mRNA fail to rescue the phenotype.

In our data set, neither intellectual disability nor CAKUT/genital defects had a predictable severity, though we did not utilize biochemical assays to explore this possibility thoroughly. Several studies have demonstrated generally that *DYRK1A* mutations which occur more C-terminally retain more kinase function (145, 183, 185). For instance, the *A498fs* mutation loses 50% of kinase activity (185) and has mild intellectual disability (145). Given that the mutations we modeled result in complete loss of kinase activity (185), it may be that *DYRK1A*'s role in nephrogenesis is dependent on it as intellectual disability seems to be.

Specific mutations can also retain partial kinase activity or even lead to hyperactivity (185). The DYRK1A A195T mutation leads to a 2-fold increase in kinase activity but still leads to mild intellectual disability and other DYRK1A-syndrome characteristic features such as language impairment and global developmental delay (208). However, these features can also be found in Down syndrome patients, which have an additional copy of *DYRK1A* (209). Therefore, the resulting clinical features may be a result of DYRK1A hyperactivation. Though we had no patients in this cohort with the A195T mutation, it has been shown that some Down syndrome patients who have an extra copy of *DYRK1A* have kidney cysts and tubule dilation (192, 193). In fact, I demonstrate that *DYRK1A* overexpression may also affect kidney development through loss of tubule convolution indicative of developmental delay (Figure 13). Additionally, I have preliminary data showing that overexpression of *dyrk1a* leads to cyst-like formation in the *Xenopus* kidney, though further replications need to be performed to validate this (Figure 16). Though DYRK1A dose is an important factor in clinical urogenital manifestations, it is still unknown which pathway or pathways DYRK1A is acting through.

In this dissertation, I attempted to uncover if Dyrk1a acts through the canonical Wnt pathway in *Xenopus* kidney development, though most of my efforts can only confidently demonstrate that it is acting through Wnt signaling during embryogenesis. It is possible that Dyrk1a is altering the Wnt pathway through GSK3 β as DYRK1A has been found to phosphorylate GSK3 β at residue T356, which inhibits its activity (201). *Xenopus* does not share the conserved T356 residue, but it has at least two possible Dyrk1a consensus sequences that could be

phosphorylated to inhibit GSK3 β , including T309. Though I did not do experiments to implicate GSK3 β I found that changes to Dyrk1a alter β -catenin. I show that loss of Dyrk1a leads to lowered total and active β -catenin expression by Western blot, as well as GFP loss in a Wnt reporter *Xenopus* line. Additionally, I found that overexpressing *dyrk1a* in the Wnt reporter frogs leads to increased GFP expression which suggests Dyrk1a is increasing canonical Wnt signaling during embryogenesis. Furthermore, I demonstrate ventralization of embryos when Dyrk1a MO is injected into the dorsal cells, similar to a loss of Wnt signaling in dorsal cells. I also show preliminary data suggesting that Dyrk1a loss leads to increased Wnt signaling in the *Xenopus* kidney, though more replicates will have to be done to verify this contradictory result. I only scratched the surface in understanding how Dyrk1a could be acting through the Wnt pathway. Future work should focus in the exact mechanism of how this occurs in the context of kidney development, as it may be a potential CAKUT therapeutic avenue.

5.11 DYRK1A's Known Interactions with Pathways Involved in Kidney Development

Given that this is the first time DYRK1A has been found to contribute to kidney development it is not known what pathway(s) it is acting through. However, Dyrk1a does interact with pathways in other tissues that have a known function during kidney development. I will briefly discuss a few pathways that DYRK1A may be acting through to exert its function on kidney development and why the Wnt pathway became an attractive candidate.

There are many different pathways that play a role in kidney development. Some key pathways include FGF, GDNF, Sonic Hedge Hog (SHH), Notch, Calcium signaling, PCP, and canonical Wnt signaling pathways (6, 210). In order to understand which pathways DYRK1A may be acting through, it is important to understand when these pathways contribute to kidney development and how DYRK1A has been shown to modulate them in other tissues.

The GDNF/Ret pathway plays a role early in kidney development by inducing ureteric bud outgrowth and subsequent branching (2). FGF signaling likewise occurs early and is critical for ureteric bud and metanephric mesenchyme formation (211). It is thought that Sprouty2, a known antagonist of FGF signaling, may coordinate Wnt11/Gdnf/Fgf7 during kidney development (212). DYRK1A has been found to positively regulate FGF through inhibiting Sprouty2 in the mouse central nervous system (213). Given that GDNF, FGF, and Sprouty2 signaling occur so early in kidney development and that loss of it leads to complete kidney or nephron loss (211, 212, 214), it is unlikely that DYRK1A is acting through either pathway via Sprouty2. However, DYRK1A has been shown to modulate Wnt11 through a direct interaction with p120 during *Xenopus* gastrulation (158). In addition, Wnt11 seems to have a role later in kidney development, specifically coordinating the development of kidney tubules, and Wnt11 loss leads to abnormal tubule formation (215). However, other Wnts such as Wnt9 and Wnt4 occur much earlier to induce renal vesicle formation and lead to more severe kidney loss (6, 41, 43, 206, 216). DYRK1A has been found to interact with downstream components of the Wnt pathway including GSK3 in mouse white adipose tissue (201) and DVL1 and DKK3

in the mouse hippocampus and in HEK293 cells (217) This leaves Wnt signaling as a potential DYRK1A pathway candidate.

SHH also has a known role in regulating proliferation and differentiation of the metanephric mesenchyme in mice (218). In the mouse brain DYRK1A has been found to positively regulate SHH through GLI3 and also can dampen SHH which is thought to be mediated through DYRK1A's negative regulation of actin dynamics (149). Though DYRK1A interacts with the SHH pathway, Loss of SHH mostly leads to ureter anomalies in mouse models, which is not seen in DYRK1A syndrome patients. However, pursuing how DYRK1A changes actin dynamics may implicate the PCP Wnt pathway.

DYRK1A has been found to negatively regulate F-actin in the mouse brain through inhibiting ABLIM proteins which stabilize actin (149). In addition, DYRK1A interacts with DVL1 to increase canonical Wnt signaling (217). It is thought that differential recruitment of DVL to the membrane acts as a switch between PCP and canonical Wnt pathways (219). In addition, mutations in different PCP genes in mice leads to duplicated, hypodysplastic, and/or misshapen kidneys. I have seen both dilated tubules and ectopic tubule buds with Dyrk1a loss and overexpression in *Xenopus* kidneys. It may be possible that these abnormalities are a result of changed actin dynamics or the PCP pathway, as PCP disruptions can lead to tubule dilation and duplicate kidneys (220). When Dyrk1a is lost these branches could arise from an increase in F-actin which increases cell movements. In addition, the resulting phenotypes could occur with activation of the PCP pathway which could inhibit the canonical Wnt pathway. Furthermore, if DYRK1A levels somehow acts as

a switch between Wnt pathways the phenotypes that arise from DYRK1A's altered state could be acting through DVL1. Therefore, the non-canonical PCP pathway may also be a viable candidate pathway.

Another pathway that DYRK1A interacts with is Notch signaling where it has been found to attenuate Notch signaling in the mouse brain (221). Notch2 plays a role in proximal nephron fates and loss of Notch2 in the metanephric mesenchyme leads to loss of glomeruli and proximal tubules (222). Loss of proximal tubules is seen in the *Xenopus* kidney, however, loss of DYRK1A would increase Notch signaling which has been shown to lead to premature tubule differentiation and dilated tubules (223) and thus is an unlikely pathway for DYRK1A to act through. However, the calcium signaling pathway may be a promising candidate.

DYRK1A has been found to regulate calcium signaling by maintaining inactive NFAT in neuronal cells (146) as well as enhancing RCAN1s ability to inhibit calcineurin in neuronal cell line PC12 (224). In addition, in zebrafish loss of *dyrk1a* led to increased calcium signaling which caused hemorrhaging in the brain (150). The Calcium/Wnt pathway has been implicated in nephrogenesis by treating primary metanephric mesenchymal cells with Wnt4. This treatment caused significant Ca²⁺ influx leading to tubule formation which could be blocked in presence of Ca²⁺ chelator (199). DYRK1A has been found to inhibit calcium signaling in multiple tissue types and loss of calcium signaling leads to widened tubules in *Xenopus*. Though the phenotype for overexpression of calcium signaling is not known, it could be how DYRK1A influences kidney development. It is known that the calcium/NFAT pathway acts downstream of canonical Wnt ligand Wnt4 (206) and that calcium signaling

inhibits canonical Wnt signaling which leads to abnormal kidney development. Therefore, it may act by throwing off the balance between the different Wnt pathways. The canonical Wnt pathway became my focus because initial experiments with Dyrk1a such as the dorsoventral experiment implicated canonical signaling. However, given that DYRK1A interacts with DVL1, which has been called the hub of the three main Wnt pathways, it is plausible that disruption of DYRK1A may lead to disruption of the synergy between Wnt pathways (Figure 24).

5.12 Overall Conclusions

Congenital anomalies of the kidney and urinary tract are a leading cause of pediatric kidney failure and result from defects in morphogenesis. This work highlights a novel gene implicated in CAKUT known as *DYRK1A*. By using *Xenopus laevis* as a model I determine that Dyrk1a is essential for kidney development, as well as the likely cause behind observed renal anomalies in DYRK1A intellectual disability syndrome patients. In addition, it shows that Dyrk1a may be acting through the canonical Wnt pathway to exert its effects on nephrogenesis. Overall, this dissertation reveals a new gene important for kidney development and disease which has the potential to impact diagnostic patient treatment strategies for DYRK1A-syndrome patients.

5.2 Future Directions

My data indicate that Dyrk1a is found in the *Xenopus* kidney and that Dyrk1a loss disrupts nephrogenesis. This kidney defect can be partially rescued by adding

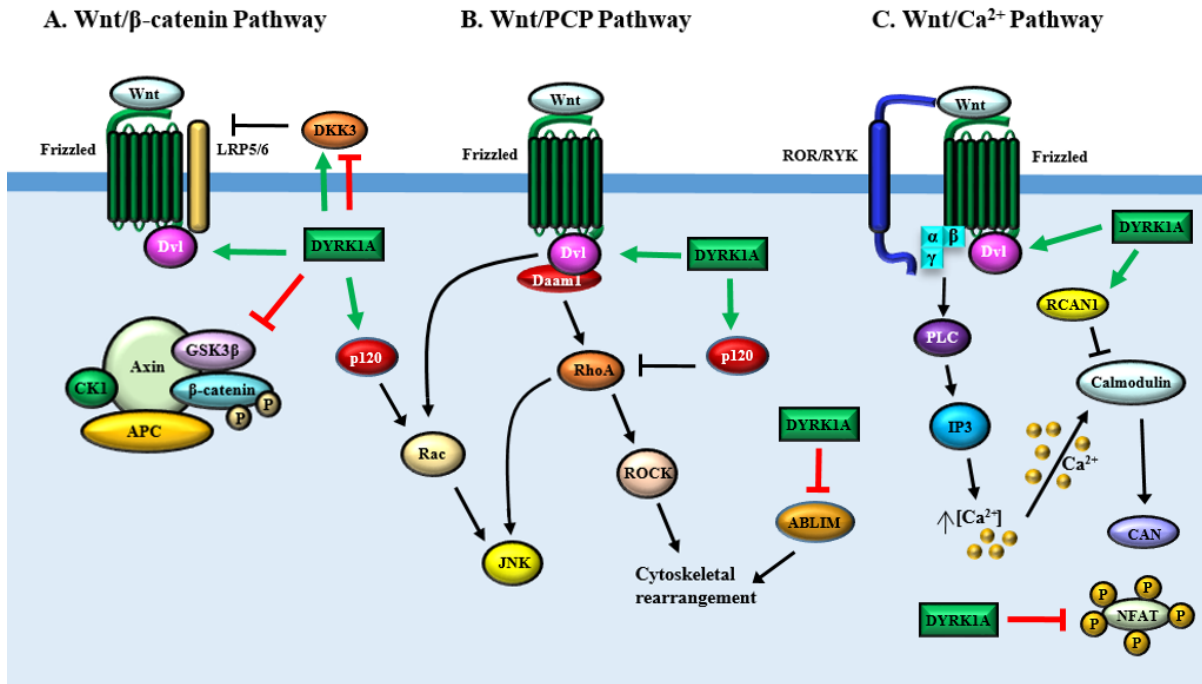


Figure 24. How DYRK1A Interacts with the Wnt Pathways.

A simplified version of Figure 3 which demonstrates the downstream Wnt components that DYRK1A, which is depicted by a green rectangle, phosphorylates of the three major Wnt pathways. Positive regulation by DYRK1A is denoted with a green arrow while negative regulation is denoted by a red inhibition bar. (A) DYRK1A has been shown to both positively and negatively regulate the canonical Wnt antagonist DKK3, and negatively regulates Wnt inhibitor GSK3β. DYRK1A has been found to positively regulate p120, which plays a transcriptional role in the canonical Wnt pathway but also (B) regulates the small GTPases Rac1 and RhoA, implicating it in the non-canonical PCP pathway. DYRK1A has been found to negatively regulate ABLIM, which serves to organize the actin cytoskeleton. (C) DYRK1A was shown to regulate the calcium pathway through several proteins. It positively regulates RCAN1, an inhibitor of the calcium pathway and it also maintains inactive NFAT, which likewise inhibits calcium signaling. (A-C) Lastly, DYRK1A positively regulates DVL, which is a common component of the three major Wnt pathways.

human *DYRK1A* mRNA, but patient-derived mutant mRNA has no such effect. However, the two mutations I modeled are both kinase dead. It would be insightful to model a patient mutation that does not result in loss of kinase function to determine if Dyrk1a's kinase domain is necessary for its role in kidney development. Though it is clear that Dyrk1a knockdown results in loss of kidney tubules, I only assess this loss by immunofluorescence and with one *in situ* marker. Being more thorough with various *in situ* markers would be insightful such as looking at nephron sections individually and the glomus, as well as assessing both early and late kidney markers. *In situ* hybridization for early kidney markers, *lim1* and *hnf1 β* , and late kidney marker, *atp1a1*, will decipher when Dyrk1a affects nephrogenesis. Additionally, detection of different regions of kidney with late markers, *slc5a1* for proximal tubules, *clckb* for distal tubules, and *nphs1* for the glomus is useful. This will let me compare expression patterns to my immunofluorescence data, as the two techniques have displayed discrepancies, especially concerning the distal and connecting tubule presence (162). Understanding why these regions were altered could also help pinpoint Dyrk1a's role in kidney development.

One indirect way to assess Dyrk1a's role would be to look at proliferation and apoptosis in Dyrk1a knockdown kidneys, as Dyrk1a has a known role in both. DYRK1A overexpression inhibits proliferation in neuronal progenitor cells (225), and DYRK1A loss leads to increased proliferation in β -cells (226). This may mean Dyrk1a loss and loss of kidney tubules in *Xenopus* is not due to Dyrk1a's effect on proliferation. In fact, DYRK1A inhibition through a compound called ID-8 was found to stimulate human kidney epithelial cell proliferation after acute injury (227).

DYRK1A is pro-survival through phosphorylation and activation of SIRT1, which promotes deacetylation of p53 (228). Therefore, it could be that DYRK1A loss leads to apoptosis ultimately loss of kidney cells and tubules.

My ambition was to implicate Dyrk1a in the Wnt pathway during kidney development. To further understand if Dyrk1a is affecting the Wnt pathway transcriptionally, qRT-PCR should be done with *Xenopus* kidneys where *dyrk1a* is overexpressed. Well established Wnt target genes that are expressed in the kidney are *fgf8*, *lef1*, *wnt4*, and *axin2*. In order to see if Dyrk1a is directly affecting the Wnt pathway, a rescue experiment of the kidney phenotype with β -catenin would be ideal.

A successful rescue by co-injecting non-phosphorylatable *β -catenin* mRNA with the Dyrk1a MO would implicate that Dyrk1a is acting through the canonical Wnt pathway. It is a difficult experiment because too much or too little Wnt signaling leads to abnormal kidney development in *Xenopus* (43, 44) and finding the correct dose that successfully rescues will be challenging. Additionally, β -catenin perturbation may also affect the adherens junction β -catenin pool, which may confound the results. To get around this I could utilize the Dex inducible Lef Δ N- β CTA-GR755A fusion construct, This construct consists of the DNA binding region of mouse Lef1 (HMB box amino acids 265-394), two HA tags, the C-terminal transactivation domain (CTA) of β -catenin, and the human glucocorticoid receptor hormone-binding domain (amino acids 512-777 with E to A substitution at 755) (44). Under normal conditions, the glucocorticoid domain ensures the construct remains in the cytoplasm, but upon addition of dexamethasone it translocates to the nucleus and induces Wnt target

genes. This allows for a more precise activation of canonical Wnt signaling that may get around some of the off target effects and difficult titration of toxic non-phosphorylatable β -catenin. An alternate approach is to alter the Wnt pathway to see if it affects Dyrk1a levels. An obvious way to do this is by stimulating the Wnt pathway with a Wnt ligand such as Wnt3 to see if it affects levels of DYRK1A in kidney cell lines. Ideally this would be done *in vivo*, but Dyrk1a antibodies do not work well in early *Xenopus* embryos. Additionally, after stimulation, CO-IP of DYRK1A and various Wnt components such as GSK3 β may illuminate where in the pathway DYRK1A is exerting its effects. Overall, this dissertation identifies a novel role for DYRK1A in kidney development and demonstrates that it may be acting through the canonical Wnt pathway.

CHAPTER 6: APPENDIX

LOSS OF P53 LEADS TO ABERRANT KIDNEY DEVELOPMENT IN *XENOPUS* AND MAY LEAD TO CONGENITAL ANOMALIES OF THE KIDNEY AND URINARY TRACT IN LI-FRAUMENI PATIENTS

6.1 Introduction

TP53, also known as p53, has long been regarded as the guardian of the genome due to its role as a tumor suppressor and maintaining genomic stability (231). Through this role, p53 acts as a tetramer to transcriptionally regulate genes important for DNA repair, cell cycle arrest, and apoptosis (232). p53 has other vital roles that are underappreciated, such as in embryonic development and organogenesis (233). In some genetic backgrounds p53 null mice development normally but develop spontaneous tumors by 6 months of age (234). However, in other backgrounds mice have neural tube defects, craniofacial malformations (235) and even congenital anomalies of the kidney and urinary tract (CAKUT) (233). Additionally, conditional *p53* deletion in mouse nephron progenitor cells leads to loss of these progenitors and the subsequent loss of cap mesenchyme (232). Furthermore, work in *Xenopus* targeting the pronephros demonstrated that dominant negative p53 overexpression leads to complete loss of the kidney (236). Given this, we speculated that p53 loss may similarly effect pronephric development.

6.2 Results

6.21 P53 Knockdown or Knockout Leads to Aberrant Kidney Development in *Xenopus*

Given that p53 is expressed in the *Xenopus* pronephros (Xenbase.org), we sought to determine when p53 is expressed. We show by Western blot that p53 is expressed across all stages of development including gastrulation and neurulation, but is reduced around stage 19 during tailbud formation (Figure 25). Western blot analysis was used to confirm that the translation-blocking antisense morpholino (MO) correctly targets *Xenopus* p53 mRNA (Figure 26). Next, I sought to determine whether loss of p53 function in *Xenopus* results in disruption of kidney development. Embryos were injected in a single V2 blastomere at the 8-cell stage to target a single kidney, leaving the other as an internal control. Knockdown with a p53 MO resulted in abnormal pronephroi when immunostained with antibodies 3G8 and 4A6, which label the proximal tubules and the distal and connecting tubules (nephric duct), respectively (Figure 27). I wanted to validate these results with a second approach, this time by knocking out the p53 gene using the CRISPR Cas9 system.

Xenopus is an allotetraploid species and has both a long and short homeolog, or four copies of most genes, including p53. I designed two single guide RNAs (sgRNAs) that each target both *Xenopus* p53 homeologs. Western blot analysis indicates that using both guides together leads to visibly lowered p53 protein expression at tadpole stage 37 (Figure 28A). Though, this does not mean that a single guide does not affect p53, as Sanger sequencing indicates that the genomic sequence of the p53 long homeolog has been edited in whole embryos using

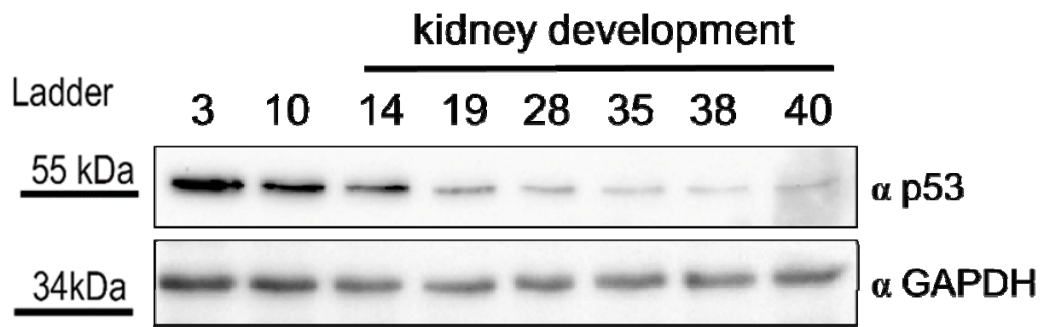


Figure 25. p53 Expression Across Developmental Stages.

Xenopus laevis lysates were made to assess p53 expression from blastula (3), gastrula (10), neurula (14-19), and through tailbud (28) to tadpole (35-40) developmental stages (168). Kidney development in *Xenopus* occurs from stage 12.5 to stage 40 and beyond. The blot demonstrates that p53 expression is high in early stages and is greatly reduced in later stages. GAPDH was used as a loading control. The bar under the molecular weight indicates its position on the blot.

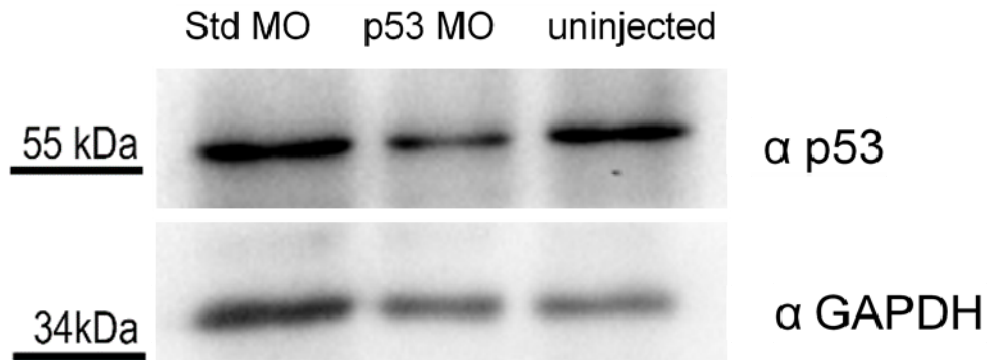


Figure 26. The p53 Morpholino Correctly Targets p53 mRNA in *Xenopus*.

Western blot analysis demonstrates that p53 protein levels are reduced in blastula embryos (stage 10-12) upon morpholino knockdown indicating that the MO correctly targets p53 mRNA. Embryos were injected with 40 ng of p53 MO or standard (Std) MO. GAPDH is used as a loading control. The bar under the molecular weight indicates its position on the blot.

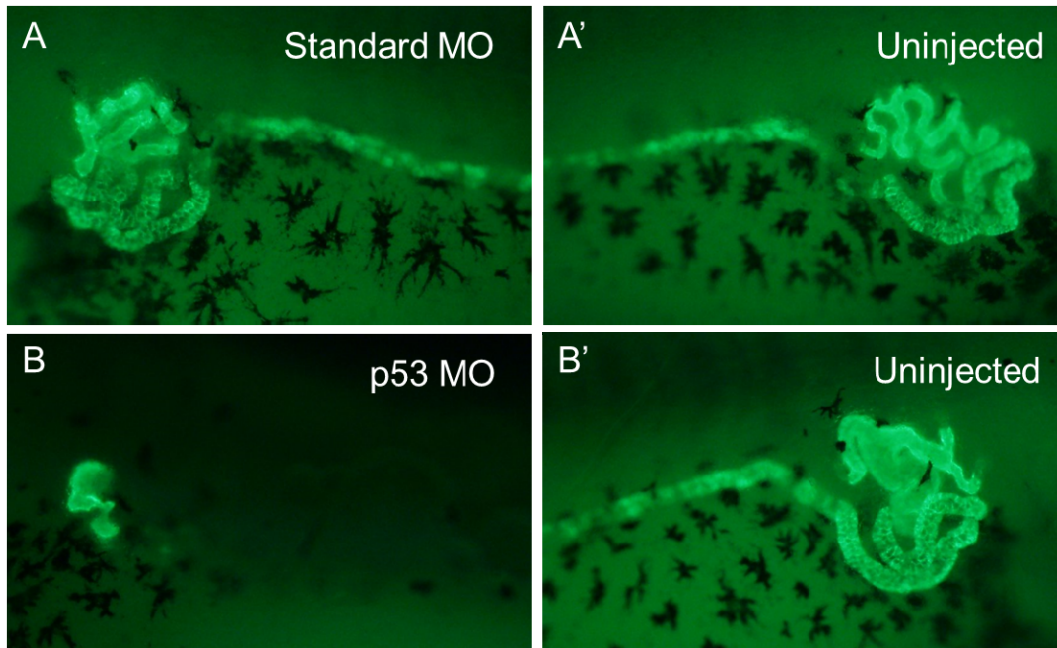


Figure 27. p53 Knockdown Leads to Loss of Kidney Tubules in *Xenopus*.

Embryos were unilaterally injected at the 8-cell stage with 20 ng of p53 MO or standard MO. Stage 40 tadpoles were immunostained with kidney antibodies 3G8, which labels the proximal tubules, and 4A6, which labels the distal and connecting tubules. Letters without apostrophes (A–B) represent the injected side, whereas letters with apostrophes (A'–B') represent the uninjected side. (A) The Standard MO has no affect while (B) knockdown with a translation-blocking p53 MO disrupts kidney development.

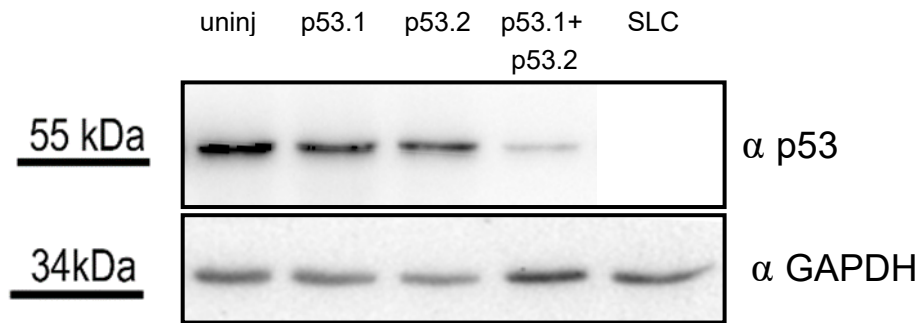
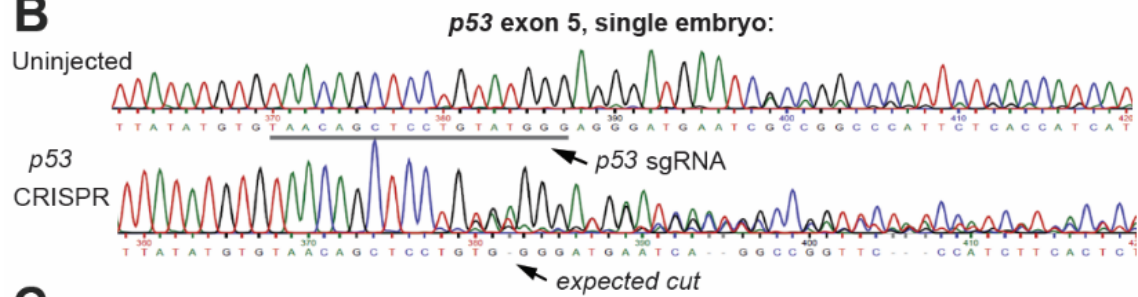
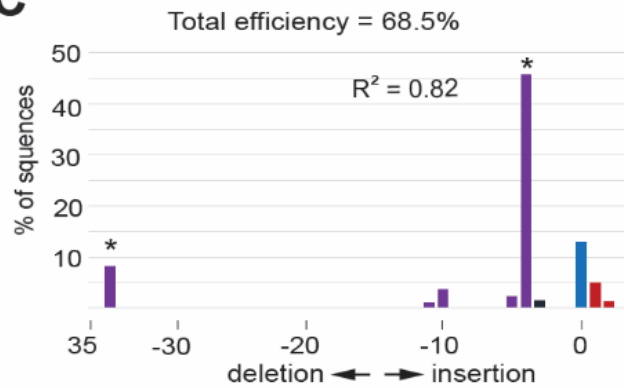
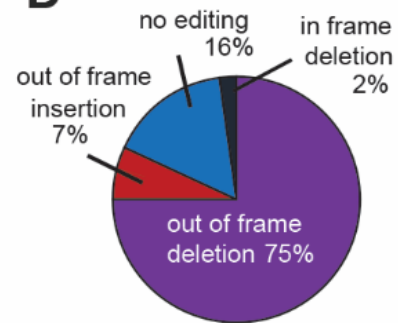
A**B****C****D**

Figure 28. p53 Can be Knocked Out with CRISPR/Cas9 Technology in *Xenopus*.

(A). Western blot analysis of stage 37-40 tadpole lysates demonstrates that injecting single cell embryos with both sgRNA 1 and 2 (p53.1 and p53.2) leads to lowered p53 expression as seen with a p53 antibody. SLC serves as the negative control while GAPDH serves as the loading control. Uninj = uninjected. The bar under the molecular weight indicates its position on the blot. (B) To verify that p53 knockout was obtained, I injected single-cell embryos and then sequenced individual embryos around the region where the Cas9 protein targets for cutting. The chromatogram of the p53 CRISPR embryo demonstrates that the sequence before the cut site appears normal, whereas after the cut site, the sequence appears to degrade and a good read was not ascertained. The chromatogram of the wild-type embryo has no degradation of its peaks. (C) TIDE analysis shows that most embryos that had Cas9 cutting lead to a four base pair deletion, most likely leading to a non-functional protein. (D) A majority of all cutting (75%) lead to out of frame deletions, followed by out of frame insertions (7%) and in frame deletions (2%). Only 16% of embryos had no editing.

sgRNA 1 alone (Figure 28B). To gain a more thorough understanding of the CRISPR edits I used TIDE analysis, which compares wild-type embryos to CRISPRed embryos and establishes the efficacy of cutting as well as the most likely types of indels that specific guide has caused. TIDE analysis showed an almost 70% cutting efficiency with 75% of cuts being out of frame deletions, a majority of which result in a 4 base pair deletion, likely leading to a non-functional p53 protein (Figure 28B).

After this validation, I injected sgRNA 1 into 8 cell embryos targeted to a single kidney. I found that the p53 CRISPR/Cas9 method phenocopied the p53 MO and lead to loss of kidney tubules (Figure 29). Because I was able to get a kidney phenotype and degraded sequence, it is likely that there is reduced p53 expression, it is just not visible by Western blot. Given that the kidney loss result could be replicated with two different methods of p53 loss, it suggests that p53 is responsible for the kidney phenotype, rather than off-target effects of either approach.

6.22 Dominant Negative RNA From Li-Fraumeni Patients Leads to Abnormal Kidney Development in *Xenopus*

Next, we sought to establish if the p53 kidney phenotype had human relevance. Mutations in *TP53* at a single allele in humans results in a dominant negative disease known as Li Fraumeni syndrome. These patients have a predisposition for developing various types of cancers that are early onset. Interestingly, it was found through unpublished MRI data that a cohort of Li Fraumeni

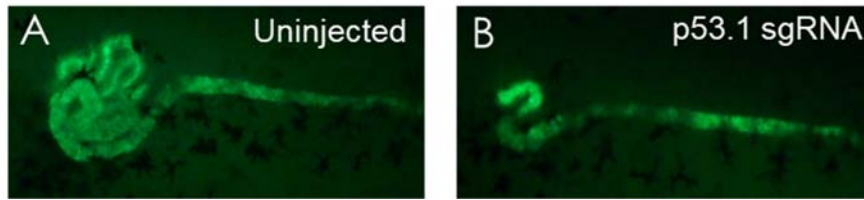


Figure 29 p53 Knock Out Leads to Loss of Kidney Tubules in *Xenopus*.

Embryos were unilaterally injected at the 8-cell stage with 500 ng of p53 sgRNA and 1 ug of Cas9 protein along with a RFP tracer. Stage 40 tadpoles were immunostained with kidney antibodies 3G8 and 4A6. (A) The uninjected side has a normal pronephros while (B) the injected side knocks out p53 and disrupts kidney development.

patients has a higher prevalence of CAKUT (31% compared to 10% in control group) including kidney hypoplasia, renal cysts or benign kidney tumors, or agenesis, ovarian cysts, or uterine agenesis. Of the 29 Li-Fraumeni patients examined, 45% had glomerular filtration rates lower than 90, which is a clinical readout of kidney function and under 90 demonstrates impairment. These mutations can result in functional loss of p53, but also can result in dominant negative function in patients. Because p53 acts as a tetramer to bind DNA, mutant p53 can form tetramers with wild-type p53, resulting in inhibition of wild-type p53 function (237).

We chose to model two different human mutations in *Xenopus* that are thought to have a dominant negative effect as it has been shown that overexpressing a dominant negative form of p53 leads to loss of kidney tubules in *Xenopus* (236). The first mutation, p53^{R248W}, is found in the DNA binding domain of p53 and has been previously characterized in *Xenopus* (236). It is also known to disrupt DNA binding by eliminating essential minor groove contacts (238). A patient with this mutation in this cohort was found to have a simple kidney cyst 6.8 cm in diameter. The second, p53^{R282W}, is novel and is also found in p53's DNA binding domain and is speculated to also have dominant negative function. The patient suffers from a complex kidney cyst 3.4 cm in diameter and kidney lesions.

We used site-directed mutagenesis to obtain both mutations and synthesized mRNA, along with human wild-type p53. The constructs all contain two flag epitopes. Western blot analysis with both p53 and flag antibodies was used to confirm that the wild-type human p53, p53^{R248W}, and p53^{R282W} mRNA are successfully expressed in

Xenopus embryos (Figure 30). From Western blot analysis, it appears that the $p53^{R282W}$ mutation has lower levels of expression than wild-type or $p53^{R248W}$. This is likely due to protein stability, as the mutation may interfere with maintaining the correct protein conformation. We then injected either wild-type *p53*, $p53^{R248W}$, or $p53^{R282W}$ mRNA into the V2 blastomere of 8-cell embryos to target a single kidney to find a subphenotypic dose of wild-type *p53*, as too much *p53* has been shown to cause abnormal kidney development (239). We found that 300 pg elicits a moderate loss of kidney tubules with either $p53^{R248W}$ or $p53^{R282W}$, but not with wild-type *p53* that is statistically significant (Figure 31).

6.3 Discussion

p53 is perhaps the most well-known tumor suppressor, but it has other important roles in both embryogenesis and organogenesis (233). Conditional *p53* deletion in mouse nephron progenitor cells leads to loss of cap mesenchyme, which is where nephrons arise from (232). Previous work in *Xenopus* has even shown that dominant negative *p53* overexpression alters kidney development (236). Given that loss of *p53* by two independent methods or overexpression of dominant negative *p53* which can inhibit wild-type *p53* leads to kidney abnormalities, it likely plays a role in nephrogenesis.

Here, we report that *p53* affects *Xenopus* nephrogenesis: loss of *p53* with either MO (Figure 27) or CRISPR/Cas9 (Figure 29) strategies led to loss of kidney tubule formation. Both methodologies were verified with Western blot analysis and/or

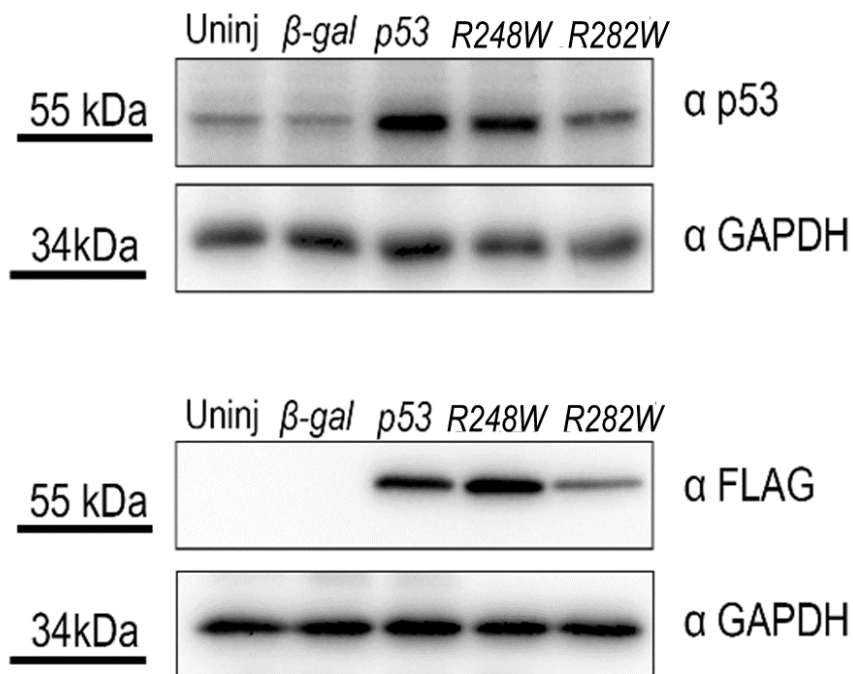


Figure 30. Human p53 Wild-type and Mutant Proteins are Expressed in Neurula Stage *Xenopus* Embryos.

Single-cell embryos were injected with 1 ng of either wild-type, *R248W*, or *R282W* human p53 mRNA along with a membrane RFP tracer. Western blot analysis demonstrates that human wild-type and mutant p53 mRNA can be successfully translated in *Xenopus* embryos. Of note, the *R282W* mutant has lower expression than either the wild-type or other mutant p53. This may represent that this mutant protein is less stable than the *R248W* mutant. β-gal serves as a negative control. The two point (C742T, p53^{R248W} and C844T, p53^{R282W}) mutant constructs were generated with site-directed mutagenesis from a wild-type human pCdna3-Flag-p53 vector. GAPDH was used as a loading control. The bar under the molecular weight indicates its position on the blot. Western blot was performed by undergraduate Amisheila Kinua and is used here with her permission.

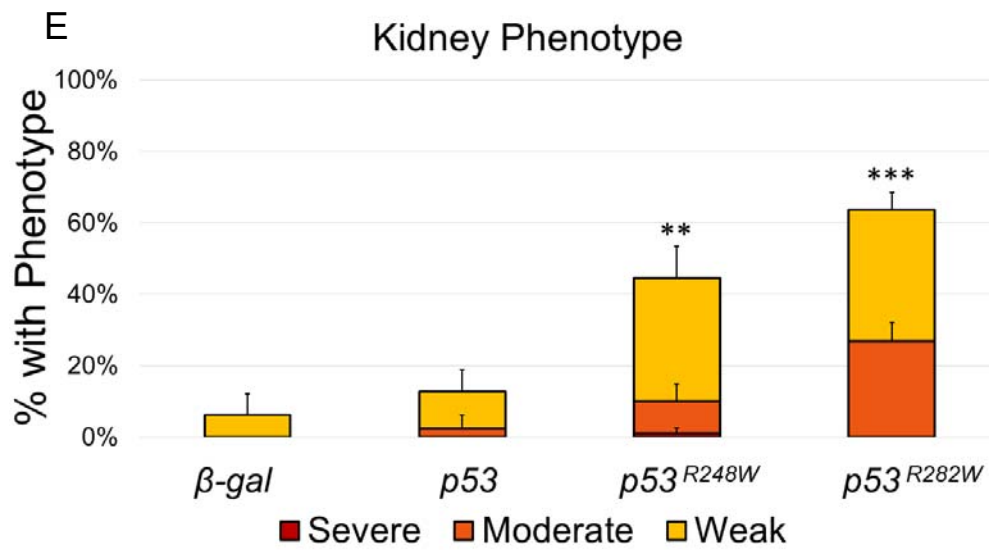
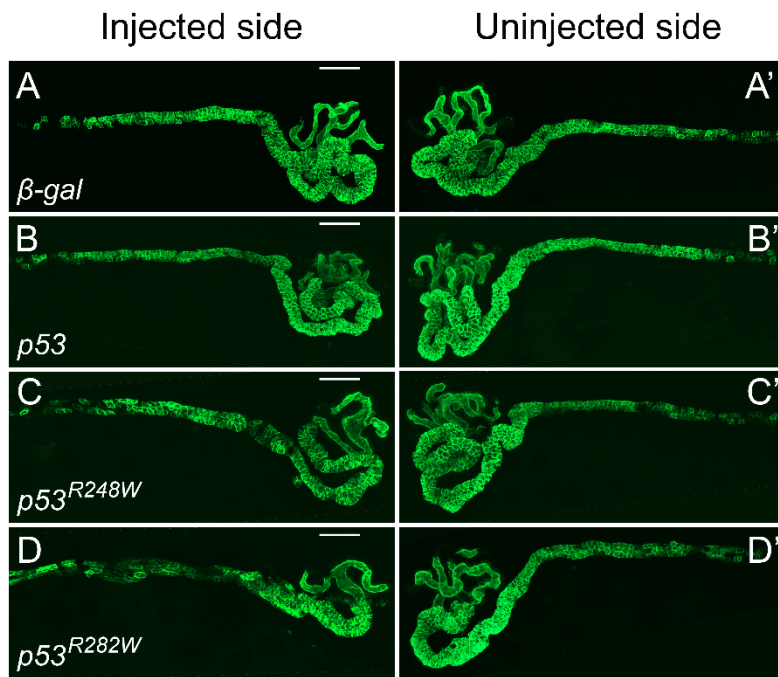


Figure 31. Mutant Human p53 Disrupts Kidney Development in *Xenopus*.

(A–D) Embryos were unilaterally injected at the 8-cell stage with 300 pg of *β-gal*, wild-type, *p53^{R248W}*, or *p53^{R282W}* mRNA. Stage 40 tadpoles were stained with kidney antibodies 3G8, which labels the proximal tubules, and 4A6, which labels the distal and connecting tubules. Letters without apostrophes (A–D) represent the injected side, whereas letters with apostrophes (A'–D') represent the uninjected side. (C–D) Overexpression of mutant p53 disrupts kidney development while (B) wild-type p53 does not. (A) *β-gal* serves as a negative control and scale bars represent 100 μm. (E) The graph demonstrates a significant difference between embryos injected with either *p53^{R248W}*, or *p53^{R282W}* mRNA compared to those injected with wild-type *p53* mRNA. Significance was established against embryos that had a weak (yellow bar), moderate (orange bar) or severe kidney (red bar) phenotype using a two tailed T-test. Double asterisk (**) indicates $p < 0.007$ while triple asterisk (***) indicates $p < 0.0006$. Error bars represent standard error. For scoring system of *Xenopus* embryonic kidneys, please refer to Figure 14.

Sanger sequencing/TIDE analysis. Because p53 has an essential role in apoptosis, future research should include both proliferation and apoptosis assays to assess if either accounts for the kidney phenotype found in these embryos.

Furthermore, we present a novel genetic contribution of p53 to CAKUT in patients with Li-Fraumeni syndrome. Our collaborator Zubaida Saifudeen identified from clinical MRIs that nine of twenty-nine (31%) Li-Fraumeni patients in this study with both non-functional and dominant negative mutations have a higher prevalence of CAKUT. Additionally, thirteen of the twenty-nine (45%) Li-Fraumeni patients examined had glomerular filtration rates lower than 90, which indicates loss of kidney function.

We found that overexpression of Li-Fraumeni patient mutant mRNA led to a similar phenotype as loss of p53, though the kidney defect was less severe. This indicates that dominant negative variants in this gene are likely causative for the observed CAKUT phenotype in some patients. The human mutant mRNA may elicit a more attenuated phenotype because it may not exert a dominant negative affect to every DNA binding tetramer it forms or not all p53 tetramers acquire mutant monomers. Western blot also demonstrates mutant p53 is potentially less stable, thus a portion of it could degrade before kidney development is finished ultimately leading to a lessened effect. In summary, p53 plays a role in both *Xenopus* and human kidney development. Based on our data, we empirically recommend that individuals with Li-Fraumeni syndrome undergo a renal and urogenital ultrasound as part of their clinical workup.

CHAPTER 7: BIBLIOGRAPHY

1. Lawrence, E. A., D. Doherty, and R. Dhanda. 2018. Function of the nephron and the formation of urine. *Anaesth. Intensive Care Med.* .
2. Little, M. H., and A. P. McMahon. 2012. Mammalian kidney development: Principles, progress, and projections. *Cold Spring Harb. Perspect. Biol.* .
3. Black, M. J., M. R. Sutherland, and L. Gubhaju. 2012. Effects of Preterm Birth on the Kidney. *Basic Nephrol. Acute Kidney Inj.* .
4. Rosselot, C., L. Spraggon, I. Chia, E. Batourina, P. Riccio, B. Lu, K. Niederreither, P. Dolle, G. Duester, P. Chambon, F. Costantini, T. Gilbert, A. Molotkov, and C. Mendelsohn. 2010. Non-cell-autonomous retinoid signaling is crucial for renal development. *Development* 137: 283–292.
5. Al-Maawali, A., A. Walfisch, and G. Koren. 2012. Taking angiotensin-converting enzyme inhibitors during pregnancy: Is it safe? *Can. Fam. Physician* 58: 49–51.
6. Davidson, A. 2008. Mouse kidney development. *StemBook* .
7. Takasato, M., and M. H. Little. 2015. The origin of the mammalian kidney: Implications for recreating the kidney in vitro. *Dev.*
8. Costantini, F. 2012. Genetic controls and cellular behaviors in branching morphogenesis of the renal collecting system. *Wiley Interdiscip. Rev. Dev. Biol.* .
9. Dressler, G. R. 2006. The Cellular Basis of Kidney Development. *Annu. Rev. Cell Dev. Biol.* 22: 509–529.
10. Bertram, J. F., R. N. Douglas-Denton, B. Diouf, M. D. Hughson, and W. E. Hoy.

2011. Human nephron number: Implications for health and disease. In *Pediatric Nephrology* vol. 26. 1529–1533.
11. Short, K. M., A. N. Combes, J. Lefevre, A. L. Ju, K. M. Georgas, T. Lamberton, O. Cairncross, B. A. Rumballe, A. P. McMahon, N. A. Hamilton, I. M. Smyth, and M. H. Little. 2014. Global quantification of tissue dynamics in the developing mouse kidney. *Dev. Cell* 29: 188–202.
12. T.P. Fleming. 2012. Epithelial Organization and Development. *Springer Sci. Bus. Media* 385.
13. Raciti, D., L. Reggiani, L. Geffers, Q. Jiang, F. Bacchion, A. E. Subrizi, D. Clements, C. Tindal, D. R. Davidson, B. Kaissling, and A. W. Brändli. 2008. Organization of the pronephric kidney revealed by large-scale gene expression mapping. *Genome Biol.* 9: R84.
14. Fox, H. 1963. The Amphibian Pronephros. *Q. Rev. Biol.* 38: 1–25.
15. Vize, P. D., T. J. Carroll, and J. B. Wallingford. 2003. Induction, Development, and Physiology of the Pronephric Tubules. In *The Kidney: From Normal Development to Congenital Disease* 19–50.
16. Tena, J. J., A. Neto, E. de la Calle-Mustienes, C. Bras-Pereira, F. Casares, and J. L. Gómez-Skarmeta. 2007. Odd-skipped genes encode repressors that control kidney development. *Dev. Biol.* 301: 518–531.
17. Drews, C., S. Senkel, and G. U. Ryffel. 2011. The nephrogenic potential of the transcription factors *osr1*, *osr2*, *hnf1b*, *lhx1* and *pax8* assessed in *Xenopus* animal

caps. *BMC Dev. Biol.* 11.

18. Boualia, S. K., Y. Gaitan, M. Tremblay, R. Sharma, J. Cardin, A. Kania, and M. Bouchard. 2013. A core transcriptional network composed of Pax2/8, Gata3 and Lim1 regulates key players of pro/mesonephros morphogenesis. *Dev. Biol.* 382: 555–566.

19. Buisson, I., R. Le Bouffant, M. Futel, J. F. Riou, and M. Umbhauer. 2015. Pax8 and Pax2 are specifically required at different steps of *Xenopus* pronephros development. *Dev. Biol.* 397: 175–190.

20. DeLay, B. D., M. E. Corkins, H. L. Hanania, M. Salanga, J. M. Deng, N. Sudou, M. Taira, M. E. Horb, and R. K. Miller. 2018. Tissue-specific Gene Inactivation in *Xenopus laevis*: Knockout of *lhx1* in the Kidney with CRISPR/Cas9. *Genetics* 208: 673–686.

21. Shawlot, W., and R. R. Behringer. 1995. Requirement for *lim1* in head-organizer function. *Nature* 374: 425–430.

22. Bouchard, M., A. Souabni, M. Mandler, A. Neubüser, and M. Busslinger. 2002. Nephric lineage specification by Pax2 and Pax8. *Genes Dev.* 16: 2958–2970.

23. Gong, Y., Z. Ma, V. Patel, E. Fischer, T. Hiesberger, M. Pontoglio, and P. Igarashi. 2009. HNF-1 Regulates Transcription of the PKD Modifier Gene *Kif12*. *J. Am. Soc. Nephrol.* 20: 41–47.

24. Costantini, F., and R. Kopan. 2010. Patterning a complex organ: Branching morphogenesis and nephron segmentation in kidney development. *Dev. Cell* 18:

698–712.

25. Møbjerg, N., E. H. Larsen, and Å. Jespersen. 2000. Morphology of the kidney in larvae of *Bufo viridis* (amphibia, anura, bufonidae). *J. Morphol.* 245: 177–195.

26. Urban, A. E., X. Zhou, J. M. Ungos, D. W. Raible, C. R. Altmann, and P. D. Vize. 2006. FGF is essential for both condensation and mesenchymal-epithelial transition stages of pronephric kidney tubule development. *Dev. Biol.* 297: 103–117.

27. Wessely, O., and U. Tran. 2011. *Xenopus* pronephros development-past, present, and future. In *Pediatric Nephrology*.

28. Zhou, X., and P. D. Vize. 2004. Proximo-distal specialization of epithelial transport processes within the *Xenopus* pronephric kidney tubules. *Dev. Biol.* 271: 322–338.

29. Eid, S. R., A. Terrettaz, K. Nagata, and A. W. Brändli. 2002. Embryonic expression of *Xenopus* SGLT-1L, a novel member of the solute carrier family 5 (SLC5), is confined to tubules of the pronephric kidney. *Int. J. Dev. Biol.* 46: 177–184.

30. Zhou, X., and P. D. Vize. 2005. Pronephric regulation of acid-base balance; coexpression of carbonic anhydrase type 2 and sodium-bicarbonate cotransporter-1 in the late distal segment. *Dev. Dyn.* 233: 142–144.

31. Christensen, E. I., D. Raciti, L. Reggiani, P. J. Verroust, and A. W. Brändli. 2008. Gene expression analysis defines the proximal tubule as the compartment for endocytic receptor-mediated uptake in the *Xenopus* pronephric kidney. *Pflügers*

Arch. Eur. J. Physiol. 456: 1163–1176.

32. Reggiani, L., D. Raciti, R. Airik, A. Kispert, and A. W. Brändli. 2007. The prepattern transcription factor *Ir3* directs nephron segment identity. *Genes Dev.* 21: 2358–2370.

33. Vize, P. D. 2003. The chloride conductance channel *ClC-K* is a specific marker for the *Xenopus* pronephric distal tubule and duct. *Gene Expr. Patterns* 3: 347–350.

34. Zhou, X., and P. D. Vize. 2005. Amino acid cotransporter *SLC3A2* is selectively expressed in the early proximal segment of *Xenopus* pronephric kidney nephrons. *Gene Expr. Patterns* 5: 774–777.

35. Lindström, N. O., T. Tran, J. Guo, E. Rutledge, R. K. Parvez, M. E. Thornton, B. Grubbs, J. A. McMahon, and A. P. McMahon. 2018. Conserved and Divergent Molecular and Anatomic Features of Human and Mouse Nephron Patterning. *J. Am. Soc. Nephrol.* ASN.2017091036.

36. Kaminski, M. M., J. Tosić, C. Kresbach, H. Engel, J. Klockenbusch, A.-L. Müller, R. Pichler, F. Grahammer, O. Kretz, T. B. Huber, G. Walz, S. J. Arnold, and S. S. Lienkamp. 2016. Direct reprogramming of fibroblasts into renal tubular epithelial cells by defined transcription factors. *Nat. Cell Biol.* 18: 1269–1280.

37. Komiya, Y., and R. Habas. 2008. Wnt signal transduction pathways. *Organogenesis* .

38. Huelsken, J., and J. Behrens. 2002. The Wnt signalling pathway. *J. Cell Sci.* .

39. MacDonald, B. T., K. Tamai, and X. He. 2009. Wnt/ β -Catenin Signaling:

Components, Mechanisms, and Diseases. *Dev. Cell* .

40. Yamanaka, H., T. Moriguchi, N. Masuyama, M. Kusakabe, H. Hanafusa, R. Takada, S. Takada, and E. Nishida. 2002. JNK functions in the non-canonical Wnt pathway to regulate convergent extension movements in vertebrates. *EMBO Rep.*

41. Carroll, T. J., J. S. Park, S. Hayashi, A. Majumdar, and A. P. McMahon. 2005. Wnt9b plays a central role in the regulation of mesenchymal to epithelial transitions underlying organogenesis of the mammalian urogenital system. *Dev. Cell* 9: 283–292.

42. Iglesias, D. M., P.-A. Hueber, L. Chu, R. Campbell, A.-M. Patenaude, A. J. Dziarmaga, J. Quinlan, O. Mohamed, D. Dufort, and P. R. Goodyer. 2007. Canonical WNT signaling during kidney development. *Am. J. Physiol. Renal Physiol.* 293: F494-500.

43. Saulnier, D. M. E., H. Ghanbari, and A. W. Brändli. 2002. Essential Function of Wnt-4 for Tubulogenesis in the *Xenopus* Pronephric Kidney. *Dev. Biol.* 248: 13–28.

44. Lyons, J. P., R. K. Miller, X. Zhou, G. Weidinger, T. Deroo, T. Denayer, J. Il Park, H. Ji, J. Y. Hong, A. Li, R. T. Moon, E. A. Jones, K. Vleminckx, P. D. Vize, and P. D. McCrea. 2009. Requirement of Wnt/ β -catenin signaling in pronephric kidney development. *Mech. Dev.* 126: 142–159.

45. Park, J.-S., M. T. Valerius, and A. P. McMahon. 2007. Wnt/beta-catenin signaling regulates nephron induction during mouse kidney development. *Development* 134: 2533–2539.

46. Bridgewater, D., B. Cox, J. Cain, A. Lau, V. Athaide, P. S. Gill, S. Kuure, K. Sainio, and N. D. Rosenblum. 2008. Canonical WNT/ β -catenin signaling is required for ureteric branching. *Dev. Biol.* 317: 83–94.
47. Karner, C. M., A. Das, Z. Ma, M. Self, C. Chen, L. Lum, G. Oliver, and T. J. Carroll. 2011. Canonical Wnt9b signaling balances progenitor cell expansion and differentiation during kidney development. *Development* 138: 1247–1257.
48. Vivante, A., M. Mark-Danieli, M. Davidovits, O. Harari-Steinberg, D. Omer, Y. Gnatek, R. Cleper, D. Landau, Y. Kovalski, I. Weissman, I. Eisenstein, M. Soudack, H. R. Wolf, N. Issler, D. Lotan, Y. Anikster, and B. Dekel. 2013. Renal Hypodysplasia Associates with a Wnt4 Variant that Causes Aberrant Canonical Wnt Signaling. *J. Am. Soc. Nephrol.* 24: 550–558.
49. Naylor, R. W., and E. a Jones. 2009. Notch activates Wnt-4 signalling to control medio-lateral patterning of the pronephros. *Development* 136: 3585–95.
50. Kim, M. S., S. K. Yoon, F. Bollig, J. Kitagaki, W. Hur, N. J. Whye, Y. P. Wu, M. N. Rivera, J. Y. Park, H. S. Kim, K. Malik, D. W. Bell, C. Englert, A. O. Perantoni, and S. B. Lee. 2010. A novel wilms tumor 1 (WT1) target gene negatively regulates the WNT signaling pathway. *J. Biol. Chem.* 285: 14585–14593.
51. Murugan, S., J. Shan, S. J. Kühl, A. Tata, I. Pietilä, M. Kühl, and S. J. Vainio. 2012. WT1 and Sox11 regulate synergistically the promoter of the Wnt4 gene that encodes a critical signal for nephrogenesis. *Exp. Cell Res.* 318: 1134–1145.
52. Saadi-Kheddouci, S., D. Berrebi, B. Romagnolo, F. Cluzeaud, M. Peuchmaur, a Kahn, a Vandewalle, and C. Perret. 2001. Early development of polycystic kidney

disease in transgenic mice expressing an activated mutant of the beta-catenin gene. *Oncogene* 20: 5972–81.

53. Vivante, A., S. Kohl, D. Y. Hwang, G. C. Dworschak, and F. Hildebrandt. 2014. Single-gene causes of congenital anomalies of the kidney and urinary tract (CAKUT) in humans. In *Pediatric Nephrology* vol. 29. 695–704.

54. Yosypiv, I. V. 2012. Congenital anomalies of the kidney and urinary tract: A genetic disorder? *Int. J. Nephrol.* 2012.

55. Van Der Ven, A. T., D. M. Connaughton, H. Ityel, N. Mann, M. Nakayama, J. Chen, A. Vivante, D. Hwang, J. Schulz, D. A. Braun, J. M. Schmidt, D. Schapiro, R. Schneider, J. K. Warejko, A. Daga, A. J. Majmundar, W. Tan, T. Jobst-Schwan, T. Hermle, E. Widmeier, S. Ashraf, A. Amar, C. A. Hoogstraaten, H. Hugo, T. M. Kitzler, F. Kause, C. M. Kolvenbach, R. Dai, L. Spaneas, K. Amann, D. R. Stein, M. A. Baum, M. J. G. Somers, N. M. Rodig, M. A. Ferguson, A. Z. Traum, G. H. Daouk, R. Bogdanovic, N. Stajic, N. A. Soliman, J. A. Kari, S. El Desoky, H. M. Fathy, D. Milosevic, M. Al-Saffar, H. S. Awad, L. A. Eid, A. Selvin, P. Senguttuvan, S. Sanna-Cherchi, H. L. Rehm, D. G. MacArthur, M. Lek, K. M. Laricchia, M. W. Wilson, S. M. Mane, R. P. Lifton, R. S. Lee, S. B. Bauer, W. Lu, H. M. Reutter, V. Tasic, S. Shril, and F. Hildebrandt. 2018. Whole-exome sequencing identifies causative mutations in families with congenital anomalies of the kidney and urinary tract. *J. Am. Soc. Nephrol.*

56. Sanna-Cherchi, S., R. Westland, G. M. Ghiggeri, and A. G. Gharavi. 2018. Genetic basis of human congenital anomalies of the kidney and urinary tract. *J. Clin.*

Invest. 128: 4–15.

57. Hurtado del Pozo, C., E. Garreta, J. C. Izpisúa Belmonte, and N. Montserrat.

2018. Modeling epigenetic modifications in renal development and disease with organoids and genome editing. *Dis. Model. Mech.* 11: dmm035048.

58. Hellsten, U., R. M. Harland, M. J. Gilchrist, D. Hendrix, J. Jurka, V. Kapitonov, I.

Ovcharenko, N. H. Putnam, S. Shu, L. Taher, I. L. Blitz, B. Blumberg, D. S.

Dichmann, I. Dubchak, E. Amaya, J. C. Detter, R. Fletcher, D. S. Gerhard, D.

Goodstein, T. Graves, I. V Grigoriev, J. Grimwood, T. Kawashima, E. Lindquist, S.

M. Lucas, P. E. Mead, T. Mitros, H. Ogino, Y. Ohta, A. V Poliakov, N. Pollet, J.

Robert, A. Salamov, A. K. Sater, J. Schmutz, A. Terry, P. D. Vize, W. C. Warren, D.

Wells, A. Wills, R. K. Wilson, L. B. Zimmerman, A. M. Zorn, R. Grainger, T.

Grammer, M. K. Khokha, P. M. Richardson, and D. S. Rokhsar. 2010. The genome of the Western clawed frog *Xenopus tropicalis*. *Science* 328: 633–6.

59. Quassinti, L., E. Maccari, O. Murri, and M. Bramucci. 2007. Comparison of ACE activity in amphibian tissues: *Rana esculenta* and *Xenopus laevis*. *Comp. Biochem. Physiol. - A Mol. Integr. Physiol.* 146: 119–123.

60. Gribouval, O., V. Morinière, A. Pawtowski, C. Arrondel, S. L. Sallinen, C.

Saloranta, C. Clericuzio, G. Viot, J. Tantau, S. Blesson, S. Cloarec, M. C. Machet, D.

Chitayat, C. Thauvin, N. Laurent, J. R. Sampson, J. A. Bernstein, A. Clemenson, F.

Prieur, L. Daniel, A. Levy-Mozziconacci, K. Lachlan, J. L. Alessandri, F. Cartault, J.

P. Rivière, N. Picard, C. Baumann, A. L. Delezoide, M. B. Ortega, N. Chassaing, P.

Labrune, S. Yu, H. Firth, D. Wellesley, M. Bitzan, A. Alfares, N. Braverman, L.

Krogh, J. Tolmie, H. Gaspar, B. Doray, S. Majore, D. Bonneau, S. Triau, C. Loirat, A. David, D. Bartholdi, A. Peleg, D. Brackman, R. Stone, R. DeBerardinis, P. Corvol, A. Michaud, C. Antignac, and M. C. Gubler. 2012. Spectrum of mutations in the renin-angiotensin system genes in autosomal recessive renal tubular dysgenesis. *Hum. Mutat.* 33: 316–326.

61. Holbrook, J. D., and C. J. Danpure. 2002. Molecular basis for the dual mitochondrial and cytosolic localization of alanine:glyoxylate aminotransferase in amphibian liver cells. *J. Biol. Chem.* 277: 2336–2344.

62. Hoff, S., J. Halbritter, D. Epting, V. Frank, T.-M. T. Nguyen, J. van Reeuwijk, C. Boehlke, C. Schell, T. Yasunaga, M. Helmstädter, M. Mergen, E. Filhol, K. Boldt, N. Horn, M. Ueffing, E. A. Otto, T. Eisenberger, M. W. Elting, J. A. E. van Wijk, D. Bockenhauer, N. J. Sebire, S. Rittig, M. Vyberg, T. Ring, M. Pohl, L. Pape, T. J. Neuhaus, N. A. S. Elshakhs, S. J. Koon, P. C. Harris, F. Grahammer, T. B. Huber, E. W. Kuehn, A. Kramer-Zucker, H. J. Bolz, R. Roepman, S. Saunier, G. Walz, F. Hildebrandt, C. Bergmann, and S. S. Lienkamp. 2013. ANKS6 is a central component of a nephronophthisis module linking NEK8 to INVS and NPHP3. *Nat. Genet.* 45: 951–956.

63. Taskiran, E. Z., E. Korkmaz, S. Gucer, C. Kosukcu, F. Kaymaz, C. Koyunlar, E. C. Bryda, M. Chaki, D. Lu, K. Vadnagara, C. Candan, R. Topaloglu, F. Schaefer, M. Attanasio, C. Bergmann, and F. Ozaltin. 2014. Mutations in ANKS6 Cause a Nephronophthisis-Like Phenotype with ESRD. *J. Am. Soc. Nephrol.* 25: 1653–1661.

64. Tran, U., L. M. Pickney, B. D. Özpolat, and O. Wessely. 2007. Xenopus

Bicaudal-C is required for the differentiation of the amphibian pronephros. *Dev. Biol.* 307: 152–164.

65. Tran, U., L. Zakin, A. Schweickert, R. Agrawal, R. Doger, M. Blum, E. M. De Robertis, and O. Wessely. 2010. The RNA-binding protein bicaudal C regulates polycystin 2 in the kidney by antagonizing miR-17 activity. *Development* 137: 1107–1116.

66. Kraus, M. R. C., S. Clauin, Y. Pfister, M. Di Maïo, T. Ulinski, D. Constam, C. Bellanné-Chantelot, and A. Grapin-Botton. 2012. Two mutations in human BICC1 resulting in wnt pathway hyperactivity associated with cystic renal dysplasia. *Hum. Mutat.* 33: 86–90.

67. Lian, P., A. Li, Y. Li, H. Liu, D. Liang, B. Hu, D. Lin, T. Jiang, G. Moeckel, D. Qin, and G. Wu. 2014. Loss of polycystin-1 inhibits Bicc1 expression during mouse development. *PLoS One* 9.

68. Bracken, C. M., K. Mizeracka, and K. A. McLaughlin. 2008. Patterning the embryonic kidney: BMP signaling mediates the differentiation of the pronephric tubules and duct in *Xenopus laevis*. *Dev. Dyn.* 237: 132–144.

69. Weber, S., J. C. Taylor, P. Winyard, K. F. Baker, J. Sullivan-Brown, R. Schild, T. Knuppel, A. M. Zurowska, A. Caldas-Alfonso, M. Litwin, S. Emre, G. M. Ghiggeri, A. Bakkaloglu, O. Mehls, C. Antignac, E. Network, F. Schaefer, and R. D. Burdine. 2008. SIX2 and BMP4 Mutations Associate With Anomalous Kidney Development. *J. Am. Soc. Nephrol.* 19: 891–903.

70. Neugebauer, J. M., S. Kwon, H.-S. Kim, N. Donley, A. Tilak, S. Sopory, and J. L.

Christian. 2015. The prodomain of BMP4 is necessary and sufficient to generate stable BMP4/7 heterodimers with enhanced bioactivity in vivo. *Proc. Natl. Acad. Sci. U. S. A.* 112: E2307-16.

71. Wang, S., M. Krinks, L. Kleinwaks, and M. Moos. 1997. A novel *Xenopus* homologue of bone morphogenetic protein-7 (BMP-7). *Genes Funct.* 1: 259–271.

72. Hwang, D. Y., G. C. Dworschak, S. Kohl, P. Saisawat, A. Vivante, A. C. Hilger, H. M. Reutter, N. A. Soliman, R. Bogdanovic, E. O. Kehinde, V. Tasic, and F. Hildebrandt. 2014. Mutations in 12 known dominant disease-causing genes clarify many congenital anomalies of the kidney and urinary tract. *Kidney Int.* 85: 1429–1433.

73. Simon, D. B., R. S. Bindra, T. A. Mansfield, C. NelsonWilliams, E. Mendonca, R. Stone, S. Schurman, A. Nayir, H. Alpay, A. Bakkaloglu, J. RodriguezSoriano, J. M. Morales, S. A. Sanjad, C. M. Taylor, D. Pilz, A. Brem, H. Trachtman, W. Griswold, G. A. Richard, E. John, and R. P. Lifton. 1997. Mutations in the chloride channel gene, *CLCNKB*, cause Bartter's syndrome type III. *Nat Genet* 17: 171–178.

74. Seys, E., O. Andrini, M. Keck, L. Mansour-Hendili, P.-Y. Courand, C. Simian, G. Deschenes, T. Kwon, A. Bertholet-Thomas, G. Bobrie, J. S. Borde, G. Bourdat-Michel, S. Decramer, M. Cailliez, P. Krug, P. Cozette, J. D. Delbet, L. Dubourg, D. Chaveau, M. Fila, N. Jourde-Chiche, B. Knebelmann, M.-P. Lavocat, S. Lemoine, D. Djeddi, B. Llanas, F. Louillet, E. Merieau, M. Mileva, L. Mota-Vieira, C. Mousson, F. Nobili, R. Novo, G. Roussey-Kesler, I. Vrillon, S. B. Walsh, J. Teulon, A. Blanchard, and R. Vargas-Poussou. 2017. Clinical and Genetic Spectrum of Bartter Syndrome

Type 3. *J. Am. Soc. Nephrol.* ASN.2016101057.

75. Abdelhak, S., V. Kalatzis, R. Heilig, S. Compain, D. Samson, C. Vincent, D. Weil, C. Cruaud, I. Sahly, M. Leibovici, M. Bitner-Glindzicz, M. Francis, D. Lacombe, J. Vigneron, R. Charachon, K. Boven, P. Bedbeder, N. Van Regemorter, J. Weissenbach, and C. Petit. 1997. A human homologue of the *Drosophila* eyes absent gene underlies branchio-oto-renal (BOR) syndrome and identifies a novel gene family. *Nat. Genet.* 15: 157–164.

76. Li, Y., J. M. Manaligod, and D. L. Weeks. 2010. EYA1 mutations associated with the branchio-oto-renal syndrome result in defective otic development in *Xenopus laevis*. *Biol. Cell* 102: 277–92.

77. Nakano, T., F. Niimura, K. Hohenfellner, E. Miyakita, and I. Ichikawa. 2003. Screening for Mutations in BMP4 and FOXC1 Genes in Congenital Anomalies of the Kidney and Urinary Tract in Humans. *Tokai J. Exp. Clin. Med.* 28: 121–126.

78. Maguire, R. J., H. V. Isaacs, and M. E. Pownall. 2012. Early transcriptional targets of MyoD link myogenesis and somitogenesis. *Dev. Biol.* 371: 256–268.

79. Yildirim-Toruner, C., K. Subramanian, L. El Manjra, E. Chen, S. Goldstein, and E. Vitale. 2004. A novel frameshift mutation of FOXC2 gene in a family with hereditary lymphedema-distichiasis syndrome associated with renal disease and diabetes mellitus. *Am. J. Med. Genet. A* 131: 281–6.

80. White, J. T., B. Zhang, D. M. Cerqueira, U. Tran, and O. Wessely. 2010. Notch signaling, wt1 and foxc2 are key regulators of the podocyte gene regulatory network in *Xenopus*. *Development* 137: 1863–1873.

81. Deconinck, A. E., P. E. Mead, S. G. Tevosian, J. D. Crispino, S. G. Katz, L. I. Zon, and S. H. Orkin. 2000. FOG acts as a repressor of red blood cell development in *Xenopus*. *Development* 127: 2031–2040.
82. Van Esch, H., P. Groenen, M. A. Nesbit, S. Schuffenhauer, P. Lichtner, G. Vanderlinden, B. Harding, R. Beetz, R. W. Bilous, I. Holdaway, N. J. Shaw, J.-P. Fryns, W. Van de Ven, R. V. Thakker, and K. Devriendt. 2000. GATA3 haplo-insufficiency causes human HDR syndrome. *Nature* 406: 419–422.
83. Kyuno, J., and E. A. Jones. 2007. GDNF expression during *Xenopus* development. *Gene Expr. Patterns* 7: 313–7.
84. Prato, A. P., M. Musso, I. Ceccherini, G. Mattioli, C. Giunta, G. M. Ghiggeri, and V. Jasonni. 2009. Hirschsprung disease and congenital anomalies of the kidney and urinary tract (CAKUT): A novel syndromic association. *Medicine (Baltimore)*. 88: 83–90.
85. Bohn, S., H. Thomas, G. Turan, S. Ellard, C. Bingham, A. T. Hattersley, and G. U. Ryffel. 2003. Distinct molecular and morphogenetic properties of mutations in the human HNF1beta gene that lead to defective kidney development. *J. Am. Soc. Nephrol.* 14: 2033–2041.
86. Roose, M., K. Sauert, G. Turan, N. Solomentsew, D. Werdien, K. Pramanik, S. Senkel, G. U. Ryffel, and C. Waldner. 2009. Heat-shock inducible cre strains to study organogenesis in transgenic *xenopus laevis*. *Transgenic Res.* 18: 595–605.
87. Nagamani, S. C. S., A. Erez, J. Shen, C. Li, E. Roeder, S. Cox, L. Karaviti, M. Pearson, S. H. L. Kang, T. Sahoo, S. R. Lalani, P. Stankiewicz, V. R. Sutton, and S.

- W. Cheung. 2010. Clinical spectrum associated with recurrent genomic rearrangements in chromosome 17q12. *Eur. J. Hum. Genet.* 18: 278–284.
88. Verdeguer, F., S. Le Corre, E. Fischer, C. Callens, S. Garbay, A. Doyen, P. Igarashi, F. Terzi, and M. Pontoglio. 2010. A mitotic transcriptional switch in polycystic kidney disease. *Nat. Med.* 16: 106–110.
89. Sauert, K., S. Kahnert, M. Roose, M. Gull, A. W. Brandli, G. U. Ryffel, and C. Waldner. 2012. Heat-shock mediated overexpression of HNF1beta mutations has differential effects on gene expression in the *Xenopus* pronephric kidney. *PLoS One* 7: e33522.
90. Halbritter, J., J. D. Porath, K. A. Diaz, D. A. Braun, S. Kohl, M. Chaki, S. J. Allen, N. A. Soliman, F. Hildebrandt, and E. A. Otto. 2013. Identification of 99 novel mutations in a worldwide cohort of 1,056 patients with a nephronophthisis-related ciliopathy. *Hum. Genet.* 132: 865–884.
91. Miner, J. H., R. Morello, K. L. Andrews, C. Li, C. Antignac, A. S. Shaw, and B. Lee. 2002. Transcriptional induction of slit diaphragm genes by Lmx1b is required in podocyte differentiation. *J. Clin. Invest.* 109: 1065–1072.
92. Haldin, C. E., K. L. Massé, S. Bhamra, S. Simrick, J. ichi Kyuno, and E. A. Jones. 2008. The *Imx1b* gene is pivotal in glomus development in *Xenopus laevis*. *Dev. Biol.* 322: 74–85.
93. Edwards, N., S. J. Rice, S. Raman, A. M. Hynes, S. Srivastava, I. Moore, M. Al-Hamed, Y. Xu, M. Santibanez-Koref, D. T. Thwaites, D. P. Gale, and J. A. Sayer. 2015. A novel LMX1B mutation in a family with end-stage renal disease of “unknown

cause.” *Clin. Kidney J.* 8: 113–119.

94. Zalli, D., R. Bayliss, and A. M. Fry. 2012. The Nek8 protein kinase, mutated in the human cystic kidney disease nephronophthisis, is both activated and degraded during ciliogenesis. *Hum. Mol. Genet.* 21: 1155–1171.

95. Olbrich, H., M. Fliegauf, J. Hoefele, A. Kispert, E. Otto, A. Volz, M. T. Wolf, G. Sasmaz, U. Trauer, R. Reinhardt, R. Sudbrak, C. Antignac, N. Gretz, G. Walz, B. Schermer, T. Benzing, F. Hildebrandt, and H. Omran. 2003. Mutations in a novel gene, NPHP3, cause adolescent nephronophthisis, tapeto-retinal degeneration and hepatic fibrosis. *Nat. Genet.* 34: 455–459.

96. Vivante, A., N. Mann, H. Yonath, A.-C. Weiss, M. Getwan, M. M. Kaminski, T. Bohnenpoll, C. Teyssier, J. Chen, S. Shril, A. T. van der Ven, H. Ityel, J. M. Schmidt, E. Widmeier, S. B. Bauer, S. Sanna-Cherchi, A. G. Gharavi, W. Lu, D. Magen, R. Shukrun, R. P. Lifton, V. Tasic, H. C. Stanescu, V. Cavaillès, R. Kleta, Y. Anikster, B. Dekel, A. Kispert, S. S. Lienkamp, and F. Hildebrandt. 2017. A Dominant Mutation in Nuclear Receptor Interacting Protein 1 Causes Urinary Tract Malformations *via* Dysregulation of Retinoic Acid Signaling. *J. Am. Soc. Nephrol.* ASN.2016060694.

97. Woolf, A. S. 2000. A molecular and genetic view of human renal and urinary tract malformations. *Kidney Int.*

98. Lu, W., X. Shen, A. Pavlova, M. Lakkis, C. J. Ward, L. Pritchard, P. C. Harris, D. R. Genest, A. R. Perez-Atayde, and J. Zhou. 2001. Comparison of Pkd1-targeted mutants reveals that loss of polycystin-1 causes cystogenesis and bone defects. *Hum Mol Genet* 10: 2385–2396.

99. Burtsey, S., C. Leclerc, E. Nabais, P. Munch, C. Gohory, M. Moreau, and M. Fontés. 2005. Cloning and expression of the amphibian homologue of the human PKD1 gene. *Gene* 357: 29–36.
100. Deltas, C. C. 2001. Mutations of the human polycystic kidney disease 2 (PKD2) gene. *Hum. Mutat.* 18: 13–24.
101. Kim, I., T. Ding, Y. Fu, C. Li, L. Cui, A. Li, P. Lian, D. Liang, D. W. Wand, C. Guo, J. Ma, P. Zhao, R. J. Coffey, Q. Zhan, and G. Wu. 2009. Conditional Mutation of Pkd2 Causes Cystogenesis and Upregulates β -Catenin. *J Am Soc Nephrol* 20: 2556–2569.
102. Carroll, T., J. B. Wallingford, D. Seufert, and P. D. Vize. 1998. Molecular Regulation of Pronephric Development. *Curr. Top. Dev. Biol.* 44: 67–100.
103. Skinner, M. A., S. D. Safford, J. G. Reeves, M. E. Jackson, and A. J. Freemerman. 2008. Renal Aplasia in Humans Is Associated with RET Mutations. *Am. J. Hum. Genet.* 82: 344–351.
104. Nishinakamura, R. 2003. Kidney development conserved over species: Essential roles of Sall1. *Semin. Cell Dev. Biol.* 14: 241–247.
105. Ruf, R. G., P.-X. Xu, D. Silvius, E. A. Otto, F. Beekmann, U. T. Muerb, S. Kumar, T. J. Neuhaus, M. J. Kemper, R. M. Raymond, P. D. Brophy, J. Berkman, M. Gattas, V. Hyland, E.-M. Ruf, C. Schwartz, E. H. Chang, R. J. H. Smith, C. A. Stratakis, D. Weil, C. Petit, and F. Hildebrandt. 2004. SIX1 mutations cause branchio-oto-renal syndrome by disruption of EYA1-SIX1-DNA complexes. *Proc. Natl. Acad. Sci.* 101: 8090–8095.

106. Yan, B., K. M. Neilson, R. Ranganathan, T. Maynard, A. Streit, and S. A. Moody. 2015. Microarray identification of novel genes downstream of Six1, a critical factor in cranial placode, somite, and kidney development. *Dev. Dyn.* 244: 181–210.
107. Suzuki, N., K. Hirano, H. Ogino, and H. Ochi. 2015. Identification of distal enhancers for Six2 expression in pronephros. *Int. J. Dev. Biol.* 59: 241–246.
108. Sinner, D., P. Kirilenko, S. Rankin, E. Wei, L. Howard, M. Kofron, J. Heasman, H. R. Woodland, and A. M. Zorn. 2006. Global analysis of the transcriptional network controlling *Xenopus* endoderm formation. *Development* 133: 1955–66.
109. Gimelli, S., G. Caridi, S. Beri, K. McCracken, R. Bocciardi, P. Zordan, M. Dagnino, P. Fiorio, L. Murer, E. Benetti, O. Zuffardi, R. Giorda, J. M. Wells, G. Gimelli, and G. M. Ghiggeri. 2010. Mutations in SOX17 are associated with congenital anomalies of the kidney and the urinary tract. *Hum. Mutat.* 31: 1352–1359.
110. Romaker, D., V. Kumar, D. M. Cerqueira, R. M. Cox, and O. Wessely. 2014. MicroRNAs are critical regulators of tuberous sclerosis complex and mTORC1 activity in the size control of the *Xenopus* kidney. *Proc. Natl. Acad. Sci.* 111: 6335–6340.
111. Kim, S. K., A. Shindo, T. J. Park, E. C. Oh, S. Ghosh, R. S. Gray, R. A. Lewis, C. A. Johnson, T. Attie-Bittach, N. Katsanis, and J. B. Wallingford. 2010. Planar Cell Polarity Acts Through Septins to Control Collective Cell Movement and Ciliogenesis. *Science* (80-.). 329: 1337–1340.
112. Suspitsin, E. N., and E. N. Imyanitov. 2016. Bardet-Biedl Syndrome. *Mol.*

Syndromol. 7: 62–71.

113. Moody, S. A. 1987. Fates of the blastomeres of the 32-cell-stage *Xenopus* embryo. *Dev. Biol.* 122: 300–319.

114. Dale, L., and J. M. W. Slack. 1987. Fate map for the 32-cell stage of *Xenopus laevis*. *Development* 99: 527–51.

115. DeLay, B. D., V. Krneta-Stankic, and R. K. Miller. 2016. Technique to Target Microinjection to the Developing *Xenopus* Kidney. *J Vis Exp*.

116. Aslan, Y., E. Tadjuidje, A. M. Zorn, and S.-W. Cha. 2017. High efficiency non-mosaic CRISPR mediated knock-in and mutations in F0 *Xenopus*. *Development dev.*152967.

117. Denayer, T., F. Van Roy, and K. Vleminckx. 2006. In vivo tracing of canonical Wnt signaling in *Xenopus* tadpoles by means of an inducible transgenic reporter tool. *FEBS Lett.* 580: 393–398.

118. Rankin, S. A., A. M. Zorn, and D. R. Buchholz. 2011. New doxycycline-inducible transgenic lines in *Xenopus*. *Dev. Dyn.* 240: 1467–1474.

119. Zhuo, X., M. Haeri, E. Solessio, and B. E. Knox. 2013. An inducible expression system to measure rhodopsin transport in transgenic *Xenopus* rod outer segments. *PLoS One* 8.

120. Beck, C. W., and J. M. Slack. 2001. An amphibian with ambition: a new role for *Xenopus* in the 21st century. *Genome Biol.* 2: REVIEWS1029.

121. Blum, M., and T. Ott. 2019. *Xenopus*: An undervalued model organism to study

and model human genetic disease. *Cells Tissues Organs*.

122. Gresh, L., E. Fischer, A. Reimann, M. Tanguy, S. Garbay, X. Shao, T.

Hiesberger, L. Fiette, P. Igarashi, M. Yaniv, and M. Pontoglio. 2004. A transcriptional network in polycystic kidney disease. *EMBO J.* 23: 1657–1668.

123. Wolf, M. T. F., and F. Hildebrandt. 2011. Nephronophthisis. *Pediatr. Nephrol.* 26: 181–94.

124. Lienkamp, S., A. Ganner, C. Boehlke, T. Schmidt, S. J. Arnold, T. Schäfer, D.

Romaker, J. Schuler, S. Hoff, C. Powelske, A. Eifler, C. Krönig, A. Bullerkotte, R.

Nitschke, E. W. Kuehn, E. Kim, H. Burkhardt, T. Brox, O. Ronneberger, J. Gloy, and

G. Walz. 2010. Inversin relays Frizzled-8 signals to promote proximal pronephros development. *Proc. Natl. Acad. Sci. U. S. A.* 107: 20388–20393.

125. Stokman, M., M. Lilien, and N. Knoers. 2016. Nephronophthisis. *Gene Rev.*

126. Srivastava, S., E. Molinari, S. Raman, and J. A. Sayer. 2018. Many Genes—One Disease? Genetics of Nephronophthisis (NPHP) and NPHP-Associated Disorders. *Front. Pediatr.* 5: 1–15.

127. Wing, M. R., J. M. Devaney, M. M. Joffe, D. Xie, H. I. Feldman, E. A. Dominic,

N. J. Guzman, A. Ramezani, K. Susztak, J. G. Herman, L. Cope, B. Harmon, B.

Kwabi-Addo, H. Gordish-Dressman, A. S. Go, J. He, J. P. Lash, J. W. Kusek, and D.

S. Raj. 2014. DNA methylation profile associated with rapid decline in kidney function: Findings from the CRIC Study. *Nephrol. Dial. Transplant.* 29: 864–872.

128. Bendl, J., J. Stourac, O. Salanda, A. Pavelka, E. D. Wieben, J. Zendulka, J.

Brezovsky, and J. Damborsky. 2014. PredictSNP: Robust and Accurate Consensus Classifier for Prediction of Disease-Related Mutations. *PLoS Comput. Biol.* 10.

129. Capriotti, E., R. B. Altman, and Y. Bromberg. 2013. Collective judgment predicts disease-associated single nucleotide variants. *BMC Genomics* 14 Suppl 3: S2.

130. Xue, Y., Y. Chen, Q. Ayub, N. Huang, E. V. Ball, M. Mort, A. D. Phillips, K. Shaw, P. D. Stenson, D. N. Cooper, and C. Tyler-Smith. 2012. Deleterious- and disease-allele prevalence in healthy individuals: Insights from current predictions, mutation databases, and population-scale resequencing. *Am. J. Hum. Genet.* 91: 1022–1032.

131. Matsumura, Y., S. Uchida, Y. Kondo, H. Miyazaki, S. B. Ko, a Hayama, T. Morimoto, W. Liu, M. Arisawa, S. Sasaki, and F. Marumo. 1999. Overt nephrogenic diabetes insipidus in mice lacking the CLC-K1 chloride channel. *Nat. Genet.* 21: 95–98.

132. Corkins, M. E., H. L. Hanania, V. Krneta-Stankic, B. D. DeLay, E. J. Pearl, M. Lee, H. Ji, A. J. Davidson, M. E. Horb, and R. K. Miller. 2018. Transgenic *Xenopus laevis* line for in vivo labeling of nephrons within the kidney. *Genes (Basel)*. 9.

133. Schmitt, S. M., M. Gull, and A. W. Brändli. 2014. Engineering *Xenopus* embryos for phenotypic drug discovery screening. *Adv. Drug Deliv. Rev.* 69–70: 225–246.

134. Galceran, J., K. De Graaf, F. J. Tejedor, and W. Becker. 2003. The MNB/DYRK1A protein kinase: Genetic and biochemical properties. *J. Neural*

Transm. Suppl.

135. Aranda, S., A. Laguna, and S. de la Luna. 2011. DYRK family of protein kinases: evolutionary relationships, biochemical properties, and functional roles.

FASEB J.

136. Lochhead, P. A., G. Sibbet, N. Morrice, and V. Cleghon. 2005. Activation-loop autophosphorylation is mediated by a novel transitional intermediate form of DYRKs.

Cell.

137. Møller, R. S., S. Kübart, M. Hoeltzenbein, B. Heye, I. Vogel, C. P. Hansen, C. Menzel, R. Ullmann, N. Tommerup, H. H. Ropers, Z. Tümer, and V. M. Kalscheuer. 2008. Truncation of the Down Syndrome Candidate Gene DYRK1A in Two Unrelated Patients with Microcephaly. *Am. J. Hum. Genet.*

138. Dowjat, W. K., T. Adayev, I. Kuchna, K. Nowicki, S. Palminiello, Y. W. Hwang, and J. Wegiel. 2007. Trisomy-driven overexpression of DYRK1A kinase in the brain of subjects with Down syndrome. *Neurosci. Lett.* 413: 77–81.

139. Himpel, S., W. Tegge, R. Frank, S. Leder, H. G. Joost, and W. Becker. 2000. Specificity determinants of substrate recognition by the protein kinase DYRK1A. *J. Biol. Chem.*

140. Campbell, L. E., and C. G. Proud. 2002. Differing substrate specificities of members of the DYRK family of arginine-directed protein kinases. *FEBS Lett.*

141. Helfrich, C. 1986. Role of the optic lobes in the regulation of the locomotor activity rhythm of drosophila melanogaster: Behavioral analysis of neural mutants. *J.*

142. Becker, W., Y. Weber, K. Wetzel, K. Eirnbter, F. J. Tejedor, and H. G. Joost. 1998. Sequence characteristics, subcellular localization, and substrate specificity of DYRK-related kinases, a novel family of dual specificity protein kinases. *J. Biol. Chem.*

143. Kentrup, H., H. G. Joost, G. Heimann, and W. Becker. 2000. [Minibrain/DYRK1A gene: candidate gene for mental retardation in Down's syndrome?]. *Klin. Pädiatrie.*

144. Hämmerle, B., C. Elizalde, J. Galceran, W. Becker, and F. J. Tejedor. 2003. The MNB/DYRK1A protein kinase: neurobiological functions and Down syndrome implications. *J. Neural Transm. Suppl.* 129–37.

145. Van Bon, B. W. M., B. P. Coe, R. Bernier, C. Green, J. Gerdts, K. Witherspoon, T. Kleefstra, M. H. Willemsen, R. Kumar, P. Bosco, M. Fichera, D. Li, D. Amaral, F. Cristofoli, H. Peeters, E. Haan, C. Romano, H. C. Mefford, I. Scheffer, J. Gecz, B. B. A. De Vries, and E. E. Eichler. 2016. Disruptive de novo mutations of DYRK1A lead to a syndromic form of autism and ID. *Mol. Psychiatry.*

146. Becker, W., and W. Sippl. 2011. Activation, regulation, and inhibition of DYRK1A. *FEBS J.*

147. Liu, Q., Y. Tang, L. Chen, N. Liu, F. Lang, H. Liu, P. Wang, and X. Sun. 2016. E3 ligase SCF β TrCP-induced DYRK1A protein degradation is essential for cell cycle progression in HEK293 cells. *J. Biol. Chem.*

148. Granno, S., J. Nixon-Abell, D. C. Berwick, J. Tosh, G. Heaton, S. Almudimeegh, Z. Nagda, J. C. Rain, M. Zanda, V. Plagnol, V. L. J. Tybulewicz, K. Cleverley, F. K. Wiseman, E. M. C. Fisher, and K. Harvey. 2019. Downregulated Wnt/ β -catenin signalling in the Down syndrome hippocampus. *Sci. Rep.*
149. Singh, R., and M. Lauth. 2017. Emerging roles of DYRK kinases in embryogenesis and Hedgehog pathway control. *J. Dev. Biol.*
150. Cho, H. J., J. G. Lee, J. H. Kim, S. Y. Kim, Y. H. Huh, H. J. Kim, K. S. Lee, K. Yu, and J. S. Lee. 2019. Vascular defects of DYRK1A knockouts are ameliorated by modulating calcium signaling in zebrafish. *DMM Dis. Model. Mech.*
151. Park, J., J. Y. Sung, J. Park, W. J. Song, S. Chang, and K. C. Chung. 2012. Dyrk1a negatively regulates the actin cytoskeleton through threonine phosphorylation of N-WASP. *J. Cell Sci.*
152. Knoers, N. V. A. M., and K. Y. Renkema. 2019. The genomic landscape of CAKUT; you gain some, you lose some. *Kidney Int.*
153. Sanna-Cherchi, S., K. Kiryluk, K. E. Burgess, M. Bodria, M. G. Sampson, D. Hadley, S. N. Nees, M. Verbitsky, B. J. Perry, R. Sterken, V. J. Lozanovski, A. Materna-Kiryluk, C. Barlassina, A. Kini, V. Corbani, A. Carrea, D. Somenzi, C. Murtas, N. Ristoska-Bojkovska, C. Izzi, B. Bianco, M. Zaniew, H. Flogelova, P. L. Weng, N. Kacak, S. Giberti, M. Gigante, A. Arapovic, K. Drnasin, G. Caridi, S. Curioni, F. Allegri, A. Ammenti, S. Ferretti, V. Goj, L. Bernardo, V. Jobanputra, W. K. Chung, R. P. Lifton, S. Sanders, M. State, L. N. Clark, M. Saraga, S. Padmanabhan, A. F. Dominiczak, T. Foroud, L. Gesualdo, Z. Gucev, L. Allegri, A. Latos-Bielenska,

- D. Cusi, F. Scolari, V. Tasic, H. Hakonarson, G. M. Ghiggeri, and A. G. Gharavi. 2012. Copy-number disorders are a common cause of congenital kidney malformations. *Am. J. Hum. Genet.*
154. Nicolaou, N., K. Y. Renkema, E. M. H. F. Bongers, R. H. Giles, and N. V. A. M. Knoers. 2015. Genetic, environmental, and epigenetic factors involved in CAKUT. *Nat. Rev. Nephrol.*
155. Rosenblum, S., A. Pal, and K. Reidy. 2017. Renal development in the fetus and premature infant. *Semin. Fetal Neonatal Med.*
156. Esther, C. R., E. M. Marino, T. E. Howard, a Machaud, P. Corvol, M. R. Capecchi, and K. E. Bernstein. 1997. The critical role of tissue angiotensin-converting enzyme as revealed by gene targeting in mice. *J. Clin. Invest.* 99: 2375–85.
157. Chan, S. K., P. R. Riley, K. L. Price, F. McElduff, P. J. Winyard, S. J. M. Welham, A. S. Woolf, and D. A. Long. 2010. Corticosteroid-induced kidney dysmorphogenesis is associated with deregulated expression of known cystogenic molecules, as well as indian hedgehog. *Am. J. Physiol. - Ren. Physiol.*
158. Hong, J. Y., J.-I. Park, M. Lee, W. A. Muñoz, R. K. Miller, H. Ji, D. Gu, J. Ezan, S. Y. Sokol, and P. D. McCrea. 2012. Down's-syndrome-related kinase Dyrk1A modulates the p120-catenin–Kaiso trajectory of the Wnt signaling pathway. *J. Cell Sci.*
159. Gurdon, J. B. 1995. Normal table of *Xenopus laevis* (Daudin). *Trends Genet.*

160. Kim, S. W., X. Fang, H. Ji, A. F. Paulson, J. M. Daniel, M. Ciesiolka, F. Van Roy, and P. D. McCrea. 2002. Isolation and characterization of XKaiso, a transcriptional repressor that associates with the catenin Xp120ctn in *Xenopus laevis*. *J. Biol. Chem.* 277: 8202–8208.
161. Davidson, L. A., M. Marsden, R. Keller, and D. W. DeSimone. 2006. Integrin $\alpha 5 \beta 1$ and Fibronectin Regulate Polarized Cell Protrusions Required for *Xenopus* Convergence and Extension. *Curr. Biol.* 16: 833–844.
162. Bainbridge, M. N., M. Wang, Y. Wu, I. Newsham, D. M. Muzny, J. L. Jefferies, T. J. Albert, D. L. Burgess, and R. A. Gibbs. 2011. Targeted enrichment beyond the consensus coding DNA sequence exome reveals exons with higher variant densities. *Genome Biol.*
163. Bekheirnia, M. R., N. Bekheirnia, M. N. Bainbridge, S. Gu, Z. H. C. Akdemir, T. Gambin, N. K. Janzen, S. N. Jhangiani, D. M. Muzny, M. Michael, E. D. Brewer, E. Elenberg, A. S. Kale, A. A. Riley, S. J. Swartz, D. A. Scott, Y. Yang, P. R. Srivaths, S. E. Wenderfer, J. Bodurtha, C. D. Applegate, M. Velinov, A. Myers, L. Borovik, W. J. Craigie, N. A. Hanchard, J. A. Rosenfeld, R. A. Lewis, E. T. Gonzales, R. A. Gibbs, J. W. Belmont, D. R. Roth, C. Eng, M. C. Braun, J. R. Lupski, and D. J. Lamb. 2017. Whole-exome sequencing in the molecular diagnosis of individuals with congenital anomalies of the kidney and urinary tract and identification of a new causative gene. *Genet. Med.*
164. Lupski, J. R., C. Gonzaga-Jauregui, Y. Yang, M. N. Bainbridge, S. Jhangiani, C. J. Buhay, C. L. Kovar, M. Wang, A. C. Hawes, J. G. Reid, C. Eng, D. M. Muzny,

and R. A. Gibbs. 2013. Exome sequencing resolves apparent incidental findings and reveals further complexity of SH3TC2 variant alleles causing Charcot-Marie-Tooth neuropathy. *Genome Med.*

165. Richards, S., N. Aziz, S. Bale, D. Bick, S. Das, J. Gastier-Foster, W. W. Grody, M. Hegde, E. Lyon, E. Spector, K. Voelkerding, and H. L. Rehm. 2015. Standards and guidelines for the interpretation of sequence variants: A joint consensus recommendation of the American College of Medical Genetics and Genomics and the Association for Molecular Pathology. *Genet. Med.*

166. Morin, R. D., E. Chang, A. Petrescu, N. Liao, M. Griffith, R. Kirkpatrick, Y. S. Butterfield, A. C. Young, J. Stott, S. Barber, R. Babakaiff, M. C. Dickson, C. Matsuo, D. Wong, G. S. Yang, D. E. Smailus, K. D. Wetherby, P. N. Kwong, J. Grimwood, C. P. Brinkley, M. Brown-John, N. D. Reddix-Dugue, M. Mayo, J. Schmutz, J. Beland, M. Park, S. Gibson, T. Olson, G. G. Bouffard, M. Tsai, R. Featherstone, S. Chand, A. S. Siddiqui, W. Jang, E. Lee, S. L. Klein, R. W. Blakesley, B. R. Zeeberg, S. Narasimhan, J. N. Weinstein, C. P. Pennacchio, R. M. Myers, E. D. Green, L. Wagner, D. S. Gerhard, M. A. Marra, S. J. M. Jones, and R. A. Holt. 2006. Sequencing and analysis of 10,967 full-length cDNA clones from *Xenopus laevis* and *Xenopus tropicalis* reveals post-tetraploidization transcriptome remodeling. *Genome Res.*

167. Eid, S. R., and A. W. Brändli. 2001. *Xenopus* Na,K-ATPase: Primary sequence of the $\beta 2$ subunit and in situ localization of $\alpha 1$, $\beta 1$, and γ expression during pronephric kidney development. *Differentiation.*

168. Nieuwkoop P., F. J. 1994. *Normal Table of Xenopus Laevis (Daudin): A Systematical & Chronological Survey of the Development from the Fertilized Egg till the End of Metamorphosis*.
169. Sive, H. L., R. M. Grainger, and R. M. Harland. 2000. Early Development of *Xenopus Laevis*: A Laboratory Manual. *Spring*.
170. Moody, S. A., and M. J. Kline. 1990. Segregation of fate during cleavage of frog (*Xenopus laevis*) blastomeres. *Anat. Embryol. (Berl)*. 182: 347–362.
171. Hong, J. Y., J.-I. Park, M. Lee, W. a. Munoz, R. K. Miller, H. Ji, D. Gu, J. Ezan, S. Y. Sokol, and P. D. McCrea. 2012. Down's-syndrome-related kinase Dyrk1A modulates the p120-catenin-Kaiso trajectory of the Wnt signaling pathway. *J. Cell Sci*. 125: 3012–3012.
172. DeLay, B. D., T. A. Baldwin, and R. K. Miller. 2019. Dynamin binding protein is required for *Xenopus laevis* kidney development. *Front. Physiol*.
173. Vize, P. D., E. A. Jones, and R. Pfister. 1995. Development of the *Xenopus* pronephric system. *Dev. Biol*. 171: 531–540.
174. Tărlungeanu, D. C., and G. Novarino. 2018. Genomics in neurodevelopmental disorders: an avenue to personalized medicine. *Exp. Mol. Med*.
175. Shashi, V., A. McConkie-Rosell, B. Rosell, K. Schoch, K. Vellore, M. McDonald, Y. H. Jiang, P. Xie, A. Need, and D. B. Goldstein. 2014. The utility of the traditional medical genetics diagnostic evaluation in the context of next-generation sequencing for undiagnosed genetic disorders. *Genet. Med*.

176. O’Roak, B. J., P. Deriziotis, C. Lee, L. Vives, J. J. Schwartz, S. Girirajan, E. Karakoc, A. P. MacKenzie, S. B. Ng, C. Baker, M. J. Rieder, D. A. Nickerson, R. Bernier, S. E. Fisher, J. Shendure, and E. E. Eichler. 2011. Exome sequencing in sporadic autism spectrum disorders identifies severe de novo mutations. *Nat. Genet.*

177. Fitzgerald, T. W., S. S. Gerety, W. D. Jones, M. Van Kogelenberg, D. A. King, J. McRae, K. I. Morley, V. Parthiban, S. Al-Turki, K. Ambridge, D. M. Barrett, T. Bayzetenova, S. Clayton, E. L. Coomber, S. Gribble, P. Jones, N. Krishnappa, L. E. Mason, A. Middleton, R. Miller, E. Prigmore, D. Rajan, A. Sifrim, A. R. Tivey, M. Ahmed, N. Akawi, R. Andrews, U. Anjum, H. Archer, R. Armstrong, M. Balasubramanian, R. Banerjee, D. Baralle, P. Batstone, D. Baty, C. Bennett, J. Berg, B. Bernhard, A. P. Bevan, E. Blair, M. Blyth, D. Bohanna, L. Bourdon, D. Bourn, A. Brady, E. Bragin, C. Brewer, L. Brueton, K. Brunstrom, S. J. Bumpstead, D. J. Bunyan, J. Burn, J. Burton, N. Canham, B. Castle, K. Chandler, S. Clasper, J. Clayton-Smith, T. Cole, A. Collins, M. N. Collinson, F. Connell, N. Cooper, H. Cox, L. Cresswell, G. Cross, Y. Crow, M. D’Alessandro, T. Dabir, R. Davidson, S. Davies, J. Dean, C. Deshpande, G. Devlin, A. Dixit, A. Dominiczak, C. Donnelly, D. Donnelly, A. Douglas, A. Duncan, J. Eason, S. Edkins, S. Ellard, P. Ellis, F. Elmslie, K. Evans, S. Everest, T. Fendick, R. Fisher, F. Flinter, N. Foulds, A. Fryer, B. Fu, C. Gardiner, L. Gaunt, N. Ghali, R. Gibbons, S. L. Gomes Pereira, J. Goodship, D. Goudie, E. Gray, P. Greene, L. Greenhalgh, L. Harrison, R. Hawkins, S. Hellens, A. Henderson, E. Hobson, S. Holden, S. Holder, G. Hollingsworth, T. Homfray, M. Humphreys, J. Hurst, S. Ingram, M. Irving, J. Jarvis, L. Jenkins, D. Johnson, D. Jones, E. Jones, D. Josifova, S. Joss, B. Kaemba, S. Kazembe, B. Kerr, U. Kini, E. Kinning, G. Kirby, C.

Kirk, E. Kivuva, A. Kraus, D. Kumar, K. Lachlan, W. Lam, A. Lampe, C. Langman, M. Lees, D. Lim, G. Lowther, S. A. Lynch, A. Magee, E. Maher, S. Mansour, K. Marks, K. Martin, U. Maye, E. McCann, V. McConnell, M. McEntagart, R. McGowan, K. McKay, S. McKee, D. J. McMullan, S. McNerlan, S. Mehta, K. Metcalfe, E. Miles, S. Mohammed, T. Montgomery, D. Moore, S. Morgan, A. Morris, J. Morton, H. Mugalaasi, V. Murday, L. Nevitt, R. Newbury-Ecob, A. Norman, R. O'Shea, C. Ogilvie, S. Park, M. J. Parker, C. Patel, J. Paterson, S. Payne, J. Phipps, D. T. Pilz, D. Porteous, N. Pratt, K. Prescott, S. Price, A. Pridham, A. Procter, H. Purnell, N. Ragge, J. Rankin, L. Raymond, D. Rice, L. Robert, E. Roberts, G. Roberts, J. Roberts, P. Roberts, A. Ross, E. Rosser, A. Saggarr, S. Samant, R. Sandford, A. Sarkar, S. Schweiger, C. Scott, R. Scott, A. Selby, A. Seller, C. Sequeira, N. Shannon, S. Sharif, C. Shaw-Smith, E. Shearing, D. Shears, I. Simoncic, D. Simpkin, R. Singzon, Z. Skitt, A. Smith, B. Smith, K. Smith, S. Smithson, L. Sneddon, M. Splitt, M. Squires, F. Stewart, H. Stewart, M. Suri, V. Sutton, G. J. Swaminathan, E. Sweeney, K. Tatton-Brown, C. Taylor, R. Taylor, M. Tein, I. K. Temple, J. Thomson, J. Tolmie, A. Torokwa, B. Treacy, C. Turner, P. Turnpenny, C. Tysoe, A. Vandersteen, P. Vasudevan, J. Vogt, E. Wakeling, D. Walker, J. Waters, A. Weber, D. Wellesley, M. Whiteford, S. Widaa, S. Wilcox, D. Williams, N. Williams, G. Woods, C. Wragg, M. Wright, F. Yang, M. Yau, N. P. Carter, M. Parker, H. V. Firth, D. R. FitzPatrick, C. F. Wright, J. C. Barrett, and M. E. Hurles. 2015. Large-scale discovery of novel genetic causes of developmental disorders. *Nature*.

178. O'Roak, B. J., L. Vives, W. Fu, J. D. Egerton, I. B. Stanaway, I. G. Phelps, G. Carvill, A. Kumar, C. Lee, K. Ankenman, J. Munson, J. B. Hiatt, E. H. Turner, R.

- Levy, D. R. O'Day, N. Krumm, B. P. Coe, B. K. Martin, E. Borenstein, D. A. Nickerson, H. C. Mefford, D. Doherty, J. M. Akey, R. Bernier, E. E. Eichler, and J. Shendure. 2012. Multiplex targeted sequencing identifies recurrently mutated genes in autism spectrum disorders. *Science* (80-.).
179. Courcet, J. B., L. Faivre, P. Malzac, A. Masurel-Paulet, E. Lopez, P. Callier, L. Lambert, M. Lemesle, J. Thevenon, N. Gigot, L. Duplomb, C. Ragon, N. Marle, A. L. Mosca-Boidron, F. Huet, C. Philippe, A. Moncla, and C. Thauvin-Robinet. 2012. The DYRK1A gene is a cause of syndromic intellectual disability with severe microcephaly and epilepsy. *J. Med. Genet.*
180. Luco, S. M., D. Pohl, E. Sell, J. D. Wagner, D. A. Dymont, and H. Daoud. 2016. Case report of novel DYRK1A mutations in 2 individuals with syndromic intellectual disability and a review of the literature. *BMC Med. Genet.* 17.
181. Ji, J., H. Lee, B. Argiropoulos, N. Dorrani, J. Mann, J. A. Martinez-Agosto, N. Gomez-Ospina, N. Gallant, J. A. Bernstein, L. Hudgins, L. Slattery, B. Isidor, C. Le Caignec, A. David, E. Obersztyn, B. Wiśniowiecka-Kowalik, M. Fox, J. L. Deignan, E. Vilain, E. Hendricks, M. H. Harr, S. E. Noon, J. R. Jackson, A. Wilkens, G. Mirzaa, N. Salamon, J. Abramson, E. H. Zackai, I. Krantz, A. M. Innes, S. F. Nelson, W. W. Grody, and F. Quintero-Rivera. 2015. DYRK1A haploinsufficiency causes a new recognizable syndrome with microcephaly, intellectual disability, speech impairment, and distinct facies. *Eur. J. Hum. Genet.*
182. Lek, M., K. J. Karczewski, E. V. Minikel, K. E. Samocha, E. Banks, T. Fennell, A. H. O'Donnell-Luria, J. S. Ware, A. J. Hill, B. B. Cummings, T. Tukiainen, D. P.

Birnbaum, J. A. Kosmicki, L. E. Duncan, K. Estrada, F. Zhao, J. Zou, E. Pierce-
 Hoffman, J. Berghout, D. N. Cooper, N. Deflaux, M. DePristo, R. Do, J. Flannick, M.
 Fromer, L. Gauthier, J. Goldstein, N. Gupta, D. Howrigan, A. Kiezun, M. I. Kurki, A.
 L. Moonshine, P. Natarajan, L. Orozco, G. M. Peloso, R. Poplin, M. A. Rivas, V.
 Ruano-Rubio, S. A. Rose, D. M. Ruderfer, K. Shakir, P. D. Stenson, C. Stevens, B.
 P. Thomas, G. Tiao, M. T. Tusie-Luna, B. Weisburd, H. H. Won, D. Yu, D. M.
 Altshuler, D. Ardissino, M. Boehnke, J. Danesh, S. Donnelly, R. Elosua, J. C. Florez,
 S. B. Gabriel, G. Getz, S. J. Glatt, C. M. Hultman, S. Kathiresan, M. Laakso, S.
 McCarroll, M. I. McCarthy, D. McGovern, R. McPherson, B. M. Neale, A. Palotie, S.
 M. Purcell, D. Saleheen, J. M. Scharf, P. Sklar, P. F. Sullivan, J. Tuomilehto, M. T.
 Tsuang, H. C. Watkins, J. G. Wilson, M. J. Daly, D. G. MacArthur, H. E. Abboud, G.
 Abecasis, C. A. Aguilar-Salinas, O. Arellano-Campos, G. Atzmon, I. Aukrust, C. L.
 Barr, G. I. Bell, S. Bergen, L. Bjørkhaug, J. Blangero, D. W. Bowden, C. L. Budman,
 N. P. Burt, F. Centeno-Cruz, J. C. Chambers, K. Chambert, R. Clarke, R. Collins, G.
 Coppola, E. J. Córdova, M. L. Cortes, N. J. Cox, R. Duggirala, M. Farrall, J. C.
 Fernandez-Lopez, P. Fontanillas, T. M. Frayling, N. B. Freimer, C. Fuchsberger, H.
 García-Ortiz, A. Goel, M. J. Gómez-Vázquez, M. E. González-Villalpando, C.
 González-Villalpando, M. A. Grados, L. Groop, C. A. Haiman, C. L. Hanis, A. T.
 Hattersley, B. E. Henderson, J. C. Hopewell, A. Huerta-Chagoya, S. Islas-Andrade,
 S. B. Jacobs, S. Jalilzadeh, C. P. Jenkinson, J. Moran, S. Jiménez-Morale, A.
 Kähler, R. A. King, G. Kirov, J. S. Kooner, T. Kyriakou, J. Y. Lee, D. M. Lehman, G.
 Lyon, W. MacMahon, P. K. Magnusson, A. Mahajan, J. Marrugat, A. Martínez-
 Hernández, C. A. Mathews, G. McVean, J. B. Meigs, T. Meitinger, E. Mendoza-

Caamal, J. M. Mercader, K. L. Mohlke, H. Moreno-Macías, A. P. Morris, L. A. Najmi, P. R. Njølstad, M. C. O'Donovan, M. L. Ordóñez-Sánchez, M. J. Owen, T. Park, D. L. Pauls, D. Posthuma, C. Revilla-Monsalve, L. Riba, S. Ripke, R. Rodríguez-Guillén, M. Rodríguez-Torres, P. Sandor, M. Seielstad, R. Sladek, X. Soberón, T. D. Spector, S. E. Tai, T. M. Teslovich, G. Walford, L. R. Wilkens, and A. L. Williams. 2016. Analysis of protein-coding genetic variation in 60,706 humans. *Nature*.

183. Evers, J. M. G., R. A. Laskowski, M. Bertolli, J. Clayton-Smith, C. Deshpande, J. Eason, F. Elmslie, F. Flinter, C. Gardiner, J. A. Hurst, H. Kingston, U. Kini, A. K. Lampe, D. Lim, A. Male, S. Naik, M. J. Parker, S. Price, L. Robert, A. Sarkar, V. Straub, G. Woods, J. M. Thornton, The DDD Study, and C. F. Wright. 2017. Structural analysis of pathogenic mutations in the DYRK1A gene in patients with developmental disorders. *Hum. Mol. Genet.*

184. Widowati, E. W., S. Ernst, R. Hausmann, G. Müller-Newen, and W. Becker. 2018. Functional characterization of DYRK1A missense variants associated with a syndromic form of intellectual deficiency and autism. *Biol. Open*.

185. Arranz, J., E. Balducci, K. Arató, G. Sánchez-Elexpuru, S. Najas, A. Parras, E. Rebollo, I. Pijuan, I. Erb, G. Verde, I. Sahun, M. J. Barallobre, J. J. Lucas, M. P. Sánchez, S. de la Luna, and M. L. Arbonés. 2019. Impaired development of neocortical circuits contributes to the neurological alterations in DYRK1A haploinsufficiency syndrome. *Neurobiol. Dis.*

186. Blackburn, A. T. M., and R. K. Miller. 2019. Modeling congenital kidney diseases in *Xenopus laevis*. *DMM Dis. Model. Mech.*

187. Bower, M., R. Salomon, J. Allanson, C. Antignac, F. Benedicenti, E. Benetti, G. Binenbaum, U. B. Jensen, P. Cochat, S. Decramer, J. Dixon, R. Drouin, M. J. Falk, H. Feret, R. Gise, A. Hunter, K. Johnson, R. Kumar, M. P. Lavocat, L. Martin, V. Morinière, D. Mowat, L. Murer, H. T. Nguyen, G. Peretz-Amit, E. Pierce, E. Place, N. Rodig, A. Salerno, S. Sastry, T. Sato, J. A. Sayer, G. C. P. Schaafsma, L. Shoemaker, D. W. Stockton, W. H. Tan, R. Tenconi, P. Vanhille, A. Vats, X. Wang, B. Warman, R. G. Weleber, S. M. White, C. Wilson-Brackett, D. J. Zand, M. Eccles, L. A. Schimmenti, and L. Heidet. 2012. Update of PAX2 mutations in renal coloboma syndrome and establishment of a locus-specific database. *Hum. Mutat.* 33: 457–466.
188. Kobayashi, A., K. M. Kwan, T. J. Carroll, A. P. McMahon, C. L. Mendelsohn, and R. R. Behringer. 2005. Distinct and sequential tissue-specific activities of the LIM-class homeobox gene *Lim1* for tubular morphogenesis during kidney development. *Development.*
189. Gruenwald, P. 1941. The relation of the growing müllerian duct to the wolffian duct and its importance for the genesis of malformations. *Anat. Rec.*
190. Jansson, E., A. Mattsson, J. Goldstone, and C. Berg. 2016. Sex-dependent expression of anti-Müllerian hormone (amh) and amh receptor 2 during sex organ differentiation and characterization of the Müllerian duct development in *Xenopus tropicalis*. *Gen. Comp. Endocrinol.*
191. Piprek, R. P., A. Pecio, M. Kloc, J. Z. Kubiak, and J. M. Szymura. 2014. Evolutionary trend for metamery reduction and gonad shortening in anurans

revealed by comparison of gonad development. *Int. J. Dev. Biol.* .

192. Ariel, I., T. R. Wells, B. H. Landing, and D. B. Singer. 1991. The urinary system in down syndrome: A study of 124 autopsy cases. *Fetal Pediatr. Pathol.* .

193. Málaga, S., R. Pardo, I. Málaga, G. Orejas, and J. Fernández-Toral. 2005. Renal involvement in Down syndrome. *Pediatr. Nephrol.*

194. Nestor, J. G., E. E. Groopman, and A. G. Gharavi. 2018. Towards precision nephrology: the opportunities and challenges of genomic medicine. *J. Nephrol.*

195. Woolf, A. S. 2000. A molecular and genetic view of human renal and urinary tract malformations. *Kidney Int.* 58: 500–512.

196. Gbadegesin, R. A., P. D. Brophy, A. Adeyemo, G. Hall, I. R. Gupta, D. Hains, B. Bartkowiak, C. E. Rabinovich, S. Chandrasekharappa, A. Homstad, K. Westreich, G. Wu, Y. Liu, D. Holanda, J. Clarke, P. Lavin, A. Selim, S. Miller, J. S. Wiener, S. S. Ross, J. Foreman, C. Rotimi, and M. P. Winn. 2013. TNXB mutations can cause vesicoureteral reflux. *J. Am. Soc. Nephrol.*

197. Chatterjee, R., E. Ramos, M. Hoffman, J. Vanwinkle, D. R. Martin, T. K. Davis, M. Hoshi, S. P. Hmiel, A. Beck, K. Hruska, D. Coplen, H. Liapis, R. Mitra, T. Druley, P. Austin, and S. Jain. 2012. Traditional and targeted exome sequencing reveals common, rare and novel functional deleterious variants in RET-signaling complex in a cohort of living US patients with urinary tract malformations. *Hum. Genet.*

198. Sanna-Cherchi, S., R. V. Sampogna, N. Papeta, K. E. Burgess, S. N. Nees, B. J. Perry, M. Choi, M. Bodria, Y. Liu, P. L. Weng, V. J. Lozanovski, M. Verbitsky, F.

- Lugani, R. Sterken, N. Paragas, G. Caridi, A. Carrea, M. Dagnino, A. Materna-Kiryluk, G. Santamaria, C. Murtas, N. Ristoska-Bojkovska, C. Izzi, N. Kacak, B. Bianco, S. Giberti, M. Gigante, G. Piaggio, L. Gesualdo, D. Kosuljandic Vukic, K. Vukojevic, M. Saraga-Babic, M. Saraga, Z. Gucev, L. Allegri, A. Latos-Bielenska, D. Casu, M. State, F. Scolari, R. Ravazzolo, K. Kiryluk, Q. Al-Awqati, V. D. D'Agati, I. A. Drummond, V. Tasic, R. P. Lifton, G. M. Ghiggeri, and A. G. Gharavi. 2013. Mutations in DSTYK and dominant urinary tract malformations. *N. Engl. J. Med.*
199. Gilbert, T., C. Leclerc, and M. Moreau. 2011. Control of kidney development by calcium ions. *Biochimie.*
200. McCright, B. 2003. Notch signaling in kidney development. *Curr. Opin. Nephrol. Hypertens.*
201. Song, W. J., E. A. C. Song, M. S. Jung, S. H. Choi, H. H. Baik, B. K. Jin, J. H. Kim, and S. H. Chung. 2015. Phosphorylation and inactivation of glycogen synthase kinase 3 β (GSK3 β) by dual-specificity tyrosine phosphorylation-regulated kinase 1A (Dyrk1A). *J. Biol. Chem.* 290: 2321–2333.
202. Duñach, M., B. Del Valle-Pérez, and A. García de Herreros. 2017. p120-catenin in canonical Wnt signaling. *Crit. Rev. Biochem. Mol. Biol.* 52: 327–339.
203. Hikasa, H., and S. Y. Sokol. 2013. Wnt signaling in vertebrate axis specification. *Cold Spring Harb. Perspect. Biol.* 5.
204. Tran, H. T., and K. Vleminckx. 2014. Design and use of transgenic reporter strains for detecting activity of signaling pathways in *Xenopus*. *Methods.*

205. Liao, G., Q. Tao, M. Kofron, J. S. Chen, A. Schloemer, R. J. Davis, J. C. Hsieh, C. Wylie, J. Heasman, and C. Y. Kuan. 2006. Jun NH₂-terminal kinase (JNK) prevents nuclear β -catenin accumulation and regulates axis formation in *Xenopus* embryos. *Proc. Natl. Acad. Sci. U. S. A.*
206. Tanigawa, S., H. Wang, Y. Yang, N. Sharma, N. Tarasova, R. Ajima, T. P. Yamaguchi, L. G. Rodriguez, and A. O. Perantoni. 2011. Wnt4 induces nephronic tubules in metanephric mesenchyme by a non-canonical mechanism. *Dev. Biol.*
207. Davis, M. A., R. C. Ireton, and A. B. Reynolds. 2003. A core function for p120-catenin in cadherin turnover. *J. Cell Biol.*
208. Dang, T., W. Y. Duan, B. Yu, D. L. Tong, C. Cheng, Y. F. Zhang, W. Wu, K. Ye, W. X. Zhang, M. Wu, B. B. Wu, Y. An, Z. L. Qiu, and B. L. Wu. 2018. Autism-associated Dyrk1a truncation mutants impair neuronal dendritic and spine growth and interfere with postnatal cortical development. *Mol. Psychiatry.*
209. Agarwal Gupta, N., and M. Kabra. 2014. Diagnosis and management of Down syndrome. *Indian J. Pediatr.*
210. Krause, M., A. Rak-Raszewska, I. Pietilä, S. Quaggin, and S. Vainio. 2015. Signaling during Kidney Development. *Cells.*
211. Bates, C. M. 2011. Role of fibroblast growth factor receptor signaling in kidney development. *Am J Physiol Ren. Physiol.*
212. Chi, L., S. Zhang, Y. Lin, R. Pruskaite-Hyyryläinen, R. Voulteenaho, P. Itäranta, and S. Vainio. 2004. Sprouty proteins regulate ureteric branching by coordinating

reciprocal epithelial Wnt11, mesenchymal Gdnf and stromal Fgf7 signalling during kidney development. *Development*.

213. Aranda, S., M. Alvarez, S. Turró, A. Laguna, and S. de la Luna. 2008.

Sprouty2-Mediated Inhibition of Fibroblast Growth Factor Signaling Is Modulated by the Protein Kinase DYRK1A. *Mol. Cell. Biol.*

214. Jain, S. 2009. The many faces of RET dysfunction in kidney. In *Organogenesis* vol. 5.

215. Nagy, I. I., Q. Xu, F. Naillat, N. Ali, I. Miinalainen, A. Samoylenko, and S. J.

Vainio. 2016. Impairment of Wnt11 function leads to kidney tubular abnormalities and secondary glomerular cystogenesis. *BMC Dev. Biol.*

216. Kispert, A., S. Vainio, and A. P. McMahon. 1998. Wnt-4 is a mesenchymal signal for epithelial transformation of metanephric mesenchyme in the developing kidney. *Development* 125: 4225–34.

217. Granno, S., J. Nixon-Abell, D. C. Berwick, J. Tosh, G. Heaton, S.

Almudimeegh, Z. Nagda, J. C. Rain, M. Zanda, V. Plagnol, V. L. J. Tybulewicz, K. Cleverley, F. K. Wiseman, E. M. C. Fisher, and K. Harvey. 2019. Downregulated Wnt/ β -catenin signalling in the Down syndrome hippocampus. *Sci. Rep.*

218. Yu, J., T. J. Carroll, and A. P. McMahon. 2002. Sonic hedgehog regulates proliferation and differentiation of mesenchymal cells in the mouse metanephric kidney. *Development*.

219. Axelrod, J. D., J. R. Miller, J. M. Shulman, R. T. Moon, and N. Perrimon. 1998.

Differential recruitment of dishevelled provides signaling specificity in the planar cell polarity and Wntless signaling pathways. *Genes Dev.*

220. Rocque, B., and E. Torban. 2015. Planar Cell Polarity Pathway in Kidney Development and Function. *Adv. Nephrol.*

221. Fernandez-Martinez, J., E. M. Vela, M. Tora-Ponsioen, O. H. Ocaña, M. A. Nieto, and J. Galceran. 2009. Attenuation of Notch signalling by the Down-syndrome-associated kinase DYRK1A. *J. Cell Sci.*

222. Surendran, K., M. Selassie, H. Liapis, H. Krigman, and R. Kopan. 2010. Reduced notch signaling leads to renal cysts and papillary microadenomas. *J. Am. Soc. Nephrol.*

223. Fujimura, S., Q. Jiang, C. Kobayashi, and R. Nishinakamura. 2010. Notch2 activation in the embryonic kidney depletes nephron progenitors. *J. Am. Soc. Nephrol.*

224. Jung, M. S., J. H. Park, Y. S. Ryu, S. H. Choi, S. H. Yoon, M. Y. Kwon, J. Y. Oh, W. J. Song, and S. H. Chung. 2011. Regulation of RCAN1 protein activity by Dyrk1A protein-mediated phosphorylation. *J. Biol. Chem.*

225. Yabut, O., J. Domogauer, and G. D'Arcangelo. 2010. Dyrk1A overexpression inhibits proliferation and induces premature neuronal differentiation of neural progenitor cells. *J. Neurosci.*

226. Dirice, E., D. Walpita, A. Vetere, B. C. Meier, S. Kahraman, J. Hu, V. Dančík, S. M. Burns, T. J. Gilbert, D. E. Olson, P. A. Clemons, R. N. Kulkarni, and B. K.

Wagner. 2016. Inhibition of DYRK1A stimulates human β -cell proliferation. *Diabetes* .

227. Monteiro, M. B., S. Ramm, V. Chandrasekaran, S. A. Boswell, E. J. Weber, K. A. Lidberg, E. J. Kelly, and V. S. Vaidya. 2018. A high-throughput screen identifies DYRK1A inhibitor ID-8 that stimulates human kidney tubular epithelial cell proliferation. *J. Am. Soc. Nephrol.*

228. Guo, X., J. G. Williams, T. T. Schug, and X. Li. 2010. DYRK1A and DYRK3 promote cell survival through phosphorylation and activation of SIRT1. *J. Biol. Chem.*

229. Zhang, Z., A. Deb, Z. Zhang, A. Pachori, W. He, J. Guo, R. Pratt, and V. J. Dzau. 2009. Secreted frizzled related protein 2 protects cells from apoptosis by blocking the effect of canonical Wnt3a. *J. Mol. Cell. Cardiol.*

230. Stark, K., S. Vainio, G. Vassileva, and A. P. McMahon. 1994. Epithelial transformation of metanephric mesenchyme in the developing kidney regulated by Wnt-4. *Nature* 372: 679–683.

231. Lane, D. P. 1992. p53, guardian of the genome. *Nature*.

232. Li, Y., J. Liu, W. Li, A. Brown, M. Baddoo, M. Li, T. Carroll, L. Oxburgh, Y. Feng, and Z. Saifudeen. 2015. P53 enables metabolic fitness and self-renewal of nephron progenitor cells. *Dev.*

233. Saifudeen, Z., S. Dipp, J. Stefkova, X. Yao, S. Lookabaugh, and S. S. El-Dahr. 2009. p53 regulates metanephric development. *J. Am. Soc. Nephrol.*

234. Donehower, L. A., M. Harvey, B. L. Slagle, M. J. McArthur, C. A. Montgomery, J. S. Butel, and A. Bradley. 1992. Mice deficient for p53 are developmentally normal but susceptible to spontaneous tumours. *Nature*.
235. Armstrong, J. F., M. H. Kaufman, D. J. Harrison, and A. R. Clarke. 1995. High-frequency developmental abnormalities in p53-deficient mice. *Curr. Biol*.
236. Wallingford, J. B., D. W. Seufert, V. C. Virta, and P. D. Vize. 1997. p53 activity is essential for normal development in *Xenopus*. *Curr. Biol.* 7: 747–57.
237. Wallingford, J. B., D. W. Seufert, V. C. Virta, and P. D. Vize. 1997. p53 activity is essential for normal development in *Xenopus*. *Curr. Biol*.
238. Cho, Y., S. Gorina, P. D. Jeffrey, and N. P. Pavletich. 1994. Crystal structure of a p53 tumor suppressor-DNA complex: Understanding tumorigenic mutations. *Science* (80-.).
239. Hoeber, M., J. H. Clement, D. Wedlich, M. Montenarh, and W. Knöchel. 1994. Overexpression of wild-type p53 interferes with normal development in *Xenopus laevis* embryos. *Oncogene*.

Vita

Alexandria Tamara Michelle Blackburn was born in Stockton, California, the daughter of Andrea Shannon Loeppke and Blake Edward Loeppke. After completing her work at The Woodlands College Park High School, The Woodlands, Texas in 2009, she entered Lonestar College in Tomball, Texas. She received the degree of Associate of Science there in May 2013. In December 2015 she received a Bachelor of Science with a major in Biology from The University of St. Thomas. For the next 6 months, she worked as a research technician in the Department of Microbiology & Molecular Genetics at UTHealth. In August of 2016 she entered The University of Texas MD Anderson Cancer Center UTHealth Graduate School of Biomedical Sciences.

Permanent address:

13010 Thorn Valley Ct

Tomball, Texas 77377